

BULLETIN

OF THE AMERICAN PHYSICAL SOCIETY

PROGRAM OF THE 54th ANNUAL
GASEOUS ELECTRONICS CONFERENCE



October 9–12, 2001
Penn State University
University Park, Pennsylvania

October 2001
Volume 46, No. 6

BULLETIN

OF THE AMERICAN PHYSICAL SOCIETY

Coden BAPSA6

Series II, Vol. 46, No. 6

ISSN: 0003-0503

October 2001

APS COUNCIL 2001

President

George H. Trilling,* *Lawrence Berkeley National Laboratory*

President-Elect

William F. Brinkman,* *Bell Labs-Lucent Technologies*

Vice President

Myriam P. Sarachik,* *City College of New York-CUNY*

Executive Officer

Judy R. Franz,* *University of Alabama, Huntsville (on leave)*

Treasurer

Thomas McIlrath,* *University of Maryland (emeritus)*

Editor-in-Chief

Martin Blume,* *Brookhaven National Laboratory (emeritus)*

Past-President

James Langer,* *University of California, Santa Barbara*

General Councillors

Jonathan A. Bagger, Beverly Berger, Philip Bucksbaum,* L. Craig Davis, Stuart Freedman, Leon Lederman,* Cynthia McIntyre, Margaret Murnane, Cherry Ann Murray, Roberto Peccei, Philip Phillips, Helen Quinn,* Jin-Joo Song, James Trefil

Chair, Nominating Committee

Curtis G. Callan, Jr.

Chair, Panel on Public Affairs

William R. Frazer

Division, Forum and Section Councillors

Steven Holt* (*Astrophysics*), Harold Metcalf (*Atomic, Molecular, and Optical*), Robert Eisenberg (*Biological*), Sylvia Ceyer (*Chemical*), E. Dan Dahlberg,* Arthur Hebard,* Allen Goldman (*Condensed Matter*), Steve White (*Computational*), Jerry Gollub* (*Fluid Dynamics*), Peter Zimmerman (*Forum on Education*), Gloria Lubkin* (*Forum on History of Physics*), Stuart Wolf (*Forum on Industrial and Applied Physics*), Ed Gerjuoy (*Forum on Physics and Society*), Carl Lineberger (*Laser Science*), G. Slade Cargill, III (*Materials*), John D. Walecka (*Nuclear*), Sally Dawson, Peter Meyers (*Particles and Fields*), Alexander Chao (*Physics of Beams*), Richard Hazeltine (*Plasma*), Timothy P. Lodge (*Polymer*), Kannan Jagannathan (*New England*), Joe Hamilton (*Southeastern*)

**Members of the APS Executive Board*

ADVISORS

Representatives from Other Societies

John Hubisz, *AAPT*; Marc Brodsky, *AIP*

International Advisors

Gordon Drake, *Canadian Association of Physicists*,
Dr. Gerardo C. Puente, *Mexican Physical Society*

Editor: Donna M. Baudrau, CMP

Meetings Publications Coordinator:

Vinaya K. Sathyasheelappa

APS MEETINGS DEPARTMENT

One Physics Ellipse

College Park, MD 20740-3844

Telephone: (301) 209-3286

FAX: (301) 209-0866

Donna Baudrau, *Director of Meetings and Conventions*

Terri Adorjan, *Senior Meeting Planner*

Karen MacFarland, *Meeting Planner*

Don Wise, *Registrar*

Staff Representatives

Alan Chodos, *Associate Executive Officer*; Irving Lerch, *Director of International Affairs*; Fredrick Stein, *Director of Education and Outreach*; Robert L. Park, *Director, Public Information*; Michael Lubell, *Director, Public Affairs*; Stanley Brown, *Editorial Director*; Charles Muller, *Director, Journal Operations*; Robert Kelly, *Director of Journal Information Systems*; Michael Stephens, *Controller and Assistant Treasurer*

The *Bulletin of The American Physical Society* is published 11X in 2001—March, April, May, June, July, October (3X), November (2X), and December—by The American Physical Society through the American Institute of Physics. It contains information about meetings of the Society, including abstracts of papers to be presented, as well as transactions of past meetings. Reprints of papers can be obtained only by writing directly to the authors.

The *Bulletin* is delivered, on subscription, by Periodicals mail. Complete volumes are also available on microfilm. **APS Members** may subscribe to individual issues, or for the entire year. **Nonmembers** may subscribe to the *Bulletin* at the following rates: Domestic \$500; Foreign Surface \$520; Air Freight \$545. Information on prices, as well as subscription orders, renewals, and address changes, should be addressed as follows: **For APS Members**—Membership Department, The American Physical Society, One Physics Ellipse, College Park, MD 20740-3844. **For Nonmembers**—Circulation and Fulfillment Division, The American Institute of Physics, Suite 1N01, 2 Huntington Quadrangle, Melville, NY 11747-4502. Allow at least 6 weeks advance notice. For address changes, please send both the old and new addresses, and, if possible, include a mailing label from a recent issue. Requests from subscribers for missing issues will be honored without charge only if received within 6 months of the issue's actual date of publication.

The *Bulletin of The American Physical Society* (ISSN: 0003-0503) is published eleven times a year for The American Physical Society by the American Institute of Physics. 2001 subscription rate is \$500 for domestic nonmembers. Postmaster: Send address changes to *Bulletin of The American Physical Society*, AIP, Suite 1N01, 2 Huntington Quadrangle, Melville, NY 11747-4502. Periodicals postage paid at Huntington Station, NY, and additional mailing offices.

On the Cover: Materials Research Institute, Penn State University.

BULLETIN

OF THE AMERICAN PHYSICAL SOCIETY

Vol. 46, No. 6, October 2001

54th Gaseous Electronics Conference

TABLE OF CONTENTS

General Information.....	3
Special Sessions.....	3
Arranged Oral and Poster Sessions.....	3
Presentation Formats.....	4
GEC Student Award for Excellence.....	4
Registration.....	5
Opening Reception.....	5
Conference Banquet.....	5
E-mail and Other Business Services.....	5
Audio-Visual Equipment.....	5
Dining Options.....	5
Guest Programs.....	5
Call for Nominations for GEC General and Executive Committees.....	5
GEC Executive Committee.....	6
Conference Secretary.....	6
Please Note.....	6
Epitome.....	7
Main Text.....	9

<i>Tuesday, October 9, 2001</i>	9
<i>Wednesday, October 10, 2001</i>	31
<i>Thursday, October 11, 2001</i>	53
<i>Friday, October 12, 2001</i>	63
Author Index	69
Maps	At End of Issue
Condensed Epitome	Back Cover

54th Annual Gaseous Electronics Conference

October 9–12, 2001

Penn State University

University Park, Pennsylvania

GENERAL INFORMATION

Welcome to the 54th Annual Gaseous Electronics Conference (GEC), a topical conference of the American Physical Society. The GEC01 program will include the GEC Foundation Talk and the annual GEC Student Award for Excellence. Oral sessions with both invited and contributed papers and two poster sessions will address a broad range of topics. The Nittany Lion Inn will serve as headquarters for the conference.

SPECIAL SESSIONS

The GEC01 Foundation Talk will be given by Dr. William McConkey from the University of Windsor on Wednesday, October 10, 2001, at 10:00. The title that Bill has chosen for this year's lecture is *Giving Electrons an Honourable Discharge: Measuring Their Cross Sections*.

A brown-bag lunch and open discussion on *Plasma Modeling: Needs and Opportunities* is scheduled for Tuesday, October 9, 2001, at 11:45. Among the many issues to be addressed are the status and limitations of databases for fundamental processes, the integration of equipment and feature scale models, technology transfer from model developers to users, and the roadmap for future model development and applications. Dr. Peter Ventzek from Motorola will serve as discussion leader. Participants will be able to purchase a brown-bag lunch at the meeting room.

An informal *Workshop on Positive Columns* is scheduled for Tuesday evening, October 9, 2001, at 19:15. The workshop is planned to establish the relative merits of various popular theoretical methods of treating the low-pressure positive column, and to benchmark various modeling techniques using this classic problem in Gaseous Electronics. Drs. John Ingold (Bratenahl Physics) and Jim Lawler (Univ. of Wisconsin) will serve as discussion leaders.

On Friday afternoon, October 12, 2001, GEC attendees are invited to participate in a Workshop entitled

Innovations in Gaseous Electronics Education, addressing essential course content and educational methodology for training the next generation of experts in gaseous electronics. Professor Charles Fleddermann from the University of New Mexico will serve as workshop coordinator.

Laboratory Tours: Conference participants will have an opportunity to visit selected research laboratories at The Pennsylvania State University. Among the laboratories to be included in the tour are the National Science Foundation – National Nanofabrication Users Network (NNUN) site at Penn State, and laboratories within the University's Materials Research Institute. Tour buses will be departing from the main entrance of the Nittany Lion Inn beginning at 15:00 on Thursday, October 11, 2001.

ARRANGED ORAL AND POSTER SESSIONS

- Electron Collisions with Rare Gases (*Session AT1*)
- Plasma Propulsion (*Session AT2*)
- Dusty Plasmas and Plasmas for Nanostructured Materials (*Session BT1*)
- Plasma Modeling: Needs and Opportunities (*Session BT2*)
- Plasma Modeling — Discussion (*Session CT1*)
- Poster Session I (*Session DTP*)
 - High Pressure Plasmas, Breakdown and Surface Discharges
 - Magnetically-Enhanced Plasmas: ECR, Helicon, Magnetron, Other
 - Sheaths
 - Clusters and Dusty Plasmas
 - Plasma Diagnostics I
 - Negative Ion Plasmas
 - Electron Collisions and Plasma Transport Properties
- Lighting (*Session ET1*)
- Glows: DC, Pulsed, RF, Microwave, Inductive, Other (*Session ET2*)

- Positive Column Workshop (*Session FT1*)
- Collisions with Molecules (*Session GW1*)
- Computational Methods for Plasmas (*Session GW2*)
- Foundations of Gaseous Electronics (*Session HW1*)
- GEC Business Meeting (*Session IW1*)
- Poster Session II (*Session JWP*)
 - Environmental Applications and Innovative Applications
 - Capacitive Plasmas
 - Computational Methods
 - Distribution Functions
 - Inductively Coupled Plasmas
 - Glows: DC, Pulsed, RF, Microwave, Inductive, Other
 - Plasma Interactions with Surfaces
 - Plasma Diagnostics II
 - Lighting and Displays
 - Surface Processing
- Plasmas for Nanostructured Materials (*Session KW1*)
- Electron Collisions with Metal Vapors (*Session KW2*)
- Materials Processing (*Session LR1*)
- Environmental Applications and Thermal Plasmas (*Session LR2*)
- Inductively-Coupled Plasmas and Magnetically-Enhanced Plasma (*Session MR1*)
- Fluorocarbon Plasmas (*Session MR2*)
- Plasma Diagnostics III (*Session NR1*)
- Atmospheric Pressure & Dielectric Barrier Discharges (*Session NR2*)
- Laboratory Tours: Penn State's NSF Nanofabrication Facility (*Session OR1*)
- GEC Banquet (*Session PR1*)
- Plasma Boundaries: Sheaths and Presheaths (*Session QF1*)
- Plasma Interactions with Surfaces (*Session QF2*)
- Plasma Diagnostics IV (*Session RF1*)
- Low and Ultralow Energy Electron-Molecule Interactions (*Session RF2*)
- Workshop: Innovations in Gaseous Electronics Education (*Session SF1*)

PRESENTATION FORMATS

Papers that have been accepted for presentation are listed in the technical program. Invited papers are allotted 25 minutes, with 5 additional minutes for questions and discussion. Oral contributed presentations are allotted 12 minutes, with an additional 3 minutes for discussion. Presenters at the Poster Sessions will be provided with 96" by 48" posterboards. Presenters may mount their poster materials anytime earlier in the day upon

which their presentation is scheduled. Poster materials must be removed the evening of the scheduled presentation.

GEC STUDENT AWARD FOR EXCELLENCE

In order to recognize the outstanding contributions students make to the Gaseous Electronics Conference and encourage further student participation, the GEC will continue to award a prize for the best paper presented by a student. A subcommittee of the GEC executive committee will choose the award winner. Students competing for the \$500 award this year are:

Corey Collard (University of Michigan): "Carbon nanostructure Growth in an ICP-GEC Reference Cell" (*Session KW1*)

Peter Kurunczi (Stevens Institute): "Time-Resolved Emission Spectroscopy of High-Pressure Discharge Plasmas in Ne and Ne/H₂ Gas Mixtures" (*Session NR2*)

Antonio Maresca (University of Minnesota): "'Evaporative cooling' of electrons in the afterglow of low pressure plasmas" (*Session MR1*)

Catherine Thompson (Queen's University Belfast): "Laser Thomson scattering in Ar and N₂ gas plasmas" (*Session NR1*)

Boris Le Drogoff (INRS Energy and Materials, Quebec): "Influence of the dynamic expansion of laser-produced gold plasmas on nanostructured thin films grown in various atmospheres" (*Session BT1*)

Stephane Laville (University of Montreal): "Results from the numerical modelling (for various laser pulsewidths) of laser-induced ablation and the subsequent plasma expansion" (*Session GW2*)

Dominik Hammer (University of Texas-Austin): "Sonoluminescence, a weakly ionized plasma" (*Session ET2*)

John L. Kline (West Virginia University): "Effects of Boundary Conditions on the Inherent Ion Heating in a Helicon Plasma" (*Session MR1*)

David J. Smith (University of Strathclyde): "Complementary optical diagnostics of noble gas plasmas" (*Session NR1*)

Luc Stafford (University of Montreal): "Sputter-Etching Characteristics of BST and SBT using a Surface-Wave High-Density Plasma Reactor" (*Session LR1*)

George Gozadinos (Dublin City University): "Pressure Heating of Electrons by Capacitive RF Sheaths" (*Session ET2*)

Ian McAninch (NASA-Ames Research Center): "Plasma CVD of Carbon Nanotubes" (*Session KW1*)

REGISTRATION

The registration desk will be located in the Nittany Lion Inn. Registration hours will be 18:30 to 21:00 on Monday, October 8, 2001 and 7:30 to 15:00 on Tuesday through Thursday, October 9-11, 2001. The on-site conference registration fee is \$300.00. Students and retirees pay only \$150 for registration. The registration fee includes the opening reception, refreshment breaks, and conference materials. For students and retirees, the banquet is also included in the registration fee.

OPENING RECEPTION

A reception for GEC participants and their guests will start at 19:00 on Monday, October 8, 2001, in the Nittany Lion Inn Ballroom.

CONFERENCE BANQUET

A banquet will be held on Thursday, October 11, 2001 in the Nittany Lion Inn Ballroom. Conference participants and guests are encouraged to attend the banquet. The banquet will be preceded by a reception starting at 18:30 in the Atrium of the Nittany Lion Inn.

E-MAIL AND OTHER BUSINESS SERVICES

Free e-mail access will be available to conference participants in the Mt. Nittany Room located on the ground floor of the Nittany Lion Inn. Fax, photocopy services, and office supplies will also be available from the conference hotel services.

AUDIO-VISUAL EQUIPMENT

Each conference room will be equipped with overhead projector and slide projector. If additional equipment is required, please contact the conference secretary.

DINING OPTIONS

A complete listing of dining options in the State College area is included in the registration packet provided to each conference participant.

GUEST PROGRAMS

Information on local attractions and activities can be obtained from the GEC Secretary's staff or from the Nittany Lion Inn.

CALL FOR NOMINATIONS FOR GEC GENERAL AND EXECUTIVE COMMITTEES

The GEC Executive Committee (ExComm) is the governing body of the GEC. It is the responsibility of ExComm to oversee all aspects of the conference. This includes selection of meeting sites, budgetary decisions, selection of special topics and invited speakers, accepting/rejecting abstracts and arranging of the program. The General Committee and ExComm meet during the GEC, and the ExComm meets again during the summer to plan the program of the next GEC. There are numerous communications between members of the ExComm (usually e-mail) during the year to insure the successful completion of their duties. We have been fortunate over the years to have a dedicated group of volunteers who have been willing to take on these very necessary roles.

The by-laws of the Gaseous Electronics Conference describe the process whereby members of the ExComm are elected. At the GEC Business Meeting (to be held on Wednesday, October 10, at 11:30 in the Ballroom at the Nittany Lion Inn) nominations are accepted for members of the GEC General Committee (GenComm). The GenComm consists of the ExComm and 6 at-large members elected at the Business Meeting. The eligible voting membership of the GEC (defined as those attending the Business Meeting) elect these 6 at-large members. The GenComm then meets to fulfill its only duty: to elect new members of the ExComm.

The ExComm membership consists of the Chair, Treasurer, Past-Secretary, Secretary, Secretary-elect, past or incoming Chair and 4 at-large members. The Chair is a 4-year term (1-year incoming, 2-years chair, 1-year past-chair), the secretary is a 3-year term (1-year incoming, 1-year secretary, 1-year past-secretary), and

all other ExComm members serve 2 years. (The secretary is the person who manages the local arrangements for the meeting and is usually "recruited" and appointed to the ExComm.)

The ExComm welcomes nominations, including self-nominations, for both the GenComm and ExComm. Becoming a GenComm and/or ExComm member provides a unique opportunity to see both how the GEC is run and to influence its future direction by helping to define the programs and choose future sites. Please submit your nominations to the GEC Chair or any member of the ExComm. The ExComm also welcomes inquiries on hosting future GECs.

GEC EXECUTIVE COMMITTEE

Tim Sommerer, Chair

GE Corporate Research

Gerry Hays, Past-Chair

Sandia National Labs

Robert McGrath, Secretary

Pennsylvania State University

Demetre Economou

Past-Secretary

University of Houston

Uwe Kortshagen

Secretary-Elect

University of Minnesota

Winifred Huo, Treasurer

NASA Ames

Klaus Bartschat

Drake University

Ara Chutjian

Jet Propulsion Laboratory

Steven Buckman

Australian National University

Bill Graham

The Queen's University

Peter Ventzek

Motorola, Inc.

Yukio Watanabe

Kyushu University

CONFERENCE SECRETARY

Dr. Robert McGrath

Penn State University

304 Old Main

University Park, PA 16802

Voice: (814) 863-9580

FAX: (814) 863-9659

Email: mcgrath@psu.edu

PLEASE NOTE

The APS has made every effort to provide accurate and complete information in this *Bulletin*. Changes and corrections, however, may occasionally be necessary and may be made without notice after the date of publication. To ensure that you receive the most up-to-date information, please check the meeting *Corrigenda* contributed with this *Bulletin*.

Epitome of the Gaseous Electronics Conference 2001 of the American Physical Society

**8:00 TUESDAY MORNING
9 OCTOBER 2001**

- AT1 **Electron Colisions with Rare Gases**
Williams, Madison
Ballroom C, Nittany Lion Inn
- AT2 **Plasma Propulsion**
Spanjers
Ballroom AB, Nittany Lion Inn

**10:00 TUESDAY MORNING
9 OCTOBER 2001**

- BT1 **Dusty Plasmas and Plasmas for Nanostructured Materials**
Ballroom AB, Nittany Lion Inn
- BT2 **Plasma Modeling: Needs and Opportunities**
Ballroom C, Nittany Lion Inn

**11:45 TUESDAY MORNING
9 OCTOBER 2001**

- CT1 **Plasma Modeling Discussion**
Ballroom C, Nittany Lion Inn

**13:15 TUESDAY AFTERNOON
9 OCTOBER 2001**

- DTP **Poster Session I**
Board Room, Nittany Lion Inn

**15:30 TUESDAY AFTERNOON
9 OCTOBER 2001**

- ET1 **Lighting**
Ballroom C, Nittany Lion Inn
- ET2 **Glows: DC Pulsed RF, Microwave, Inductive, Other**
Ballroom AB, Nittany Lion Inn

**19:15 TUESDAY EVENING
9 OCTOBER 2001**

- FT1 **Positive Column Workshop**
Assembly Room, Nittany Lion Inn

**8:00 WEDNESDAY MORNING
10 OCTOBER 2001**

- GW1 **Collisions with Molecules**
Surko, Becker
Ballroom C, Nittany Lion Inn
- GW2 **Computational Methods for Plasmas**
Ballroom AB, Nittany Lion Inn

**10:00 WEDNESDAY MORNING
10 OCTOBER 2001**

- HW1 **Foundations of Gaseous Electronics**
McConkey
Ballroom C, Nittany Lion Inn

**11:15 WEDNESDAY MORNING
10 OCTOBER 2001**

- IW1 **GEC Business Meeting**
Ballroom C, Nittany Lion Inn

**13:15 WEDNESDAY AFTERNOON
10 OCTOBER 2001**

- JWP **Poster Session II**
Board Room, Nittany Lion Inn

**15:30 WEDNESDAY AFTERNOON
10 OCTOBER 2001**

- KW1 **Plasmas for Nanostructured Materials**
Hori, i Cabarrocas
Ballroom C, Nittany Lion Inn

KW2 **Electron Collisions with Metal Vapors**
Hanne, Fursa, Bogaerts
 Ballroom AB, Nittany Lion Inn

15:00 THURSDAY AFTERNOON
 11 OCTOBER 2001

OR1 **Laboratory Tours: Penn State's NSF National Nanofabrication Users Network (NNUN) and Other Selected Materials Research Institute Facilities**
 Nanfab Facility, Materials Research Institute

8:00 THURSDAY MORNING
 11 OCTOBER 2001

LR1 **Materials Processing**
 Ballroom C, Nittany Lion Inn

18:30 THURSDAY EVENING
 11 OCTOBER 2001

LR2 **Environmental Applications and Thermal Plasmas**
 Ballroom AB, Nittany Lion Inn

PR1 **GEC Reception and Banquet**
 Ballroom C, Nittany Lion Inn

8:15 FRIDAY MORNING
 12 OCTOBER 2001

10:00 THURSDAY MORNING
 11 OCTOBER 2001

MR1 **Inductively-Coupled Plasmas and Magnetically-Enhanced Plasmas**
 Ballroom C, Nittany Lion Inn

QF1 **Plasma Boundaries: Sheaths and Poesheaths**
 Ballroom C, Nittany Lion Inn

MR2 **Fluorocarbon Plasmas**
Steffens, Booth, Tatsumi
 Ballroom AB, Nittany Lion Inn

QF2 **Plasma Interactions with Surfaces**
Winograd, d'Agostino
 Ballroom AB, Nittany Lion Inn

10:00 FRIDAY MORNING
 12 OCTOBER 2001

13:15 THURSDAY AFTERNOON
 11 OCTOBER 2001

NR1 **Plasma Diagnostics III**
 Ballroom C, Nittany Lion Inn

RF1 **Plasma Diagnostic V**
 Ballroom C, Nittany Lion Inn

NR2 **Atmospheric Pressure & Dielectric Barrier Discharges**
Massines
 Ballroom AB, Nittany Lion Inn

RF2 **Low and Ultralow Energy Electron-Molecule Interactions**
Gopalan, Bass
 Ballroom A, B, Nittany Lion Inn

13:30 FRIDAY AFTERNOON
 12 OCTOBER 2001

SF1 **Workshop: Innovations in Gaseous Electronics Education**
 Ballroom C, Nittany Lion Inn

MAIN TEXT

SESSION AT1: ELECTRON COLISIONS WITH RARE GASES

Tuesday morning, 9 October 2001; Ballroom C Nittany Lion Inn at 8:00; Klaus Bartschat, Drake University, presiding

Invited Papers

8:00

AT1 1 Spin and orbital angular momenta effects in electron collisions with rare gas atoms.JIM WILLIAMS, *The University of Western Australia, Perth. WA 6009. Australia*

The periodic table of the elements reflects the relative strengths of the Coulomb and spin-orbit interactions, as well as other spin-effects and the consequences of the Pauli principle. Observations of the scattered electrons or radiated photons or residual ions in traditional scattering experiments explored angular and polarization phenomena which generally reflect integrated effects of the Coulomb interactions. Subsequent coincidence detection of the angular and polarization correlations of the outgoing particles have given descriptions of the size, shape and rotation (i.e. alignment and orientation) of the angular momentum of the charge cloud of excited (ionized) states. Now spin-polarised electron scattering allows the angular momentum properties of incident transversely polarised electrons, radiated photons and scattering symmetries to be combined to reveal the weaker effects of exchange and spin-orbit coupling relative to the Coulomb effects. Observations will be reported for excitation of the $4d[7/2]$ and $5s, 6s[3/2]$ ($J=2$) states of neon and the $np(n+1)p[3/2, 5/2]$ $J = 1, 2, 3$ states with $n = 3, 5$ and 6 for Ne, Kr and Xe respectively. States with a dominant triplet component reflect exchange and the spin-orbit interaction effects, while states with a dominant singlet component indicate mainly spin-orbit interaction effects. The ionization-with-excitation collision process will be discussed for the ionic doublet D ($J=3/2$) state of zinc and the $5p$ quartet P ($J=3/2, 5/2, 7/2$) states of krypton.

8:30

AT1 2 Electron Impact Excitation of Inert Gases.DON MADISON, *University of Missouri-Rolla*

The last decade has witnessed enormous advances in technology which has permitted both experimentalists and theoreticians to perform measurements and calculations that were previously thought to be impossible. As a result of these advances, theory and experiment are now in reasonable accord for hydrogen and helium. In fact, theoretical calculations have been so successful for excitation of these atoms that, if there is a disagreement between experiment and theory, the experiment would be questioned. However, the situation is much different for the inert gases where disagreement between experiment and theory, often by orders of magnitude, is common. An overview of the current status of theoretical calculations for electron excitation of the inert gases will be given in this talk.

Contributed Papers

9:00

AT1 3 Measurement of the electron-impact excitation cross sections out of the metastable levels of krypton*

JOHN B. BOFFARD, TOM STONE, L. W. ANDERSON, CHUN C. LIN, *University of Wisconsin - Madison* We have measured cross sections for electron-impact excitation out of the metastable levels of krypton into seven of the ten levels of the $4p^5 5p$ configuration ($2p_n$ in Paschen's notation). Two sources of metastable krypton atoms are used. A hollow cathode discharge is used for measurements with an electron beam energy below the threshold for ground state excitation (< 11 eV). For measurements at high energies (11 to 500 eV), the metastable atoms are formed via near-resonant charge exchange between a 2 keV krypton ion beam and a cesium vapor. Both sources produce targets with a mixture of atoms in the 3P_0 ($1s_3$) and 3P_2 ($1s_5$) metastable levels. A laser is used with the hollow cathode experiment to quench one of the metastable levels,

allowing us to determine the individual cross sections out of each metastable level. Results will be compared to our previous work on excitation out of the ground state of krypton¹ and the metastable levels of other heavy rare gas atoms².

*This work supported by the National Science Foundation.

¹J. E. Chilton, *et al.*, *Phys. Rev. A*, **62**, (2000) 032714.²J. B. Boffard, *et al.*, *Phys. Rev. A*, **59**, (1999) 2749.

9:15

AT1 4 Electron Collisions with Trapped Metastable Helium

Atoms L.J. UHLMANN, *Affiliation* M. COLLA, *Affiliation* R.J. GULLEY, *Affiliation* M. HOOGERLAND, *Affiliation* K.G. BALDWIN, *Affiliation* S.J. BUCKMAN, *Australian National University, Canberra* Magneto-optical traps have been successfully used in the recent past to provide a localised source of ground state atoms for electron collision cross section measurements (eg. Rb^1). We have utilised a laser-cooled and trapped source of metastable helium atoms to measure the total electron scattering cross section from excited He (2^3S) at incident electron

energies in the intermediate energy range (> 30 eV). The magneto-optical trap used for these studies is loaded from a laser-controlled, "bright" beam of He (2^3S), and contains metastable atoms at a density of 10^9 cm $^{-3}$. The atoms are trapped and, after extinguishing the magnetic and optical trapping fields, a short pulse of electrons is directed at the trapped atoms. Electrons which collide with atoms in the trap transfer sufficient momentum to the atoms to ensure that they are ejected from the trap on a time scale which is short compared to that for the natural trap loss due to

ballistic expansion. By measuring the trap loss rate, with and without the electron beam present, the loss rate due to electron collisions can be deduced. This, combined with a measurement of the absolute electron current density, can then be used to derive the total collision cross section. Measurements at a number of incident electron energies will be presented and compared with recent theoretical calculations, including one using the convergent-close-coupling approach. ¹ Schappe et al. *Europhys. Lett.* 29, 439 (1995); *Phys. Rev. Lett.* 76 4328 (1996).

SESSION AT2: PLASMA PROPULSION

Tuesday morning, 9 October 2001; Ballroom AB Nittany Lion Inn at 8:00; Michael Micci, The Pennsylvania State University, presiding

Invited Papers

8:00

AT2 1 Plasma diagnostic development and future needs for electric propulsion applications.

GREG SPANJERS, *Air Force Research Laboratory*

An overview of the current electric propulsion research and development efforts within the United States Air Force is presented. The AFRL Propulsion Directorate conducts electric propulsion efforts in basic research, engineering development, and space flight experiments. A major component of this work is the development and implementation of advanced plasma diagnostic techniques, both in the laboratory and in space. Specific challenges in the laboratory include the capability to perform measurements on very small-scale length plasmas formed in microthrusters, and the ability to perform non-intrusive measurements in highly energetic plasmas where plasma perturbations are an issue. Diagnostics such as 2-color Herriott cell interferometry and fast-reciprocating probes and have been shown useful in addressing these challenges. Specific challenges in space applications include miniaturization of laboratory techniques for use on micro-satellites, and interpretation of remote measurements. The diagnostic package in development for the AFRL TechSat21 spacecraft will be presented as an example. A discussion will also be presented of current plasma diagnostic needs within the electric propulsion research community.

Contributed Papers

8:30

AT2 2 Lifetime Modeling of Xenon Hollow Cathodes Used in Electric Propulsion SCOTT KOVALESKI, *QSS Group, Inc., NASA Glenn Research Center Group* Xenon hollow cathodes with barium calcium aluminate impregnated tungsten inserts are widely used in electric propulsion. These high current, low power cathodes are employed in ion thrusters, Hall thrusters, and on the International Space Station in plasma contactors. The entitlement lifetime of a thermionic emission cathode impregnated with barium-containing compounds is determined by the evolution and transport of barium away from the emitter surface. A model is being developed to study the process of barium transport and loss from the emitter insert in hollow cathodes. A thermodynamic model of the chemical process of barium evolution has been adapted from that of Lipeles and Kan¹. The model accounts for the diffusion of barium and barium oxide gas through the xenon expellant and loss of barium-containing gases through the cathode orifice as well as loss by condensation. Axial barium density profiles are presented and cathode lifetimes are estimated. Results of the model are compared with experimental results from the extensive hollow cathode life test database at the NASA Glenn Research Center. 1. Lipeles, R.A., Kan, H.K.A., *Appl. Surf. Sci.* 16, 189(1983).

8:45

AT2 3 Ferroelectric Emission Cathodes for Space Applications

SCOTT KOVALESKI, *QSS Group, Inc., NASA Glenn Research Center Group* Low-power electric thrusters, spacecraft plasma contactors, and electrodynamic tether systems need electron emitters that require very low gas flow rates or no gas flow to perform their functions. In addition, expellantless neutralizers can improve the viability of very low-power colloid thrusters, Field Emission Electric Propulsion (FEEP) devices, ion engines, Hall thrusters, and gridded vacuum arc thrusters. Ferroelectric emission (FEE) cathodes are currently being studied at the NASA Glenn Research Center as zero expellant flow rate cathodes sources. The cathodes rely on the strong ferroelectric effect, induced by rapidly pulsing several kV across a ferroelectric ceramic, to emit electrons. Peak current densities as high as 100's of A/cm² have been reported in the literature. An initial parametric study of FEE cathodes has been initiated. The effects of ferroelectric dielectric constant, grid geometry, and pulse geometry are being examined. The current-voltage relationship for the cathode is also being characterized. Additionally, cathode surface modification due to operation will be studied.

9:00

AT2 4 PLASMA COAXIAL DISCHARGE EFFICIENCY

E. A. MEHANNA, A coaxial discharge system with negative central electrode has been used to study the plasma current sheath and the ejected plasma parameters. Results showed that the plasma sheath velocity reached 5×10^5 cm/s at the muzzle. The ejected plasma

velocity in the expansion chamber varied with position z according to the relation $V = k \cdot z^{-0.5}$, while the temperature and the density changed as: $T = T_0 \cdot z^{-1.8}$ and $N = N_0 \cdot z^{-1.2}$ respectively. It has been detected that the plasma current sheath and the ejected plasma are accompanied with an induced axial magnetic field, which indicated that the plasma rotates within its propagation. The input energy from the capacitor bank to the coaxial discharge system was 196 J, (Joule), the energy gained by the plasma as kinetic energy was 17 J, while the plasma internal energy was 5.6 J. Hence 8% of the energy was gained as kinetic drift of the plasma.

9:15

AT2 5 Flow Measurements in a Helicon Plasma Source Operated as a Plasma Thruster XUAN SUN, ROBERT BOIVIN, JOHN KLINE, EARL SCIME, ROBERT SPANGLER, MICHAEL WOEHRMAN, *Department of Physics, West Virginia University* Because of their high densities and efficient operation, helicon sources can potentially be employed as plasma thrusters for deep space missions. We report measurements of argon ion flow velocities parallel to the magnetic field in the exhaust and source regions of a helicon plasma source configured as a plasma thruster. Non-invasive, laser induced fluorescence measurements were used to directly determine the bulk flow velocity for argon ions. An absorption line in an iodine cell is monitored as absolute zero velocity reference during the measurements. Flow measurements as a function of source RF power, the ratio of source to exhaust region magnetic field strength, source neutral pressure, RF frequency, and distance from the center of the plasma will be presented.

SESSION BT1: DUSTY PLASMAS AND PLASMAS FOR NANOSTRUCTURED MATERIALS

Tuesday morning, 9 October 2001

Ballroom AB Nittany Lion Inn at 10:00

Themis Matsoukas, The Pennsylvania State University, presiding

10:00

BT1 1 Waves in a 2D Dusty Plasma Crystal* J. GOREE, *Dept. of Physics and Astronomy, Univ. of Iowa* S. NUNOMURA, V. NOSENKO, A dusty plasma is an ionized gas that also contains micron-size particles of solid matter, which gain a large electric charge of typically $-10,000 e$. In experiments, we shake polymer microspheres into a low-temperature argon rf discharge, and image the microspheres directly, using video microscopy. This allows us to image where all the particles are, and follow them as they move around. Due to their mutual repulsion, the particles arrange in a lattice, analogous to a crystal in an ordinary atomic solid. Here we report experiments with a monolayer crystalline lattice that is disturbed so that phonons, or sound waves, propagate through the lattice. There are two kinds of phonons, corresponding to compressional and shear motion. Experiments have been performed to observe these two waves and to measure their dispersion relations. To excite the waves, we stimulate the lattice using the radiation pressure of an argon laser.

*Work supported by U.S. Dept. of Energy and NASA.

10:15

BT1 2 Compressional and Shear Wakes in a 2D Dusty Plasma Crystal* V. NOSENKO, J. GOREE, Z.W. MA, *Dept. of Physics and Astronomy, Univ. of Iowa* D.H.E. DUBIN, *Dept. of Physics, UCSD* A 2D crystalline lattice can vibrate with two kinds of sound waves, compressional and shear (transverse), where the latter has a much slower sound speed. When these waves are excited by a moving supersonic disturbance, the superposition of the waves creates a Mach cone, i.e., a V-shaped wake. In our experiments, the supersonic disturbance was a moving spot of argon laser light, and this laser light applied a force, due to radiation pressure, on the particles. The beam was swept across the lattice in a controlled and repeatable manner. The particles were levitated in an argon rf discharge. By moving the laser spot faster than the shear sound speed c_t , but slower than the compressional sound speed c_l , we excited a shear wave Mach cone. Alternatively, by moving the laser spot faster than c_l , we excited both cones. In addition to Mach cones, we also observed a wake structure that arises from the compressional waves dispersion. We compare our results to Dubins theory (*Phys. Plasmas* 2000) and to molecular dynamics (MD) simulations.

**Work supported by U.S. Dept. of Energy and NASA.

10:30

BT1 3 Formation of Coulomb Crystals Having Multiple Lattices and Translational Motion in Dusty Plasmas* VIVEK VYAS, MARK J. KUSHNER, *University of Illinois* Particles in low temperature, partially ionized plasmas exhibit collective behavior and form Coulomb solids at moderate gas pressures, small particle sizes and lower powers in capacitively coupled, radio frequency discharges. Lattices having different radial structure functions $[g(r)]$, non-ideality factors and geometrical shapes can be formed given somewhat subtle changes in discharge properties. In particular, solid body translational motion, such as rotation of the crystals, has been observed. To address these phenomena, a dust transport simulation has been developed and used to investigate formation and translational motion of lattices. The forces included in the model are electrostatic, ion-drag, thermophoretic, fluid-drag by neutrals, gravity and particle-particle Coulomb interactions. Studies have been performed for Coulomb crystals in capacitively coupled, radio frequency discharges, sustained in 100s mTorr of Ar. We found that distinct, multiple lattices are abruptly formed when varying particles size, gas pressure and power. We will also report on the effect of the number of particles on the propensity for crystal formation, interparticle spacing and $g(r)$.

*Work supported by Sandia National Lab and NSF (CTS99-74962)

10:45

BT1 4 Determination of Plasma Dust Particle Interactions Confined within a Layer M. E. RILEY, *Sandia National Labs (SNL)* G. A. HEBNER, *SNL* D. JOHNSON, *Univ. of Illinois* P. HO, *SNL* R. J. BUSS, *SNL* The lateral interaction of dust particles suspended in an Ar plasma pre-sheath region was quantitatively determined from the lateral compression of two-dimensional (2D) plasma dust crystals confined in a potential well above a mildly parabolic lower electrode. The shape of the parabolic potential well was confirmed by observing trajectories of individual par-

ticles falling within the well. We used a simple equation of state for the 2D dust layer to relate the applied force to the density and particle separation. Nearest-neighbor particle spacing depended on the radial position and number of particles within the crystal. Comparison between measured and calculated particle separations was used to derive values for the particle screening length and the charge on the particles. No evidence of a lateral particle-particle binding was observed. The parabolic curved electrode allowed us to eliminate all the unknown forces due to ion wind, thermophoresis, and sheath potential from the analysis. The lateral interaction of the particles remained Debye-like down to approximately 1 mV.

11:00

BT1 5 Effect of Trapped Ions on Shielding and Floating Potential of a Dust Grain in a Plasma* MARTIN LAMPE, GURUDAS GANGULI, GLENN JOYCE, *Naval Research Laboratory, Washington, DC* VALERIY GAVRISHCHAKA, SAIC, *McLean, VA* The problem of electrostatic shielding around a small spherical collector immersed in plasma, and the related problem of electron and ion flow to the collector, date to the origins of plasma physics. Beginning with Mott-Smith and Langmuir (1926), calculations have typically neglected collisions, on the grounds that the mean free path is long compared to shielding length scales, i.e. the Debye length. However, investigators beginning with Bernstein and Rabinowitz (1959) have known that negative-energy trapped ions, created by occasional collisions, might be important. We present an analytic calculation of the density of trapped and untrapped ions, self-consistent with the potential. Under typical conditions for dust grains immersed in a discharge plasma, trapped ions dominate the shielding cloud in steady state, even in the limit of very long mean free path. As a result the shielded potential is different from the results of orbital motion limited theory. Collisions also greatly increase the ion current to the collector, thereby decreasing the floating potential and the grain charge by a factor as large as two to three.

*Supported by ONR and NASA

11:15

BT1 6 Materials Deposition on Trapped Particles in a Dusty PECVD JIN CAO, THEMIS MATSOUKAS, *Department of Chemical Engineering, The Pennsylvania State University, University Park, PA 16802* Controlled nanoscale deposition of metal and dielectrics is achieved on micron- and nanometer-sized particulate substrates fluidized in a custom-built PECVD system as a "dusty plasma." The major advantage of this technique is that it provides a convenient approach of the anisotropic surface coating of small particles for any desired reaction time. A low pressure capacitively-coupled rf discharge is utilized in this study. Dielectric films are grown on trapped particulates of various shapes including silica microspheres and metal nanowires from the plasma polymerization reactions of hydrocarbon/O₂/Ar. Copper metallization on the trapped particles is achieved by sputtering from the copper electrodes in an Ar plasma. Switching between the conditions of metal and dielectrics deposition during the process yields alternating conducting and insulating layers on the substrates. Copper doping of the dielectric film is realized by adding monomer in the feed gas during metallization. The chemical composi-

tion of the surface coating is studied using XPS. The dielectrics deposition rate is obtained from the film thickness at various reaction times as determined using TEM. A detailed study of the dielectrics deposition rate as a function of power, pressure, and feed gas flow rates is presented.

11:30

BT1 7 Influence of the dynamic expansion of laser-produced gold plasmas on nanostructured thin films grown in various atmospheres B. LE DROGOFF, E. IRISSOU, M. CHAKER, D. GUAY, *INRS - Energie et Materiaux - Qc, Canada* M. TRUDEAU, *IREQ - Qc, Canada*. Pulsed laser deposition (PLD) has been recently shown to be an excellent technique to produce nanoparticles and nanocrystalline thin films. However, little is yet known about the relationship between the film structure and the PLD plasma parameters. In this context, we have investigated the characteristics of gold thin films deposited by ablating a gold target with a KrF laser. The crystalline structure and the morphology of these thin films are found to depend on the nature of the ambient gas (Ar, He, N₂ and O₂), on its pressure (ranging from 10⁻⁴ to 10 torr) and on the target-to-substrate distance (from 2.5 to 10 cm). Our measurements show that, for a given gas nature and pressure (typically higher than 10 mtorr), there exists a substrate-to-target distance threshold, below which the gold films present a (111) monocrystalline structure. In contrast, above this threshold distance, the films exhibit a powder-like structure composed of crystallites with sizes as small as 5 nm. For the first time, this structure modification was actually found to be correlated to the decrease of velocity of the gold particles impinging the substrate, as determined using time-of-flight (TOF) emission spectroscopy.

11:45

BT1 8 Angular Motion of Dust Particles and Evolution of Dust Void in Plasmas R.P. DAHIYA,*G. PAEVA, W.W. STOFFELS, E. STOFFELS, G.M.W. KROESEN, *Department of Physics, Eindhoven University of Technology, PO Box 513, 5600 MB Eindhoven, Netherlands* The organised structures in strongly coupled dusty plasma are formed due to the balance of various forces on the dust particles. Motion of the particles can be different while they are in a cloud or only one or two particles are present in the plasma. In this paper, the observed angular motion of one and/or two particles and central void formation in the particle cloud suspended in rf sheath is investigated. Asymmetrical particles, few in number, execute spinning and orbiting motion. The ion wind flowing towards the sheath of the powered electrode is largely responsible for the angular motion of the particles. When a circularly symmetric cloud of particles is trapped in the electrostatic field of a ring electrode, a central void is observed to evolve in the cloud at elevated pressures and also with the increase in rf power. The void diameter grows at faster pace than the outer diameter of the cloud with pressure as well as rf power, leading to the reduction of the inter-particle distance. The void appears as a consequence of the radial ion drag force exceeding the confining electrostatic force. Addition of negative ions, by mixing oxygen with argon, closes the void due to the reduction in positive ion radial drag on the cloud.

*On leave from: Indian Institute of Technology, New Delhi-110016, India.

SESSION BT2: PLASMA MODELING: NEEDS AND OPPORTUNITIES

Tuesday morning, 9 October 2001
 Ballroom C Nittany Lion Inn at 10:00
 Peter Ventzek, Motorola, presiding

10:00

BT2 1 Vertically integrated computer aided design for device plasma processing T. MAKABE, K. MAESHIGE, *Keio University at Yokohama, Japan* We have proposed a computer aided design concept concerning vertically integrated CAD for device processing, VicAddress[1] as a long-range objective of the design of a low temperature plasma processing used for a multi-layer semiconductor manufacturing, by considering plasma/interface/surface/device-structure. That is, these are a series of modelings of a plasma structure, profile evolution, charging in a patterned wafer, and device damage during etching/deposition by using modules for each of objectives. A highly abstracted and idealized top-down design concept is employed as a ULSI design tool in the industry, in order to shorten the period of the development and to achieve high efficiency. Therefore, a lack of information about physical images will be essential in the topdown design. VicAddress will be expected to serve as a design tool complementary to the topdown design procedure. We will demonstrate one of the examples, plasma device damage due to local charging during etching to the gate oxide by using simple 2D modeling of VicAddress.[2mm] [1]T.Makabe, J.Matsui, and K. Maeshige, *Sci. Technol. of Adv. Materials* (in press), *Proc. of 22 Int. Symp. on RGD (AIP; in press)*.

10:15

BT2 2 Development of Self-Consistent Electron Collision Cross Sections and Validation of Plasma Chemistry Models W. L. MORGAN, G. I. FONT, *Kinema Research, L.L.C.** We will discuss the use of ab initio calculations of electron collision cross sections, ionization cross section measurements, and swarm analyses to construct self-consistent cross section sets for plasma modeling. We emphasize the use of such techniques to obtain dissociation cross sections of molecular gases. Examples include c-C4F8, CHF3, and C2F4. We will show plasma chemistry validation calculations where use of a self-consistent collision cross section set considerably improves the quantitative modeling results.

*Our collaborators in this work are C. Winstead and V. McKoy. Part of the research has been supported by SEMATECH.

10:30

BT2 3 On improving the continuum models for simulation of low temperature plasma discharges DEEPAK BOSE, *Eloret Corp.* DAVID HASH, T.R. GOVINDAN, M. MEYYAPPAN, *NASA Ames Research Center* We will discuss the state-of-the-art capabilities of the available continuum models for low temperature, high density plasma discharges. We will not focus on the uncertainties caused by the lack of a reliable chemistry and collision database. Instead, we will suggest possible improvements in coupling gas and plasma dynamics, self-consistent neutral transport, and gas heating models. The percentage uncertainties in electron density, temperature, ion flux, and ion impact energy predictions due to a lack of self-consistency will be estimated. We will also emphasize that certain numerical criteria, based on time and grid convergence and level of accuracy of the numerical scheme,

must be satisfied before a simulation is deemed acceptable. We will estimate the errors caused when some of these numerical standards are not met. Finally, we will show how an implicit algorithm can be efficiently used to fully couple the bulk plasma and the non-collisional sheath using the same computational mesh and the same set of governing equations.

10:45

BT2 4 A Comparison of Three Methods for Feature Profile Evolution H. H. HWANG, *NASA Ames Research Center* S. RAUF, P. J. STOUT, *Motorola Inc.* Three methods for feature scale modeling (level-set, monte-carlo, and string based) have been used to calculate the profile evolution during silicon etching of trenches with an Ar/Cl₂ plasma. The three methods have different numerical approaches in how they track a moving surface or front, but implement similar ion-enhanced etch mechanisms. The energy and angle resolved flux distributions in the feature scale simulations have been obtained from a 2-dimensional model of an Ar/Cl₂ inductively coupled plasma. Effects of the ion energy distribution (through wafer bias and frequency), the neutral to ion ratio (through Ar/Cl₂ flow rate), and photoresist aspect ratio on etch rate and etch profile will be presented. The impact of both numerical and physical differences in implementation in the simulations will be investigated. Other issues, including the general advantages and weaknesses of each methodology, will be discussed.

11:00

BT2 5 Plasma Molding over Surface Topography: IED and IAD over Steps* DEMETRE ECONOMOU, *University of Houston* DOOSIK KIM, *University of Houston* Plasma molding over surface topography finds applications in MEMS microfabrication, plasma extraction through grids, and plasma contact with internal reactor parts (e.g., wafer chuck edge). The flux, energy and angular distributions of ions incident on the target are of primary importance in these applications. These quantities depend critically on the shape of the meniscus (plasma-sheath boundary) formed over the surface topography. We have developed a 2-D simulation tool to calculate the flux, energy and angular distribution of ions (and fast neutrals) impinging on surface topography in contact with a high density plasma. Plasma molding over a step has been analyzed in detail. Simulation results will be compared to experimental data as a function of distance from the step obtained at Sandia National Labs.

*Work supported by Sandia National Labs and NSF

11:15

BT2 6 A Modeling Comparison of Ionized Physical Vapor Deposition and High Power Magnetron Deposition of Cu PHILLIP STOUT, DA ZHANG, SHAHID RAUF, PETER L. G. VENTZEK, *motorola* An integrated reactor to feature model has been applied to an ionized physical vapor deposition (IPVD) and a high power magnetron (HPM) reactor for Cu deposition. The reactor model used is HPEM which is being developed at the University of Illinois. The feature model used is being developed at Motorola. The feature model is coupled to the reactor model through "atomic sources." The atomic sources are the identity, flux rate, angular distribution, and energy distribution of specie incident on the feature surface. The 3D Monte Carlo based feature model includes physical effects of transport to surface, specular and diffusive reflection from surface, adsorption, surface diffusion, deposition, sputtering, etching, and crystal structure. The effect of IPVD and HPM reactor flow rate, pressure, target power,

coil power, and wafer bias on the flux, angular, and energy distribution of ions, neutrals, and athermals to the wafer surface will be discussed. The resulting feature Cu coverage using the IPVD and the HPM reactors will be discussed. The Cu coverage on trench and 3d via features with varying aspect ratios and side slopes will be discussed.

11:30

BT2 7 Multi-Dimensional Simulations of Fluorocarbon Plasmas with Ion Energy Resolved Surface Reaction Rates* NING ZHOU, VLADIMIR KOLOBOV, *CFD Research Corp* VLADIMIR KUDRIAVTSEV, *CFD Canada* The commercial CFD-ACE+ software has been extended to account for ion energy dependent surface reactions. The ion energy distribution function and the mean ion energy at a biased wafer were obtained using the Riley sheath model extended by the NASA group (Bose et al., *J. Appl. Phys.* v.87, 7176(2000)). The plasma chemistry model (by P. Ho et al., SAND2001-1292) consisting of 132-step gas-phase reactions and 55-step ion energy dependent surface reactions, was implemented to simulate the C2F6 plasma etching of silicon dioxide in an Inductively Coupled Plasma. Validation studies have been performed against the experimental data by Anderson et al. of UNM for a lab-scale GEC reactor. For a wide range of operating conditions (pressure: 5-25 mTorr; plasma power: 205-495 Watts; bias power: 22-148 Watts), the average etch rate calculated by CFD-ACE+ 2-D simulations agrees very well with those by 0-D AURORA predictions and the experimental data. The CFD-ACE+ simulations allow one to study the radial uniformity of the etch rate depending on discharge conditions.

*Work supported by NSF SBIR Phase-I Project DMI-0060283

SESSION DTP: POSTER SESSION I
Tuesday afternoon, 9 October 2001
Board Room Nittany Lion Inn at 13:15

DTP 1 HIGH PRESSURE PLASMAS, BREAKDOWN
AND SURFACE DISCHARGES

DTP 2 Characterization of a microwave helium-nitrogen plasma at atmospheric pressure using a Laser-Induced-Fluorescence technique K.M. BENHACENE, J. MARGOT, *Groupe de Physique des Plasmas, Université de Montréal, Montréal, Qc* J. HUBERT, *Chemistry department, ibidem* Microwave helium discharges at atmospheric pressure are commonly used as an atomization and excitation source for trace detection of non-metal analytes such as C, Br, C, etc. It has been previously observed that the addition of a small amount of nitrogen to helium could have significant effects with respect to the analyte detection limit. In some cases, nitrogen concentrations below 1% can significantly improve the detection. In order to understand these effects, we have undertaken an investigation of the influence of the

nitrogen concentration on the plasma characteristics, in particular on the concentration of metastable helium atoms and nitrogen molecules using a Laser-Induced-Fluorescence (LIF) technique, and on electron density. The results show a fair agreement with a collisional-radiative model (CRM) recently developed (1). (1) Petrov et al. *Plasma Chemistry and Plasma Processing*, vol.19, no.4 p. 467-86

DTP 3 A Simple Narrow Band Lyman-alpha (121.56 nm) Lamp* T. MCCARTHY, D.E. MURNICK, M. SALVERMOSER, *Dept. of Physics, Rutgers University, Newark NJ 07102* Lyman- α radiation can be produced efficiently via near resonant energy transfer from Ne₂⁺ excimer molecules to dissociation of H₂ to H (n=1) and H (n=2).¹ This method of Lyman- α light production has now been utilized in simple electrical discharges at pressures of about 1 atmosphere. Small bench-top light sources have been built, without external cooling, using both RF and DC discharges in Ne with 100 ppm admixtures of H₂. The UV power output is approximately 10 mW and the spectra show no significant features other than the Lyman- α line in the UV. The line center was completely self-absorbed for certain electrode and chamber geometries. Using a special geometry, the self-absorption effect was significantly reduced. For this reason our light source shows great promise as an atomic hydrogen probe. Possible applications include: trace hydrogen concentration measurements, either via absorption or opto-galvanic methods; hydrogen dissociation and/or recombination rate studies in various buffer gases; and deuterium isotopic concentration measurements. 1. J. Wieser, et al, *Journal of Physics B*, 31, 4589-97 (1998)

*Supported in part by the IAEA

DTP 4 Spectroscopic and Electrical Analysis of Capacitively Coupled VHF plasma at Atmospheric Pressure for Plasma CVM process SHOICHI KAWASHIMA, YASUSHI OSHIKANE, KENICHI TAKEMOTO, KAZUYA YAMAMURA, KATSUYOSHI ENDO, YUZO MORI, *Graduate School of Engineering, Osaka University* Plasma CVM (Chemical Vaporization Machining) process using atmospheric VHF plasma is developed and have been studied in recent years. It is required to optimize the characterization of such plasma. In this poster, we report the experimental results of spectroscopic and electrical analysis of VHF discharges in mixed gas (He/CF₄/O₂) used in CVM process. The total gas pressure is one atmosphere, and the gas concentration are He (95.99%), discharge frequency and the electric power are 150 MHz and 20 - 100 W, respectively. Electrodes are made of alumina, and the diameters are both 6 mm. The plasma gap is about 1 mm. The spatial distribution of CF and CF₂ radicals between the gap are measured by planer laser-induced fluorescence (PLIF) spectroscopy. The excitation wavelength of CF and CF₂ are 232.7 and 261.7 nm, respectively. The dependencies of the LIF intensity, emission spectra, and their 2D profiles on the concentration of CF₄ and O₂ are studied. Addition of O₂ causes the rapid decrease of LIF intensity from the radicals. This work is supported by a Grant-in-Aid for COE Research (No.08CE2004) from the Ministry of Education, Science, Sports and Culture.

DTP 5 An ultra-long spark channel thermalisation mechanism YURI V. SHCHERBAKOV, *All-Russian Electrotechnical Institute* VLADIMIR S. SYSSOEV, *Moscow Power Engineering Institute* Development of the ultra-long sparks observed in experiments at Istra (Russia) testifies to extremely low potential drop along the spark channel. At spark length of about 150-200 m, the

potential drop over the leader channel can be estimated as around 0.8-1.6 MV resulting in average absolute intrinsic electric field about 3-10 kV/m. The moderately hot (i.e. conventional) leader channel has then to become thermalised in such ultra-long sparks. The thermalisation mechanism advanced here starts in tail of the leader (at the electrode, for example) after any relatively rapid increase of the heat deposit into the channel. Positive feed-back loop through the current increase - the Joule heating increase - the channel expansion - the neutral density decrease - the reduced electric field increase - the ionisation rate plus the drift velocity increase - the electric current increase - etc results in the thermal instability wave (TIW) travelling along the moderately hot leader channel. At the front of the travelling TIW, some parameters (for instance, luminosity, field altitude) might have the maxima which can be registered by photomultiplier tubes, streak camera, electric and magnetic field probes etc. The moderately hot -to- hot leader transformation mechanism through the travelling TIW can be used to explain the dart (or step-dart) leader phenomenon observed recently in details by M.A.Uman et al at Florida.

DTP 6 Plasma breakdown and combustion ignition DONALD H. MCNEILL,*PHUOC TRAN, *National Energy Technology Laboratory, Pittsburgh, PA* Ignition in chemically reactive media and electrical breakdown are among the most widely used transient processes. The two phenomena operate together during electrical (and laser) spark ignition of combustible gases. Analogs between them show up in Semenov's early (1920's) work on chemical chain reactions and on thermal breakdown of dielectrics. Both breakdown and ignition are under active study today. The energy source for breakdown is an applied electric field, and that for ignition, an applied flux of heat or radicals. Electrons and intermediate reactants are the corresponding driver particles, with a velocity difference that implies a vast difference in the growth rates for the two processes. Combustion takes place in a fuel-oxidant mixture, and an ignited reaction can proceed until the fuel or oxidant is depleted, while a (non-afterglow, non-fusion) plasma is sustained by an external power supply. The energy balance, propagation behavior, and time evolution of some specific forms of plasma breakdown and chemical ignition are further compared in order to illustrate their physical nature.

*National Research Council Senior Research Associate

DTP 7 Influence of emission from the dielectric surface over a homogeneous barrier discharge in nitrogen YU.B. GOLUBOVSKI¹, V.A. MAIOROV^{1,2}, ¹ *State University of St. Petersburg; Physical Faculty, St. Petersburg, Russia* J. BEHNKE², J.F. BEHNKE², ² *EMA-University of Greifswald, Institute of Physics, Greifswald, Germany* The homogeneous barrier discharge at atmospheric pressure is studied theoretically using the fluid model. Since the role of electrodes is played by the dielectric barriers, the mechanisms of emission could differ from those of metal electrodes. Charge carriers are adsorbed by dielectric and may be desorbed back to the volume due to various processes. Because the discharge studied is a kind of Townsend discharge, the emission processes influence directly the discharge current. However, if one takes into account only the ion-electron emission, one obtains a series of current peaks, which does not correspond to the experimental data. The model allows us to introduce a finite lifetime of electrons and ions at the dielectric surface due to their desorption. In this case the current profile depends on time fluently. The desorption of charged particles in nitrogen could be probably caused by vibrationally excited molecules.

DTP 8 Physical Principles of Kinetic Modeling of Plasma Display Panels ROBERT ARSLANBEKOV, *CFD Research Corp.* VLADIMIR KOLOBOV, *CFD Research Corp.* ANATOLY KUDRYAVTSEV, *St. Petersburg University* LEV TSENDIN, *St. Petersburg Technical University* The plasma display panel (PDP) cells usually feature a short glow discharge with no positive column (PC). Typically, the product pressure-length of PDP cell $pL \sim 5$ cmTorr, whereas those of the cathode fall (CF) and negative glow (NG) are, respectively, $\sim 1.3-1.4$ and $3-6$ cmTorr in He. The ionization and excitation take place mostly in the NG and are produced by fast electrons streaming from the CF. These fast (non-equilibrium) electrons determine the PDP luminescence characteristics. The weak electric field in the NG is reversed to trap (and cool) most of electrons. The key parameter is the electron temperature T_e which must be calculated at the kinetic level, taking into account the distribution of superthermal electrons, heating by these electrons in Coulomb interactions and diffusion cooling. The spatial pattern of ionization in the transition region between the Faraday dark space and PC may become periodic, and the formation can take place, via kinetic mechanisms, of the standing striations similar to those observed in experiment. The description of the PDP must therefore be consistently kinetic and nonlocal for the whole electron ensemble, the fluid (or global) and local-field-approximation (LFA) models being physically inappropriate. In this paper, we present an analytical model of PDP and describe the application of a deterministic Boltzmann solver.

DTP 9 Estimations of O₃ loss factor at the wall of barrier discharge ozonizer K. OHE, T. KIMURA, S. NISHIDA, *Nagoya Institute of Technology* Recently there have been many attempts to obtain high O₃ production rate. A barrier discharge of planar disk-type with a thin gap is one of successful attempts. O₃ was produced from O₂ feed gas in a planar disk-type barrier discharge, of which lower electrode was made of 220 mm ϕ stainless steel (SUS 304) disk and the upper electrode was of 150 mm ϕ stainless steel disk. The dielectric plate made of 200 mm ϕ pyrex glass with 0.5 mm or 1.0 mm in thickness was installed just below the upper electrode. The discharge gap was varied from 0.1 to 2.0 mm. The power supply used was the high voltage commercial AC with 60Hz. A typical O₃ concentration produced for the discharge gap of 1.55 mm and the pyrex glass thickness d_g of 1.0 mm was about 5000 ppm at the dissipated power $p=3$ W for the O₂ gas flow $F=1.5$ (l/min). The O₃ concentration increased with F up to about $F=1$ (l/min) for $d_g=0.5$ mm and then decreased. If the decrease of O₃ with F is assumed due to the loss at the wall of the vessel, one can estimate the O₃ loss factor, the so-called sticking factor, γ_{sti} . The value γ_{sti} calculated for the above case was 0.005 ± 0.002 . This work is partially supported by Grant-in-Aid from JSPS.

DTP 10 Experimental studies of Arc-Anode Attachments in Cross-Flows RALF HARTMANN, *University of Minnesota, Department of Mechanical Engineering* JOACHIM HEBERLEIN, *University of Minnesota, Department of Mechanical Engineering* Understanding of arc-electrode effects is of vital importance to extending performance of a number of plasma devices, e.g. circuit breakers or plasma spray torches. There is still no general description of the physics and chemistry of arc electrodes, mainly because of the abrupt transitions from dominance of one physical effect to another when changing the operating parameters. Improved understanding of the arc anode attachment requires the investigation of the involved physical phenomena in the boundary layer. An ex-

perimental set-up has been build, characterized by a transferred arc with a superimposed cross flow. This arrangement allows a variation of the process parameters over a broad range, control of the boundary layer and easy optical access. High-speed video data are correlated to voltage fluctuations and quantitative data of the boundary layer are presented. Different modes of the arc-anode attachment have been clearly identified and are explained. A comparison to arc attachments in DC torch nozzles is given and possibilities for reduced anode wear are pointed out.

DTP 11 MAGNETICALLY-ENHANCED PLASMAS: ECR, HELICON, MAGNETRON, OTHER

DTP 12 A study of DC discharge in cylindrical magnetron in argon P. KUDRNA^{1,2}, J.F. BEHNKE¹, C. CSAMBAL¹, J. RUSZ^{1,2}, ¹ EMA-University of Greifswald, Institute of Physics, Greifswald, Germany M. TICHÝ, ² Charles University in Prague, Faculty of Mathematics and Physics, Czech Republic In the cylindrical magnetron the electric field is applied in radial direction and the magnetic field in axial direction. We study a DC discharge in the novel construction of cylindrical magnetron (cathode length 30 cm, radii of cathode and anode: 0.5 cm and 2 cm, respectively). The plasma is axially limited by 2 diaphragms biased at the cathode potential. We present results of measurements of the radial and axial profiles of the plasma density made by Langmuir probes. The probes are movable in radial direction and can be placed in one of the 5 probe ports located between each couple of total six coils generating the magnetic field. Probe tips are cylindrical (diameter 48 μm , length 2.5 mm). Also we present first results on one-dimensional PIC modeling of the DC discharge in this novel cylindrical magnetron system. Yet the experimental results show that the plasma is not axially homogeneous. The possible cause is the influence of the diaphragms limiting the discharge length.

DTP 13 Space and Time Resolved Measurements in Pulsed Sputtering Magnetron Plasma H. BCKER, J.W. BRADLEY, UMIST P.J. KELLY, R.D. ARNELL, University of Salford In the last decade magnetron sputter sources became an important tool in the deposition of thin films and coatings. Pulsing the discharge not only allows the suppression of arcs at the target but also changes the plasma intrinsic properties in a beneficial way¹. To gain information on the plasma and how it affects the film quality, measurements of the time varying properties are required. We will present and to some detail explain space and time resolved Langmuir probe measurements of T_e , n , V_p and V_f , for positions inside and outside of the magnetic trap and for different times during the pulse. These measurements have been done in Argon plasmas at 0.5 Pa using Al and Ti sputtering targets and show that: at the beginning of the duty phase a burst of hot electrons can be observed (measurements with directional probes are planned to clarify the nature of these bursts) during the reverse voltage phase V_p rises to a value above the target potential T_e and n decay and rise during the pulse (basic explanations for the characteristic time constants will be given).

¹J.W. Bradley et al., Surf. Coat. Technol. **135** (2-3) pp 221 (2001)

DTP 14 On formation of excited state densities in magnetron discharge I.A. POROKHOVA^{1,2}, J.F. BEHNKE¹, ¹ EMA-University, Institute of Physics, Greifswald, Germany YU.B. GOLUBOVSKII, ² St.Petersburg University, Department of Optics, Russia M. TICHÝ, Charles University in Prague, Faculty of Math. and Physics, Czech Republic The formation of metastable and resonance state densities of argon in cylindrical magnetron discharge (CMD) is studied experimentally by solving the system of balance equations for the densities of the 4s states with account of radiation transport, diffusion and numerous excitation and decay processes that take place in real CMD. The solution technique of Biberman-Holstein radiation transport equation is developed in conformity to CMD-geometry. The approximation of effective lifetime is considered and radial dependence of the effective probability of radiation escape obtained for the discharge between two cylindrical electrodes. An influence of the radiation imprisonment and diffusion of metastable atoms is demonstrated. The balance equations for the particle densities of metastable and resonance atoms are considered with account of the excitation and decay processes which take place in the CMD. The results of experiment and calculations are compared and discussed.

DTP 15 Comparison of cylindrical magnetron discharge via PIC and kinetic modeling J.F. BEHNKE¹, P. KUDRNA^{1,3}, I.A. POROKHOVA^{1,2}, ¹EMA - University, Institute for Physics, Greifswald, Germany YU.B. GOLUBOVSKII, ² St.Petersburg State University, Department of Optics, Russia M. TICHÝ, ³ Charles University in Prague, Faculty of Mathematics and Physics, Czech Republic The plasma in cylindrical magnetron discharge is studied on the basis of PIC simulation and self-consistent non-local modeling. Both models are the powerful tools to calculate internal plasma parameters in entire discharge gap from cathode to anode. The main features of the models are described and the obtained results discussed. The radial distribution function of electrons, charged particle densities, electric field, average energy, etc., obtained by PIC and kinetic models are compared. PIC-simulation appears to be more efficient in describing cathode region, where anisotropy of electron distribution function can be noticeable, whereas kinetic model gives more stable and detailed solutions. Discharge conditions: Ar at $p=2.8$ Pa, axial magnetic field strength $B_z=20$ mT, discharge current $I=72$ mA, discharge length $l=12$ cm, radii of inner cathode and outer anode: 0.5 cm and 3 cm respectively.

DTP 16 Possibility of significant heating of H atoms in high-density, helicon-wave excited hydrogen plasmas K. SASAKI, M. NAKAMOTO, K. KADOTA, Department of Electronics, Nagoya University, Japan In the present work, we measured the distribution of H atom density in high-density hydrogen plasmas excited by helicon-wave discharges. The measurement was carried out in a linear machine with a uniform magnetic field of 1 kG along the cylindrical axis of the vacuum chamber. Plasmas were produced in a glass tube of 3 cm diameter by applying various rf powers to a helical antenna wound around the glass tube. The hydrogen gas pressure was 30–100 mTorr. Since the plasma was confined radially by the external magnetic field, we obtained a slender plasma column of 3 cm diameter at the center of the vacuum chamber. The distribution of the H atom density was measured by (2+1)-photon laser-induced fluorescence spectroscopy. As a result, it was found that the distribution of the H atom density had a deep dip in the high-density operation. The location of the dip corresponded to the high-density plasma column. A

possible explanation for the deep dip in the plasma column is significant heating of H atoms. In general, it is known that temperatures of neutral species in low-pressure plasmas are not so far from room temperature. However, the present experimental result suggests the possibility of significant heating of neutral radicals in low-pressure, high-density plasmas. The high temperature may influence the transport and kinetics of reactive species in plasmas.

DTP 17 Particle and energy balance in a Helicon plasma source* AMNON FRUCHTMAN, *Holon Academic Institute of Technology* GENNADY MAKRINICH, *Holon Academic Institute of Technology* The plasma density in a helicon source is measured as a function of the magnetic field intensity and of the RF wave power, for various gases and mass flow rates. The measurements are compared with equilibrium calculations that are based on particle and energy balance. The momentum equation that is employed, includes the ion inertia, instead of just solving the diffusion equation. Also calculated is the ion rotation as a combined effect of the magnetic field force and collisions with neutrals. The effect of confinement by the magnetic field can be explained only when anomalous conductivity is invoked. The nonlinear dependence of the plasma density on the wave power, and the effect of the magnetic field intensity on the axial plasma profile, are discussed.

*Partially supported by the Israel Science Foundation

DTP 18 Control of Reactive Species in N₂ Helicon Plasmas ROBERT BOIVIN, JOHN KLINE, EARL SCIME, *Department of Physics, West Virginia University, Morgantown, WV 26506-6315* The control of the reactive species in Plasma-Assisted Molecular Beam Epitaxy (PAMBE) systems is of crucial importance. Studies of GaN film growth suggest that growth rates and resulting film quality depend strongly on the relative fraction of atomic nitrogen and metastable molecular nitrogen. A helicon plasma source is used to control the nitrogen plasma chemistry. This control is accomplished by varying the electron temperature of the plasma. A spectroscopy study of relevant molecular and atomic nitrogen species is carried out at different plasma conditions to identify the dominant excitation, ionization or dissociation processes in the plasmas as a function of the electron temperature. At low electron temperature, almost purely molecular plasmas are produced, while at high electron temperature atomic plasmas are observed. In parallel, electron-impact cross-sections are used to evaluate the rate coefficients of the different possible excitation/dissociation/ionization reactions in the nitrogen plasma. Formation rates of the different nitrogen species are calculated and compared to predict the dominant species at a given electron temperature. The predicted dominant species obtained from the cross-sections agrees well with the dominant nitrogen species observed in the spectroscopy study. The possible scenarios featuring the usage of a helicon source in a PAMBE system are examined.

DTP 19 A Experiment of Helicon wave propagation and mode structure KANGIL LEE, *Plasma Application Lab* MIN-JOONG JUNG, *Plasma Application Lab* TAIHYOEP LHO, *KBSI* GON-HO KIM, *Plasma Application Lab* PLASMA APPLICATION LAB TEAM, Helicon wave generation in a weakly magnetized inductively coupled Plasmas(ICP) with the floating or conducting boundaries has been issued in high density plasma source development for industrial applications. In this experiment, the characteristics of helicon wave coupled with various types of an-

tenna in conducting boundary were studied. Measurements were carried out in a weakly magnetized ICP which plasma was confined in a cylindrical S/S chamber (500mm in dia 600mm in length). Ar plasma density was approximately $10E10cm^{-3}$ with the input power 300W/1000W, respectively. Using the external Helmholtz coils, a uniform DC magnetic field was produced up to 80 Gauss. A floating B-dot probe, compensated to the capacitively coupled E-field in the signal, was employed to measure the wave field in the plasma. In case of using one turn loop antenna, It was found that $m=0$, $n=1$ mode helicon wave was launched, $m=0$, $n=2$ mode wave was generated for the two turn loop antenna and helicon wave of $m=1$, $n=2$ mode was launched for the modified Nagoya antenna respectively. The wave number was proportional to the B/n and it was fairly good agreement of experimental result and the model that was considered large aspect ratio.

DTP 20 Magnetic Tuning of Ion Energies in a Low Pressure ECR Plasma O.J. GLEMBOCKI, V. SHAMAMIAN, D. HIN-SHELWOOD, R.T. HOLM, R. FERNSLER, W. MANHEIMER, *Naval Research Laboratory, Code 6862, Washington DC, 20375* Typically in an electron-cyclotron-resonance (ECR) processing source, an RF bias is used to accelerate ions toward the substrate with a desired energy. In this paper we show that with the proper magnetic field structure, Ar ions with directed energies of up to 100 eV can be produced. Varying the field structure allows the ion energies to be tuned by a factor of 4, from 25-100 eV. Ion acceleration results from a combination of a relatively high electron temperature in the ECR region and a nozzle-like magnetic field structure. High temperature in the ECR region is obtained by operating at low pressure (0.05 to 0.1 mTorr) and by using fixed magnets that provide a multiple-cusp field structure. An external coil is added to enhance the areal expansion of the magnetic field lines and to further tune the magnetic cusp. This leads to a conversion of thermal energy to directed ion motion. We will present data for the magnetic field, profiles, the ion energies, the electron temperatures and the plasma profile that produces the energetic ions.

DTP 21 SHEATHES

DTP 22 Observation of an electron sheath at a large, transiently biased surface in the GEC cell* P.R.J. BARROY, A. GOODYEAR, N.ST.J. BRAITHWAITE, *The Open University, Oxford Research Unit, Boars Hill, Oxford, OX1 5HR, UK* Sheath reversal has been investigated in front of a biased surface embedded into the ground electrode of a capacitively coupled GEC cell. Radio frequency bursts (several tens of volts amplitude) were applied to the surface (20 mm diameter including guard ring) and fast, two dimensional observations made of the light emission using an intensified CCD camera synchronously gated within the succession of bursts. A guard ring, biased to the same potential, ensures sheath planarity. The evolution of the optical emission has been followed during the dc biasing period. If the applied RF is large enough and the timescale short enough a perturbation of the plasma sheath is observed. At the onset of the RF burst periodic,

sheath reversal is achieved as the potential of the surface exceeds that of the plasma. After several cycles of RF, the surface acquires enough negative charge to bias itself negatively, below plasma potential; sheath reversal then stops. The overall effect is accompanied by light emission from species excited by electrons accelerated towards the surface. Modelling of the phenomenon has been conducted to account for the observations.

*Work supported by the EPSRC (UK), Grant No. GR/L82380

DTP 23 How fast do ions fall into the sheath in multiple ion species plasmas?* GREG SEVERN,[†] *University of San Diego* NOAH HERSHKOWITZ, *University of Wisconsin, Madison* XU WANG, *University of Wisconsin, Madison* SHEATH TEAM, There is a fundamental open question in the science of sheaths for multiple ion species plasmas: how fast are the individual ion species traveling when they enter the sheath? The Bohm criterion furnishes only equations of constraint, e.g. $n_{e0}/T_e \geq \sum_j (n_{j0}/m_j v_{j0}^2)$, satisfying $dn_e/dx \geq (\sum_j dn_j/dx)$, where the *naught* refers to the sheath-presheath boundary, and where *j* refers to the *j*th ion species. These equations permit an infinity of solutions. Further, laser-induced fluorescence (LIF) measurements of ion velocity distribution functions within the sheath and presheath have not yet been made such plasmas. These data for ArII ions will be presented for the case of *ArI + HeI*, $P_{total} \sim 1 \text{ Torr}$ plasmas in a DC hot filament discharge with magnetic multipole confinement.

*Work supported by DOE grant no.DE-FG02-97ER54437 and NSF grant no. PHY9722658

[†]on sabbatical at the University of Wisconsin, Madison

DTP 24 Study of sheath formation in the wide range of operating pressure BO-HAN HONG, MIN-JOONG JUNG, GON-HO KIM, *Plasma Application Laboratory, Hanyang University-Ansan, 425-791 Korea* YONG-SUP CHOI, KYU-SUN CHUNG, *Applied Plasma Laboratory, Hanyang University-Seoul, 132-791 Korea* In recent years, there are arguments on the effect of collision in the sheath model and the necessity of experimental confirmations are increasing. In this study, we measured a sheath potential of the target surface using the inflection point method with the limit of zero emission of emissive probe. All experiments have been done in a DC glow discharge type of Ar and He plasma for the pressure of 1 to 600 mTorr and target bias of -30 to -110V. The results showed that the sheath thickness seemed to be proportional to the power of 3/4 of target bias in collisionless plasma and proportional to the power of 3/5 in collisional plasma, which agreed well with the result of Godyak and Sternberg. Also we observed a negative slope in potential profile in the case of collisional sheath. To explain the unusual potential profile, ionization term of ion-neutral and secondary electron-neutral, which are usually discarded in a conventional sheath model, were included in fluid equations of sheath and in a simple PIC simulation. The experimental results were compared with the various collisional sheath models. This result can be applied to understand the operating variance and processing reaction in the semiconductor process of PECVD, Sputter and etc., in which plasma is operated in high pressure.

DTP 25 PIC simulation of the presheath and sheath regions in a collisional plasma GEORGE GOZADINOS, *Dublin City University, Ireland* DAVID VENDER, *Dublin City University, Ireland* MILES M. TURNER, *Dublin City University, Ireland* The problem of sheath formation through a collisional planar presheath and the relevant Bohm criterion for the case of one and two posi-

tive ions is considered. Results are obtained from a Particle-In-Cell simulation modeling a semi-infinite planar collisional and non-ionising plasma in contact with an electrode. An investigation of the possible values of the average ion velocities compatible with the Bohm criterion, in terms of the values of the particle fluxes and the ion mean free paths, is performed. Our results indicate that the individual ion species Bohm velocities pose upper or lower boundaries to the average velocities that the ion species can attain, depending on the values of the ion mean free paths.

DTP 26 Transport of low energy ion beam with space charge compensation SVETLANA RADOVANOVA, *Varian Semiconductor Equipment Associates, Gloucester, MA 01930 USA* GORDON ANGEL, *Varian Semiconductor Equipment Associates, Gloucester, MA 01930 USA* JAMES CUMMINGS, *Varian Semiconductor Equipment Associates, Gloucester, MA 01930 USA* JAMES BUFF, *Varian Semiconductor Equipment Associates, Gloucester, MA 01930 USA* The propagation of a low energy ion beam in the field free region of a high current ion implanter, is studied here. Ion beams have electric fields in the beam interior that, at some energies and currents, cause expansion of the beam. Beam transport is then possible only with compensation of this charge by low energy electrons. The potential associated with the beam increases as the beam expands in the free space. In order to get some insight into what may be happening to beam potentials and angular distributions we have investigated these parameters for a 500 eV Boron, beam for different space charge compensation levels. Measured beam angles showed increased beam divergence at higher beam currents. When the flux of the space charge compensating electrons increased the angular spread and beam potential decreased. The calculated angular divergence for different beam currents confirmed this behavior. It has been shown that beam expansion and angles associated with it are controlled by the electric fields in the beam interior. The compensating electrons injected into the beam are effectively focussing the beam and providing efficient beam transport at low energies.

DTP 27 The anode region of an arc discharge K.-U. RIEMANN, *Ruhr-University Bochum, Theoretische Physik 1 (D-44780 Bochum, Germany)* In contrast to the cathode, the anode plays apparently no vital role in the discharge operation. There is, however, a serious difficulty to produce a sufficient number of ions in the near anode region. We investigate this problem with a plane two fluid model of the anode region of a thermal arc accounting for ionization, recombination, and charge exchange collisions. With these simplified model assumptions, we find that the anode fall is always negative and that the total current is limited by the requirement of sufficient ion production.

DTP 28 A Distribution Function for Highly Energetic Electrons in an RF Sheath F.A. HAAS, A. GOODYEAR, N.ST.J. BRAITHWAITE, *Oxford Research Unit, The Open University, Foxcombe Hall, Boars Hill, Oxford OX1 5HR, UK* Recent work using a GEC reference cell under capacitive conditions shows the electron distribution function to consist of a Maxwellian together with a high energy group of electrons at about 25 eV or higher. The distribution function is measured at the grounded electrode by using part of the surface as the probe. The latter is circular and is

separated from the earthed region by a concentric annular ring. The origin of the energetic electrons is uncertain, but the experiment suggests a simple heuristic model. Considering the probe, we assume a general distribution of energetic electrons incident at the plasma-sheath boundary. Taking account of the mean (V_0) and oscillatory (V_1) parts of the potential and assuming the transit time to be short compared with the RF period, we derive a convolution integral for the distribution at the probe. It is shown that, in general, this distribution function exists only over a limited range (or ranges) of energy. Assuming a rectangular distribution for the electrons incident at the plasma-sheath boundary the integral can be performed analytically. The distribution function of electrons reaching the probe surface is spread on passing through the RF sheath; the character of this spread can have the appearance of a thermalized high energy tail.

DTP 29 Joining Plasma and Sheath Over a Wide Range of Collisionality RAOUL FRANKLIN, *Oxford Research Unit, The Open University* The problem of joining active plasma and sheath smoothly has attracted attention ever since Bohm did his seminal work. A more significant development in terms of elucidating the structure of the plasma-sheath was the work of Su and Lam (jointly and separately) in the 1960s. This triggered a number of studies with different orderings of the physical parameters involved, both using the technique they employed of matched asymptotic approximations, and by direct computation. Results will be given covering the whole range of collisionality from collisionless plasma- collisionless sheath where the ordering is $\lambda_i > L > \lambda_{D0}$ (λ_i is the ion mean free path, L the plasma dimension and λ_{D0} the plasma Debye length) to $L \gg \lambda_{D0} > \lambda_i$ corresponding to collisional plasma-collisional sheath. Ion motion is modelled using (a) a constant collision frequency, and (b) a constant ion mean free path. The differences and similarities are discussed, as is the validity of the concept of a collisionally-modified Bohm criterion.

DTP 30 CLUSTERS AND DUSTY PLASMAS

DTP 31 Particle interactions in multilayer plasma dust crystals G. A. HEBNER, *Sandia National Laboratories* M. E. RILEY, *Sandia National Laboratories* K. E. GREENBERG, *APS Career Enrichment Center* The vertical interaction potential between dust particles suspended in a multilayer plasma dust crystal are investigated. Micron sized dust particles will, under the right conditions, form ordered, 2-D structures with a regular hexagonal close packed structure. Within a single 2-D plasma dust crystal layer, the horizontal interparticle forces are well characterized by a screened Coulomb interaction potential. However, for multi layer structures, there are a number of less well-defined mechanisms that influence the vertical layer formation and alignment. For example, the flowing ion wind present in the presheath region of the plasma where the 3-D crystal forms can produce a small potential well downstream from a dust particle suspended in the plasma. This small potential well can trap and hold a second dust particle

in a stable vertical arrangement. We are currently investigating the vertical pairing of dust particles suspended in a plasma using a number of diagnostics such as image analysis, probes and LIF. The results of recent experiments and calculations will be discussed. This work was performed at Sandia National Laboratories and supported by DoE Office of Science and the United States Department of Energy (DE-AC04-94AL85000).

DTP 32 Particulate dynamics in near-electrode regions of fluorocarbon plasmas KOSTYA OSTRIKOV, NING JIANG, SHUYAN XU, *Plasma Processing Laboratory, NIE, Nanyang Technological University, 1 Nanyang Walk, 637616 Singapore* SUNIL KUMAR, *Ian Wark Research Institute, University of South Australia, Mawson Lakes, SA 5095, Australia* HIDEO SUGAI, *Department of Electrical Engineering, Nagoya University, 464-8603 Nagoya, Japan* Dynamics of submicron-size particles, often appearing in fluorocarbon plasma etching experiments, is considered. It is shown that in inductively coupled (13.56 MHz) and microwave slot-excited (2.45 GHz) plasmas (MSEPs) of C_4F_8 and Ar gas mixtures, the charge equilibrium and relaxation processes are controlled by microscopic electron, atomic, and molecular ion (positive and negative) currents. It is revealed that in low-power MSEPs, the impact of the combined molecular ion current to the total positive microscopic current on the particle can be as high as 40 %. The particulate charge relaxation rate in fluorocarbon plasmas appears to exceed $10^8 s^{-1}$, which is higher than that from purely argon plasmas. It is also shown that in near-electrode regions of $C_4F_8 + Ar$ etching plasmas dust particles can be effectively trapped. The effect of negative ions on particulate charging and dynamics is also investigated. The equilibrium charge and forces on particles are computed as a function of the local position in the plasma pre-sheath and sheath. It is shown that despite negligible negative ion currents collected by the particles, the negative fluorine ions affect the charging and trapping of submicron-sized particles through modification of the sheath/pre-sheath structure.

DTP 33 Electron- and ion-densities in silane high frequency discharges YUKIO WATANABE, ATSUSHI HARIKAI, KAZUNORI KOGA, MASA HARU SHIRATANI, *Kyushu University* Clusters formed in SiH_4 high frequency discharges often influences on the discharge parameters, since clusters tend to be charged negatively in the discharges. Results of simulation show that the positive ion density n_i is by more than ten times as high as the electron density n_e ,¹⁾ although no experimental verification has been made. Therefore we have observed time evolution of n_i and n_e with a Langmuir probe and a microwave interferometer, as well as that of cluster-size and density by the double pulse discharge method.²⁾ The value of n_i is slightly (about 10%) higher than n_e for 13.56 MHz pure SiH_4 discharges, which is inconsistent with the results of simulation. With increasing the discharge frequency f from 13.56 to 60 MHz, their density difference increases and for 60MHz n_i is by 2-3 times as high as n_e . Since cluster-size and -density for a constant supplied power do not significantly depend on f , the higher f may bring about a higher portion of low energy electrons which tend to attach to clusters.^{1)U. Kortshagen and U. Bhandarkar, Phys. Rev. E, 60 (1999) 887. 2)K. Koga, et al., Appl. Phys. Lett, 77 (2000) 196.}

DTP 34 PLASMA DIAGNOSTICS I

DTP 35 Determination of the Gas Temperature in an Open-Air, Atmospheric Plasma Torch from the Resolved Plasma Emission JAMES M. WILLIAMSON, *Innovative Scientific Solutions, Inc., Dayton, OH* CHARLES A. DEJOSEPH JR., *Air Force Research Laboratory, Wright-Patterson AFB, OH* In principle, the gas temperature in an air plasma can be determined from the plasma emission of molecular nitrogen. The gas temperature is typically determined from the contour analysis of the emission bands in the well known, N_2 2nd positive ($C^3\Pi - B^3\Pi$) system. The N_2 2nd positive system has a large oscillator strength and is easily recognized in nitrogen discharges making it the preferred system for temperature determination. The resolved emission spectrum of an atmospheric pressure, open-air plasma torch was recorded with a 0.5 m spectrometer and CCD camera. The plasma emission under these conditions was found to be dominated by continuum radiation and emission from other species which obscured large portions of the N_2 2nd positive emission. In spite of these difficulties, the gas temperature of the torch could be determined from a fit of partially resolved N_2^+ 1st negative vibrational transitions and a blackbody fit to the continuum radiation. The vibrational temperature, determined from a Boltzmann plot, was 4300 ± 900 K while the blackbody radiation temperature was 4400 ± 400 K. As a check, spectral simulations using N_2^+ 1st negative emission, N_2 2nd positive emission, and a blackbody were compared with measured spectra over selected spectral regions.

DTP 36 Resonance Enhanced Deactivation of Ar 4p'[1/2]o State by Atomic Oxygen With Implications for Ar-Based Actinometry MICHAEL BROWN, *Innovative Scientific Solutions, Inc., Dayton, OH* BISWA GANGULY, *Air Force Research Laboratory, Wright-Patterson AFB, OH* ALAN GARCADDEN, *Air Force Research Laboratory, Wright-Patterson AFB, OH* In SiC etching plasma devices, we have recorded plasma emission from Ar, F and O atoms in SF₆/Ar/O₂ rf discharges as a function of pressure, power and mixture fraction. In particular, we have examined Ar emission at 750 nm in comparison with Ar emission from other excited states. The excited state, 4p[1/2]o (2p1), of the Ar 750 nm emission line is nearly iso-energetic with Rydberg states of atomic oxygen. We observed the resonant deactivation of this Ar excited state by O atoms in SF₆/Ar/O₂ rf-driven discharges with high O₂ dissociation fractions. Using a variable gap and peak-to-peak voltage measurements, we estimated E/n to be 300 Td at 600 mTorr. For E/n > 150 Td, 80% deposition in O₂ goes to dissociation. At fixed pressure and input power, the Ar emission at 750 nm decreases with O₂ additions up to 101/2]o (3s5) Ar state at 641 nm increases with O₂ addition. The increased emission of the 641 nm line parallels that of F at 704 nm. The divergent behavior of the Ar emission lines is a manifestation of the resonant deactivation of the 4p[1/2]o (2p1), state by O atoms which suggest the Ar 750 nm transition may not be suitable for actinometry in discharges containing oxygen and characterized by high E/n values.

DTP 37 Study of Intensity Distribution in the (0 - 0)R Branch of the $A^1\Pi \rightarrow X^1\Sigma^+$ Electronic Transition of the BH Molecule and Determination of Gas Temperature in Non-Equilibrium Plasmas M. OSIAC, J. RÖPCKE, *Institute of Low Temperature Plasma Physics, F.-L.-Jahn-Str. 19, 17489 Greifswald, Germany* B. P. LAVROV, *Faculty of Physics, St.-Petersburg State University, 198904, Russian Federation* Relative transition probabilities of spontaneous emission in the R and P branches of the $A^1\Pi \rightarrow X^1\Sigma^+$ (0 - 0) band of BH have been obtained for the first time. It was observed that they are in agreement to corresponding ratios of Hönl-London factors. Thus the non-adiabatic effect of perturbation is negligible small and Hönl-London formulas may be used for derivation of rovibronic population densities from measured line intensities. General considerations are illustrated at the example of a low-pressure plasma of a planar microwave discharge using H₂-Ar-B₂H₆ gas mixture ($p = 1 - 2.5$ mbar, $P = 1.2 - 2.4$ kW). In the framework of a corona model the rotational temperatures of $A^1\Pi^-$, $v'=0$, and $X^1\Sigma^+$, $v''=0$ vibronic states obtained from the BH spectrum are in accordance with the rotational temperatures of the $X^1\Sigma^+$, $v''=0$ state of H₂ determined from the intensities of (0 - 0)Q-branch lines of the H₂-Fulcher- α band system. This provides the opportunity to use rotational line intensities of the (0 - 0)R branch of BH for the spectroscopic determination of rotational and gas temperatures in non-equilibrium plasmas.

DTP 38 Time-resolved determination of the dissociation degree in pulsed plasmas containing H₂ by the means of OES N. LANG, J. RÖPCKE, *Institute of Low Temperature Plasma Physics, 17489 Greifswald, Germany* B.P. LAVROV, *Faculty of Physics, St.-Petersburg State University, 198904 St. Petersburg, Russia* Since the dissociation degree of hydrogen in plasmas is very important for basic research and numerous applications, simple and reliable methods of its determination are highly necessary in particular for plasma technology. The new method proposed here is applied to determine the time evolution of the dissociation degree in a pulse-modulated microwave discharge containing hydrogen by time-resolved optical emission spectroscopy (OES). This method is a modification and correction of the established method developed by Devyatov¹ with respect to following points: (1) taking into account the rotational structure of levels (previously neglected) and (2) usage of new values of cross sections, life times and transition probabilities. It is shown that in this case the determination of the dissociation degree can be reduced to the measurement of just two line intensities (one atomic and one molecular) and the gas temperature. It was found that the dissociation degree raises up from about 40% to 70% during the pulse ($p = 55$ Pa, $P_{MW} = 3.6$ kW). In spite of that corresponding atomic and molecular densities of hydrogen decrease because of the gas heating, which is in correspondence to results of TALIF experiments.

¹A. M. Devyatov et al., *Opt. Spectrosc.* **71** (1991), 525.

DTP 39 A Time Resolved Laser Study of Hydrocarbon Chemistry in H₂-CH₄ Surface Wave Plasmas LARS MECHOLD, JÜRGEN RÖPCKE, *Institute of Low Temperature Plasma Physics, F.-L.-Jahn-Str. 19, 17489 Greifswald, Germany* XAVIER DUTEN, *Laboratoire d'Ingenierie des Materiaux et des Hautes Pressions, Universite Paris 13 - Avenue J.B. Clement, 93430 Villetaneuse, France* ANTOINE ROUSSEAU, *Laboratoire de Physique des Gaz et des Plasmas, CNRS, Universite Paris-Sud - Ba-*

timent 210, 91405 Orsay Cedex, France Time resolved tunable infrared diode laser absorption spectroscopy has been used to detect the methyl radical and four related stable molecules, CH₄, C₂H₂, C₂H₄, C₂H₆, in H₂ surface wave plasmas ($f = 2.45$ GHz) containing 10 % of methane under static conditions at different pressures ($p = 0.1 - 4$ Torr). For the first time, the time dependence of the conversion of methane to the methyl radical and three stable C-2 hydrocarbons was studied in a fixed discharge volume nearly up to a stationary state. The degree of dissociation of the methane precursor was found to increase up to 96 % in the stationary state, and the methyl radical concentration was measured to be in the range of $10^{12} - 10^{13}$ molecules cm⁻³. The influence of diffusion on the spatial distribution of the hydrocarbon concentration in the discharge tube was considered. A qualitative model has been developed in order to describe the chemical processes and to identify the main plasma chemical reaction paths.

DTP 40 Absorption Spectroscopic Studies of Molecular Species in H₂-Ar-N₂-Microwave Discharges With Small Admixtures of Hydrocarbons F. HEMPEL, L. MECHOLD, J. RÖPCKE, *Institute of Low Temperature Plasma Physics (INP), Friedrich-Ludwig-Jahn-Str. 19, 17489 Greifswald, Germany* P. B. DAVIES, *Department of Chemistry, University of Cambridge, Lensfield Road, Cambridge CB21EW, United Kingdom* Results of absorption spectroscopic studies of stable and transient molecular species in hydrocarbon containing H₂-Ar-N₂-discharges in a planar microwave reactor ($f = 2.45$ GHz, $P = 1.5$ kW) are presented. Measurements were performed using various ratios of H₂ to N₂ and small admixtures of a few percent of CH₄ or CH₃OH with a discharge pressure of 1.5 mbar. TDLAS in the mid infrared region has been used to determine the concentrations of nine stable molecules like C₂H₂, C₂H₄, C₂H₆, HCN, NH₃, CH₂O or C₂N₂ as well as of the CH₃ radical. The degree of dissociation of CH₄ was found to be between 70 to 95 %, showing a considerable increase at small percentages of N₂. The CH₃OH was determined to be dissociated almost completely (about 97 %) for all mixtures. The CN radical was measured for the first time under similar discharge conditions. The experimental results will be used for modelling the plasma chemistry.

DTP 41 Diode Laser Based LIF Diagnostic for the Helix Helicon Source MICHEAL WOEHMAN, ROBERT BOIVIN, JOHN KLINE, EARL SCIME, *Department of Physics, West Virginia University, Morgantown, WV 26506-6315* A description of a diode laser based LIF diagnostic is presented. The LIF diagnostic features a tunable diode laser system developed for the Hot helicon eXperiment (HELIX) at West Virginia University. We present preliminary results for experiments conducted on Ar plasmas. The laser, tuned at 668.4 nm, is used to pump the 3d⁴F_{5/2} Ar II metastable level to the 4p⁴D_{7/2} level. The fluorescence radiation between the 4p⁴D_{7/2} and the 4s⁴P_{5/2} levels (442.6 nm) is monitored by a photomultiplier detector. The LaserTechnik SAL-665-10 laser has a Littrow external cavity. The mode-hop free tuning range is greater than 20 GHz and the total power output is about 15 mWatt. An active stabilization system using an absorption cell is used to prevent wavelength drift. Wavelength scanning is achieved by ramping the voltage on the piezoelectric controlled grating in the laser cavity. A lock-in amplifier is used to isolate the fluorescence signal from the electron-impact induced radiation.

DTP 42 TALIF Calibration with Noble Gases for Quantitative Atomic Density Measurements* K. NIEMI, V. SCHULZ-VON DER GATHEN, H.F. DÖBELE, *University of Essen, Germany* INSTITUT FÜR LASER- UND PLASMAPHYSIK TEAM, In order to obtain absolute atomic ground state densities with two-photon absorption laser-induced fluorescence spectroscopy (TALIF) a reliable calibration technique and the consideration of collisional quenching effects on the induced population are required. A comparative measurement with a noble gas having a two-photon resonance spectrally close to the atomic transition can be used as a calibration. Suitable transitions exist in krypton and xenon for the two-photon excitation of atomic hydrogen at 205.1 nm, nitrogen at 206.6 nm, and oxygen at 225.5 nm. We investigated these excitations by TALIF in order to determine the atomic data required for this calibration. The radiative lifetimes of the excited states and the quenching coefficients for collisions with several important species were obtained from time resolved measurements. The relevant ratios of the two-photon excitation cross-sections were determined from comparative measurements with known densities. The atomic reference densities were generated in a flow-tube reactor with the aid of titration methods.

*Supported by the DFG in frame of SFB 191 and Graduiertenkolleg 'Hochtemperatur-Plasmaphysik'

DTP 43 Electrical Measurements during Laser Induced Fluorescence in Ar/Cl₂ ICP* OSMOND A. OKPALUGO, C.M.O. MAHONY, S.J. LAVERTY, P.D. MAGUIRE, *University of Ulster, N. Ireland* S. GOMEZ, W.G. GRAHAM, *Queen's University of Belfast, N. Ireland* In-situ electrical measurements are increasingly required for process monitoring and control. Here, electrical data are measured and correlated with atomic chlorine densities in 13.56 MHz Ar/Cl₂ inductively coupled plasmas. In particular, positive ion fluxes and derivatives of coil currents and voltages were measured simultaneously with Cl laser induced fluorescence to determine how the electrical data scale with relative atomic chlorine densities. A Scientific Systems IFTTM was used for the ion flux measurements. The coil electrical characteristics are measured with closely coupled derivative current and voltage probes. For the LIF, the radiation field at 233 nm was generated with Nd:YAG pumped dye laser with frequency doubling and mixing. Input power range of 5-400W, chlorine fractions of up to 40 % and pressure range of 0.7-11 Pa were used in all the experiments. Together, these electrical and optical measurements provide insight into the optimisation of silver chloriding and etch process conditions of interest.

*UK EPSRC TPI Supported

DTP 44 Rotational Temperature Measurements in an RF Discharge by Using CO Rotational Emission Spectrum T. DINH, S. POPOVIC, L. VUŠKOVIC, *Department of Physics, Old Dominion University, 4600 Elkhorn Ave., Norfolk, VA 23529* Gas temperature is a necessary parameter needed to establish the kinetic model of a gas discharge. In order to verify the possible perturbation and distortion of temperature of the RF discharge to the thermocouple probe, we performed the emission spectroscopy analysis based on the rotational intensity distribution of CO bands to obtain highly accurate discharge temperature measurements. In our experiment, as well defined gas mixture with 95% of CO₂ and pressure 4-6 Torr flowed transversely to the applied RF field between two parallel circular stainless steel disks with diameters of 2.54 cm and a discharge gap of 0.4-1.0 cm. The driven RF field

had the frequency of 20–40 MHz and the power delivered to discharge was 1–5 W. It was possible in this discharge conditions to use the Angstrom Band ($B^1\Sigma^+ - A^1\Pi$ e.g. 519.8 nm, 451.0 nm) in the visible emission spectrum of CO to analyze the discharge temperature. The Q branch within $B^1\Sigma^+ - A^1\Pi$ transition, which corresponds to $\Delta J = 3D_0$ and has the most intense distribution profile, was used to identify the rotational quantum numbers. The higher rotational quantum numbers were used during the fitting in order to eliminate the possible overlap with P and R branches. The rotational temperature of the RF discharge in the gas mixture was compared to the temperature measured by thermocouple probe.

DTP 45 Measurements of Electron Temperature and Gas Temperature in a Pulsed Atmospheric Pressure Air Discharge* FRANK LEIPOLD, *Old Dominion University, Physical Electronics Research Institute, Norfolk, VA 23529* ABDELALEAM HUFNEY MOHAMED, *Old Dominion University, Physical Electronics Research Institute, Norfolk, VA 23529* KARL H. SCHOENBACH, *Old Dominion University, Physical Electronics Research Institute, Norfolk, VA 23529* The application of electrical pulses with duration shorter than the time constant for glow-to-arc transition allows us to shift the electron energy distribution in high pressure glow discharges temporally to high energy values [1]. Application of these nonequilibrium plasmas are plasma ramps, plasma reactors, and excimer light sources. In order to obtain information on the electron energy distribution, or electron energy, respectively, and the gas temperature with the required temporal resolution of 1 ns, we have explored two diagnostic methods. One is based on the evaluation of the bremsstrahlung. This method allows us to determine the electron temperature [2]. The gas temperature is obtained from the rotational spectrum of the second positive system of nitrogen. The results of measurement on a 10 ns pulsed atmospheric pressure air glow will be presented. References [1] Robert H. Stark and Karl H. Schoenbach, *J. Appl. Phys.* 89, 3568 (2001) [2] Jaeyoung Park, Ivars Henins, Hans W. Herrmann, and Gary S. Selwyn, *Physics of Plasmas* 7, 3141 (2000). [3] R. Block, O. Toedter, and K. H. Schoenbach, *Bull. APS* 43, 1478 (1998)

*This work was funded by the Air Force Office of Scientific Research

DTP 46 NEGATIVE ION PLASMAS

DTP 47 Loss mechanisms of negative oxygen ions in an inductively coupled rf discharge HANS-MICHAEL KATSCH, CLAUDIUS MANTHEY, HANS FRIEDRICH DOEBELE, *University of Essen, Institute for Laser- and Plasmaphysics* The experiment is performed in a pulsed inductively coupled 13.56 MHz rf oxygen plasma (GEC reference cell). The negative ion density is measured by photodetachment. A high fraction of negative ions (approx. 90 %) is observed during the discharge. In the center of the discharge both the axial and the radial density profiles of the negative ions nearly coincide with the density profile of the positive charge carriers. This is confirmed by calculations of the loss reactions of the negative ions. The dominant loss reactions of the

negative ions can be found from measurements of the temporal decay of the positive and negative charge carriers in the post discharge. The dominant loss process of O^- -ions is the recombination with O_2^+ -ions during the discharge. The loss reaction with atomic oxygen, which produces additional electrons, is of lower significance. The expected state of an ion-ion-plasma in the early post discharge cannot be observed due to the production of electrons in the post discharge. These observations are consistent with the determination of the atomic oxygen density and the ion species. This project is supported by the Deutsche Forschungsgesellschaft in the frame of SFB 191.

DTP 48 Experiments on Ion-Ion Plasmas From Discharges* DARRIN LEONHARDT, SCOTT WALTON,†DAVID BLACKWELL,‡DONALD MURPHY, RICHARD FERNSLER, ROBERT MEGER, *US Naval Research Laboratory, Plasma Physics Division* Use of both positive and negative ions in plasma processing of materials has been shown to be advantageous[1] in terms of better feature evolution and control. In this presentation, experimental results are given to complement recent theoretical work[2] at NRL on the formation and decay of pulsed ion-ion plasmas in electron beam generated discharges. Temporally resolved Langmuir probe and mass spectrometry are used to investigate electron beam generated discharges during the beam on (active) and off (afterglow) phases in a variety of gas mixtures. Because electron-beam generated discharges inherently[3] have low electron temperatures (<0.5eV in molecular gases), negative ion characteristics are seen in the active as well as afterglow phases since electron detachment increases with low electron temperatures. Analysis of temporally resolved plasma characteristics deduced from these measurements will be presented for pure O_2 , N_2 and Ar and their mixtures with SF_6 . Oxygen discharges show no noticeable negative ion contribution during the active or afterglow phase, presumably due to the higher energy electron attachment threshold, which is well above any electron temperature. In contrast, SF_6 discharges demonstrate ion-ion plasma characteristics in the active glow and are completely ion-ion in the afterglow. Comparison between these discharges with published cross sections and production mechanisms will also be presented. [1] T.H. Ahn, K. Nakamura & H. Sugai, *Plasma Sources Sci. Technol.*, 5, 139 (1996); T. Shibyama, H. Shindo & Y. Horiike, *Plasma Sources Sci. Technol.*, 5, 254 (1996). [2] See presentation by R. F. Fernsler, at this conference. [3] D. Leonhardt, et al., 53rd Annual GEC, Houston, TX.

*Work supported by the Office of Naval Research

†SFA Inc., Largo, MD

‡NRL/NRC Postdoctoral Research Associate

DTP 49 Characterization of Electronegative Oxygen Plasma JONG-SIK KIM, GON-HO KIM, *Department of Physics, Hanyang University-Ansan, Korea* DAE-CHUL KIM, BONG-JOO LEE, SUK-JAE YOO, *Korea Basic Science Institute(KBSI), Taejeon, Korea* ME JOUNG, MOO-HYUN CHO, *Department of Physics, Pohang University of Science Technology(POSTECH), Korea* Electronegative Oxygen plasma was investigated by using Langmuir probe and optical emission spectroscopy (OES) for an inductively coupled plasma with RF power and various operating pressure respectively. Negative ions are produced by the dissociation-attachment reactions between an oxygen atom and an electron. Hence, negative currents decreased. By using Langmuir probe for

negative ion generation could be observed by the measurement of the probe current ratio of positive and negative currents ($I^*_+/I^*_e+I^*_-$) and the potential difference ($e[V - p-V_f]/T_e$) at the plasma under a floating condition. The current ratio increased with the generation of the negative ions and had maximum value in the pressure range, 50 - 60 mTorr. The potential difference decreased with the generation of the negative ions and had minimum value in the pressure region of about 30 mTorr. Furthermore, the condition of operating pressure to achieve the maximum value, and the minimum value of potential difference was shifted from low pressure region to high pressure region because of the enhancement of the ion loss through the positive-negative ion recombination. By using OES for particle temperature and transition mechanism could be observed by the measurement of the wavelength and intensity. There is comparison between probe data and OES data. We observed intensity of O-ion and O-atom line. Then, we can predict negative ion generation.

DTP 50 Transient after Applying a DC Bias to an Ion-Ion Plasma

DEMETRE ECONOMOU, *University of Houston* BADRI RAMAMURTHI, *University of Houston* VIKAS MIDHA, *General Electric CRD* A one-dimensional fluid model was developed to investigate the initial response (transient) of a positive ion-negative ion (ion-ion) plasma to an applied DC bias voltage. The ion mass and momentum continuity equations were coupled to the Poisson equation for the electric field. The applied bias is shielded and space charge sheaths are formed within the time scale of ion response (ion plasma frequency). When the ion collision frequency is short compared to the ion plasma frequency, electric field oscillations develop in the bulk due to the ion inertia (overshoot). The net charge density in the sheath, the sheath electric field, and the flux and energy of ions bombarding the electrodes all go through maximum values at a time comparable to the ion plasma frequency. Over long time scales the sheaths are in quasi equilibrium with the bulk plasma. At this time, the ion flux on each electrode is twice the free diffusion flux. The results of this study are useful for understanding the response of an ion-ion plasma to a radio frequency (RF) bias voltage. Work supported by NSF

DTP 51 ELECTRON COLLISIONS AND PLASMA TRANSPORT PROPERTIES

DTP 52 Film morphology in electron stimulated desorption: O⁻ from O₂ on benzene

ANDREW D BASS, LUC PARENTEAU, FRITZ WEIK, LEON SANCHE, *CIHR Group in Radiation Sciences, Faculty of Medicine, University of Sherbrooke, Sherbrooke, Quebec, Canada* We investigate the effects of the film structure of multilayer benzene films on the desorption of O⁻ induced by 2 - 20 eV electron impact on varying quantities of absorbed O₂. Differences in the yield of O⁻ from O₂ doped amorphous and crystalline benzene films are attributed to the ability of O₂ to diffuse into the amorphous solid via pores and defects formed during its deposition at 20 K. In contrast, diffusion into crystalline benzene is limited and the deposited O₂ molecules remain at the surface of the film. Thermal desorption measurements support this analysis.

The data are also compared with results of similar experiments for O₂ on water. While it is apparent that some of the variation in O⁻ yield observed from ice films is similarly related to morphology, a substantial suppression of the O⁻ yield is likely to result from energy loss by electrons prior to dissociation. Quenching of intermediate anionic states of molecular oxygen by water ice may also contribute to this suppression in the range 5-12 eV.

DTP 53 A systematic analysis of elastic electron scattering from inert gases*

MEHRDAD ADIBZADEH, CONSTANTINE THEODOSIOU, *University of Toledo* As part of our simulation of gas discharges in plasma display panels we have been performing critical analyses of available experimental electron-atom cross sections. These studies include comparison between all available measurements and theoretical calculations for elastic electron scattering from inert gases at energies below 1 keV, and a multivariable fitting to obtain some predictive knowledge of these quantities. In order to produce a comprehensive coverage of energy and scattering angle ranges, still lacking experimentally and theoretically, we have developed a code that includes the effects of electron exchange and of target polarization by the incident electrons. We have studied the effect of the choices for the atomic central potential, exchange potential, and polarization potential used. Our recommended set of elastic scattering cross sections are in very good agreement with the measured values in the energies and angles that the latter are available. Furthermore, our calculations provide a comprehensive and accurate coverage of all (nonrelativistic) energies and angles and will be useful for future use in kinetic plasma simulations and for guidance to experimental investigations.

*Work supported by NSF Grant ECS9896103

DTP 54 Improved potential for first-order electron-impact excitation calculations*

CHRISTOPHER J. FONTES, ROBERT D. COWAN, GEORGE CSANAK, *Los Alamos National Laboratory* Some first-order scattering theories, such as the distorted-wave approximation, permit a different potential when solving for the initial and final free-electron wavefunctions. Other methods, such as first-order many-body theory, allow only a single (initial) potential for the solution of both the initial and final scattering orbitals. In practice, however, numerical procedures have been developed whereby free-electron orbitals are considered to arise from each of the different configurations that comprise a level. This approach results in scattering orbitals that are computed from the pertinent potential of the relevant configuration, rather than from a single potential associated with the level in question. Historically, the justifications for such a procedure have been (1) computational efficiency and (2) the lack of a general expression for obtaining a single potential associated with a level that contains mixing between states arising from more than one configuration (i.e. configuration interaction, or CI, occurs). Here we address the latter issue and present an expression for obtaining a single potential from a level that contains an arbitrary amount of CI. Numerical results will also be presented for electron-impact excitation of selected levels of rare gases and alkaline earth atoms in order to quantify the effect of this approach.

*This work was performed under the auspices of the US Department of Energy

DTP 55 Electron-Impact Excitation of Krypton from the Ground State and the Metastable Excited States A. DAS-GUPTA, *Naval Research Laboratory* K. BARTSCHAT, *Drake University* A.N. GRUM-GRZHIMAILO, *Moscow State University* D. VAID, D.H. MADISON, *University of Missouri-Rolla** We present results from non-perturbative R-matrix (close-coupling) and perturbative distorted-wave calculations for electron-impact excitation of Kr from the ground state and the metastable excited states. For some transitions, particularly from the ground state to the $2p_5$ and $2p_1$ states, i.e., $J = 0 \rightarrow 0$ transitions, the results are found to be extremely sensitive to the theoretical model for both the collision process and the target structure. Furthermore, the effect of negative-ion resonances near the excitation thresholds will be discussed. Our results will be compared with the available experimental data.

*Work supported by BMDO, ONR, NSF, and "Universities of Russia; Basic Research."

DTP 56 Calculated Electron-Mercury Cross Sections and Modeling of Fluorescent Lamps GRAEME LISTER, *OSRAM SYLVANIA*, Beverly, MA DMITRY FURSA, *The Flinders University of South Australia*, Adelaide, South Australia IGOR BRAY, *The Flinders University of South Australia*, Adelaide, South Australia The convergent close coupling method has been applied to the calculation of electron impact excitation and the electron momentum cross sections for mercury. The calculated cross sections have been included in the positive column model for low pressure lighting discharges GLOMAC [1], replacing previously used values deduced from electron swarm measurements by Rockwood [2]. Cross sections have also been calculated for transitions for which no data was previously available. The influence of this self consistent set of cross sections on modeling of mercury argon discharges is discussed. Modeling results using these cross sections are compared with experimental measurements for standard fluorescent lamps and discharges at increased power loading. Of particular interest is the ratio of visible to UV radiation as power loading is increased. [1] G G Lister and S E Coe, 1993, *Comp. Phys. Commun.* 75 160 [2] S D Rockwood, 1973, *Phys. Rev. A* 8 2348

DTP 57 Electron-impact excitation out of the $5^2P_{3/2}$ excited level of Rubidium* M. LARSEN, TODD A. ZIMMERMAN, JOHN B. BOFFARD, L. W. ANDERSON, CHUN C. LIN, *University of Wisconsin-Madison* A large fraction ($f_e \sim 0.4$) of the atoms in a magneto-optical atom trap are in the excited $Rb(5^2P_{3/2})$ level. We have previously used this source of excited atoms to measure the ionization cross section out of the 5^2P level of Rb.¹ In this work, we have used trapped atoms as a target for the measurement of electron-impact excitation cross sections. A monoenergetic electron beam is incident upon the ball of trapped atoms and the fluorescence given off by the decay of the excited atoms is detected by a PMT. If the trapping lasers are briefly turned off during the electron beam pulse, the trap contains only 5^2S atoms. By leaving the lasers on during the electron beam pulse, the trap contains both 5^2S and 5^2P atoms. Combining the ratio of signals from the two cases with the measured excited state fraction yields

the ratio of the excitation cross sections from the 5^2S and 5^2P levels. When combined with the previously measured ground state cross sections, we obtain cross section measurements out of the $5^2P_{3/2}$ level. Results for excitation into the $5^2P_{1/2}$, 5^2D , and 7^2S levels will be presented.

*This work supported by the NSF and AFOSR.

¹M.L. Keeler, *et al.*, *Phys. Rev. Lett.* 85, 3353 (2000).

DTP 58 Resonant Vibrational Excitation of CO₂ by Electron Impact* T.N. RESCIGNO, *LBNL/LLNL* W.A. ISAACS, *LLNL* A.E. OREL, *UC Davis* C.W. MCCURDY, *LBNL/UC Davis* We report the results of a theoretical study of the dynamics of resonant vibrational excitation of CO₂ by low energy electrons. We have performed first-principles electron scattering calculations for a number of different fixed-nuclei geometries to obtain the dependence of both the resonance energy surface and its lifetime on both symmetric stretch and bending. We have used this complex potential surface in a time-dependent treatment to study the nuclear dynamics and to calculate the vibrational excitation cross sections. The three-dimensional time-dependent Schrödinger equation was solved using the multi-configuration time-dependent Hartree method (MCTDH). We will show that such a treatment reveals details of the resonant vibrational excitation process that cannot be properly described in a simplified one-dimensional "boomerang" treatment.

*Work performed under auspices of US DOE by University of California LBNL and LLNL under contract numbers DE-AC03-76SF00098 and W-7405-Eng-48, respectively.

DTP 59 Electron Collisions with *c*-C₄F₆ (Hexafluorocyclobutene)* CARL WINSTEAD, VINCENT MCKOY, *Caltech* Nonsaturated fluorocarbons have attracted interest as alternative plasma etchants because of their low global warming potential. To form a basis for modeling and simulation of plasma properties, it is essential to have available electron cross section information for these gases. In this work, we have studied low-energy electron collisions with *c*-C₄F₆ using the Schwinger multichannel method, a first-principles variational method adapted to electron collisions with polyatomic targets. We report the differential, integral, and momentum-transfer elastic cross sections, as well as excitation cross sections for low-lying excited states. We compare our results to the limited experimental data available and to cross sections for related fluorocarbons.

*Work supported by DOE and Intel Corp.

DTP 60 Absolute Cross Sections for the Formation of Si Atoms Following Neutral Dissociation of SiH₄ and SiF₄ by Electron Impact T. RAYNOR, *Stevens Institute of Technology* K. BECKER, *Stevens Institute of Technology* K. MARTUS, *William Paterson University* NINA ABRAMZON, *JILA-University of Colorado* We report the results of experimental studies aimed at measuring absolute cross sections for the formation of Si atoms following neutral dissociation of SiH₄ and SiF₄ by electron impact. Electron-impact dissociation of the SiH₄ and SiF₄ parent molecules produces Si atoms in respectively the 1D and 1S state of the Si ground state electron configuration. The Si(1D) and Si(1S) atoms are probed by laser-induced fluorescence pumping either the 1S \rightarrow 1P transition at 391 nm and observing the 1P \rightarrow 1D

fluorescence at 288 nm or by pumping the 1D \rightarrow 1P transition at 288 nm and observing the 1P \rightarrow 1S fluorescence at 391 nm. After proper normalization, absolute neutral dissociation cross sections with peak values near $1 \times 10^{-17} \text{ cm}^2$ are obtained for the final-state selective formation of the ground state Si atoms following neutral electron impact dissociation of SiH₄ and SiF₄. Work supported by the US DOE, Office of Science.

DTP 61 Electron-impact ionization of methane WINIFRED HUO, *NASA Ames Research Center* CHRISTOPHER DATEO, *Eloret* We report a study of the total ionization of CH₄ by electron impact and its dissociative ionization from the 2T_2 channel. The calculation of the total ionization cross section uses the improved Binary-Encounter-Dipole model (iBED).¹ The dipole Born cross section in the model is expressed in terms of a three-term representation and the optical oscillator strengths are taken from Backx and Van der Wiel.² The nuclear dynamics for the dissociation of the 2T_2 channel is studied using the statistical model. A search of the potential energy surface of the 2T_2 state of CH₄⁺ shows two minima, of C_{2v} and C_{3v} symmetries, in agreement with earlier calculations.³ The dissociation of the CH₄⁺ to CH₃⁺ + H goes through a saddle point. Comparison with recent experimental data will be presented and the role of Jahn-Teller effect discussed.

¹W. M. Huo, Phys. Rev. A (submitted for publication).

²C. Backx and M. J. Van der Wiel, J. Phys. B **18** 3020 (1975).

³(a) K. Takeshita, J. Chem. Phys. **86**, 329 (1987). (b) R. F. Frey and E. R. Davidson, J. Chem. Phys. **88**, 1775 (1988).

DTP 62 Calculated Cross Sections for the Electron Impact Ionization of Simple Molecular Ions H. DEUTSCH, *Universitat Greifswald, Germany* K. BECKER, *Stevens Institute of Technology, USA* P. DEFRANCE, *Universite Catholique de Louvain, Belgium* U. ONTHONG, *Universitat Innsbruck, Austria* M. PROBST, *Universitat Innsbruck, Austria* S. MATT, *Universitat Innsbruck, Austria* T. MARK, *Universitat Innsbruck, Austria* We applied the semi-classical Deutsch-Mrk (DM) formalism, which was originally developed for the calculation of atomic electron-impact ionization cross sections and later extended to molecules, radicals, and clusters, to the calculation of absolute electron-impact ionization cross sections of simple molecular ions such as CO₂⁺, H₃O⁺, and H₂⁺. A comparison with available experimental data reveals significant discrepancies in the case of CO₂⁺ and H₃O⁺ which can be attributed (i) to appreciable contributions to some of the measured cross sections due to dissociative excitation channels which are not described by the DM formalism and (ii) the omission of some important dissociative ionization channels in the experiments which are, on the other hand, included in the calculated cross sections. Work supported in part by NASA, the FWF, Wien, Austria and carried out within the Association EURATOM/AW, Wien, Austria.

DTP 63 Electron-Impact Ionization of Diborane RALF BASNER, MARTIN SCHMIDT, *Institut für Niedertemperatur-Plasmaphysik, Greifswald, Germany* KURT BECKER, *Stevens Institute of Technology, Hoboken, USA* HANS DEUTSCH, *University of Greifswald, Greifswald, Germany* Diborane (B₂H₆) is one of the precursors for the plasma-assisted thin film deposition of boron or cubic boron nitride. We report measurements of absolute electron-impact ionization cross sections for the formation

of all fragment ions from threshold to 200 eV. The measurements were carried out in a well-characterized time-of-flight mass spectrometer with complete collection of fragment ions, which are formed with excess kinetic energy. Dissociative ionization of diborane is the dominant ionization process and it generates the single positive fragment ions H⁺, H₂⁺, BH_x⁺ (x=0-3), and B₂H_y⁺ (y=0-5). The parent B₂H₆⁺ ions, which are stable in the period from 10⁻⁷ to 10⁻⁵s after their formation, were detected with lower abundance. No evidence for the formation of doubly charged ions was found within the energy range studied. The experimentally determined total B₂H₆⁺ single ionization cross section is also compared to a theoretical prediction from semi-empirical calculations.

DTP 64 Electron Impact Ionization Cross Sections of n-decane CHARLES JIAO, *ISSI* CHARLES DEJOSEPH, ALAN GARSCADDEN, *Air Force Research Laboratory, WPAFB* The ionization and dissociation of hydrocarbon fuels with various plasma excitation schemes including pulsed high E/n discharges have been proposed to alleviate the problem of ignition in supersonic flow combustors and operations at high altitudes. The fuel which is also used for cooling, must not pyrolyse at operational temperatures. We have examined the electron ionization collision processes in n-decane using high resolution Fourier transform mass spectrometry that permits measurements of the 24 ions with cross sections larger than 10⁻¹⁹cm². These generally fall into two broad categories: those with five or more carbon atoms whose ionization cross sections rise rapidly and essentially saturate within twice the appearance potential and those with four carbon atoms and less whose cross sections rise more gradually and are only saturating at energies above 70 eV. The total ionization cross section is large, rising to 7x10⁻¹⁶cm². Studies were made with deuterated samples to distinguish the potential mechanisms in fragment ion induced dissociation of the parent gas. The results are compared with similar data for octane.

DTP 65 Estimation of Cross Sections for Collisions between Ions and Atoms of Different Species over Wide Energy Ranges. A.V. PHELPS, *JILA, U. of Colorado and NIST* We consider the utility of cross sections for elastic collisions of asymmetric ion-atom pairs over a wide energy range when calculated using the simple Langevin formula for scattering by a pure polarization potential¹. The Langevin cross sections depend only on the dipole polarizability of the target atom when plotted versus energy in the center-of-mass system. To evaluate the accuracy of this approximation we compare it with detailed calculations of the elastic diffusion and viscosity cross sections for several ion-atom pairs. In the H⁺ - He case², the Langevin cross sections are within $\pm 20\%$ for energies up to 2 eV, but the error increases to a factor of ~ 6 by 100 eV. For O⁺ - N and N⁺ - O collisions³, the Langevin formula is high by $\sim 40\%$ at 0.1 eV and within 5% for 5 to 50 eV. In the Na⁺ - Xe case⁴, the Langevin cross sections are low by 20% at 0.1 eV, high by about 30% at 1 eV, and low by about 50% at 300 eV.

¹E. W. McDaniel, *Collision Phenomena in Ionized Gases* (Wiley, New York, 1964) p. 72.

²P. S. Krstic and D. R. Schulz, J. Phys. B **32**, 3485 (1999).

³H. Partridge, J. R. Stallcop, and E. Levin, Chem. Phys. Lett. **184** 505 (1991).

⁴A. V. Phelps, (unpublished).

DTP 66 Composition of positive ions in high-density hydrogen plasmas K SASAKI, H. YAMAGUCHI, K. KADOTA, *Department of Electronics, Nagoya University, Japan* The particle balance of charged species in a hydrogen plasma is significantly affected by the composition of positive ions. This is because the reaction rate coefficient for recombination with molecular ions ($H_x^+ + e \rightarrow H_{x-1} + H(x = 2,3)$) is much larger than that with atomic ions ($H^+ + e \rightarrow H + h\nu$). In the present work, we adopted a time-of-flight mass spectrometer for determining the composition of positive ions in high-density, helicon-wave excited hydrogen plasmas. The experiment was carried out in a linear machine with a uniform magnetic field of 1 kG along the cylindrical axis of the vacuum chamber. The time-of-flight mass spectrometer was attached behind the end plate which had a hole of 1 mm diameter. The dominant ion was H_3^+ for electron density below $2 \times 10^{11} \text{ cm}^{-3}$, while in high-density plasmas with $n_e \geq 8 \times 10^{11} \text{ cm}^{-3}$, H^+ and H_2^+ were dominant and had a similar fractional abundance. In the afterglow plasma after the termination of the rf power, the fraction of H_2^+ decreased rapidly with a time constant of $\sim 3 \mu\text{s}$. Instead of the disappearance of H_2^+ , H_3^+ became dominant in the afterglow. The fraction of H^+ was almost constant. The above experimental results were examined by a rate equation analysis based on available reaction rate coefficients. The results of the rate equation analysis was qualitatively consistent with the experimental observations.

DTP 67 Effective Ionization Coefficients and Electron Drift Velocity in $CHF_3 - Ar$ Mixtures* EDUARDO BASURTO, *Depto. Ciencias Basicas, UAM-A* JOSE LUIS HERNANDEZ, *Depto. Energia, UAM-A* JAIME DE URQUIJO, *Centro de Ciencias Fisicas, UNAM* The Pulsed Townsend Method has been used to measure the electron drift velocity and the density-normalized effective ionization coefficient ($a - h$)/ N (a and h are the ionization and attachment coefficients, respectively), over the reduced electric field intensity E/N , from 0.26 to 140 Td ($1 \text{ Td} = 10^{-17} \text{ Vcm}^2$), at CHF_3 concentrations between 1 and 20 per cent. The drift velocities display a pronounced Ramsauer Townsend minimum and maxima, which are strongly dependent on the mixture ratio. We have found good agreement between our drift velocity values and those of Wang et al for E/N less than about 50 Td. The ($a - h$)/ N values increase sharply for E/N greater than 40 Td, and are also dependent on the mixture ratio. For E/N lower than 10 Td, ($a - h$)/ N becomes more negative as the CHF_3 share increases. We are not aware of any published value for this parameter in these mixtures.

*Supported by DGAPA, Project IN113898.

DTP 68 Observation of mutual neutralization in detached plasma TONEGAWA AKIRA, *Department of Physics, School of Science, Tokai University* SHIROTA ISAO, *Department of Physics, School of Science, Tokai University* YOSHIDA KEN'ICHI, *Department of Physics, School of Science, Tokai University* ONO MASATAKA, *Department of Nuclear Energy, School of Engineering, Tokai University* KAWAMURA KAZUTAKA, *Research Institute of Science and Technology, Tokai University* WATANABE TUGUHIRO, *National Institute for Fusion Science* OHYABU NOBUYOSHI, *National Institute for Fusion Science* SUZUKI HAJIME, *National Institute for Fusion Science* TAKAYAMA KAZUO, *Research Institute of Science and Technology, Tokai University* DEPARTMENT OF PHYSICS, SCHOOL OF SCIENCE, TOKAI UNIVERSITY TEAM, 2DEPARTMENT OF NUCLEAR ENERGY, SCHOOL OF ENGI-

NEERING, TOKAI UNIVERSITY TEAM, RESEARCH INSTITUTE OF SCIENCE AND TECHNOLOGY, TOKAI UNIVERSITY TEAM, NATIONAL INSTITUTE FOR FUSION SCIENCE COLLABORATION, Mutual neutralization in collisions between negative ions and positive ions in molecular activated recombination (MAR) has been observed in a high density magnetized sheet plasma source TPDSHEET-IV (Test Plasma produced by Directed current for SHEET plasma) device. Measurements of the negative ion density of hydrogen atom, the electron density, electron temperature, and the heat load to the target plate were carried out in hydrogen high density plasma with hydrogen gas puff. A cylindrical probe made of tungsten ($0.4 \times 2 \text{ cm}$) was used to measure the spatial profiles of H^- by a probe-assisted laser photodetachment. The Balmer spectra of visible light emission from hydrogen or helium atoms were detected in front of the target plate. A small amount of secondary hydrogen gas puffing into a hydrogen plasma reduced strongly the heat flux to the target and increased rapidly the density of negative ions of hydrogen atom in the circumference of the plasma, while the conventional radiative and three-body recombination processes were disappeared. These results can be well explained by taking the charge exchange recombination of MAR in the detached plasma into account.

DTP 69 Helium Gas Contact Cooling of Argon Plasma Jet and Population Inversion of Ari KATSUHIRO KANO, HIROSHI AKATSUKA, *Research Laboratory for Nuclear Reactors, Tokyo Institute of Technology* An experiment of He gas-contact for generating population inversion in a recombining Ar plasma jet is demonstrated in the present study. Up to the present time, population inversion of H sci and He sci was found in the hydrogen and helium plasma jets, respectively, while it was not found in argon plasma jet. It was also found that its electron temperature T_e was higher than that of helium and hydrogen plasmas. Lowering of T_e is essential to make population inversion in plasma jets in recombining phase. We discuss relaxation process of electrons in the plasma jet numerically in the present study. It is found that the electrons are relaxed mainly by elastic collisions with residual neutral gas molecules in the plasma jet. Since argon atom has Ramsauer minimum in its electron elastic scattering cross section at the energy range 0.3 - 0.5 eV, we found that collisional relaxation of electrons in these energy range is accomplished by helium contact cooling, which has no Ramsauer minimum. Consequently, population inversion between Ar sci excited states $5s' \rightarrow 4p'[1/2]_{1,2}$ and $5s' \rightarrow 4p[3/2]_{1,2}, [5/2]_{2,3}$ has been created experimentally by helium gas-contact cooling of electrons.

DTP 70 GENERATION OF EXTREMELY LOW FREQUENCY ELECTROMAGNETIC RADIATION BY BEAMS. TOIR KHAZRATOV, T. M. MUMINOV, U. S. SALIKHBAEV, *Samarkand State University, Uzbekistan* In this report the results of investigation of extremely low frequency (ELF) secondary electromagnetic radiation (SER) generated by beams of electrons of microtron MT-22S ($E=13 \text{ MeV}$, average current $I=1-10 \text{ mA}$, $t=2,5 \text{ mks}$, $f=386 \text{ Hz}$) in residual gas in dielectric electronpipe (glass, diameter $d=50 \text{ mm}$, length 120 m) have been expounded. Measurements were carried out at the final 15 m part of the electronpipe where the pressure of residual gas could be regulated within the limits of $0,1-100000 \text{ Pa}$. An on line control system (based on spectrometr CK-4-72, CAMAC system and IBM computer) with electric (synphase connected planar vibrators) and

magnetic(ferrite-rod) antennas were used to registrate ELF SER. The remote controller gave the opportunity to change the antenna orientation and its position along and transverse to the axis of electron beam. The spectrum of SER and the dependence of SER signals amplitude in close zone(U), on value of beams current(I), on the length antenna-electronpipe axis(D), spatial orientation of the antenna, on the distance the front of measured part-antenna(L) and on pressure have been investigated. The analysis of obtained results permits to make the following conclusion: the pulse beams of electrons generate ELF SER with the frequencies integer multiple of f frequency of electron pulses; the SER electric component has horizontal polarization; the dependence of U on pressure is determined by the distance L and electron beam weakening processes in the gas; the dependence of U on current I and distance D in close zone has a linear character. It is obvious that full understanding of the processes of SER generation by the charged particle in gaseous medium and the investigation of their possible practical application in experiments needs to use the heavy current particle beams.

SESSION ET1: LIGHTING

Tuesday afternoon, 9 October 2001

Ballroom C Nittany Lion Inn at 15:30

Vikas Midha, GE Research and Development, presiding

15:30

ET1 1 Modeling of Breakdown Processes in Cold and Warm Metal Halide Lamps* RICHARD MOSS, MARK J. KUSHNER, *University of Illinois* Startup processes in high pressure, metal halide lamps are of interest for lamp restart and to extend the lifetime of the lamps by reducing electrode erosion. To investigate these processes, a 2-dimensional model of metal halide lamps has been developed and applied to a parametric study of startup. The model employs an unstructured mesh, and an implicit solution for charged and neutral particle transport in concert with Poisson's equation. Electric field and secondary emission from surfaces is included, as is radiation transport for photoionization sources and a circuit model. Lamps employing trigger electrodes have been investigated while varying cold Ar fill pressure and Hg metal vapor density (as a measure of cold or hot operation). The consequences of voltage format, lamp geometry and internal and external (capacitive) trigger electrodes on breakdown will be discussed.

*Work supported by General Electric and NSF (CTS99-74962)

15:45

ET1 2 Monte Carlo Simulation of Radiation Trapping in Electrodeless Lamps: Complex Geometries and Isotope Effects* KAPIL RAJARAMAN, MARK J. KUSHNER, *University of Illinois* GRAEME G. LISTER, *Osram Sylvania Inc.* Electrodeless gas discharges are finding increasing applications as lighting sources, particularly for Ar/Hg based fluorescent lamps. The particulars of trapping of resonance radiation from Hg is an important consideration in the design of such sources. Analytical expressions

for radiation trapping factors can be obtained for simple geometries. Current lamp designs have complex geometries with non-uniform densities of photon absorbers and emitters. To address these complexities, a Monte Carlo radiation transport model has been developed which accounts for frequency resolved emission, transport and absorption while employing partial frequency redistribution. Isotope effects have also been incorporated into the model. This radiation transport model has been integrated into a 2-dimensional plasma equipment model which is a self-consistent accounting of electromagnetics, electron energy and density transport, and heavy particle transport while solving Poisson's equation. The scaling and consequences of radiation trapping in complex geometries will be discussed for low pressure inductively coupled lamps using Ar/Hg mixtures. We found that cathodoluminescence produces a nonuniform distribution of radiators which makes application of simpler scaling laws questionable.

*Work supported by Osram-Sylvania and NSF (CTS99-74962)

16:00

ET1 3 Microwave-induced electrical breakdown of high pressure gases for application to light sources* BYUNGMOO SONG, DAVID HAMMER, *Cornell University* C. GOLKOWSKI, *Superpulse* Measurements of microwave breakdown at 2.45GHz in high pressure Ar, Kr and Xe have been made in a tunable microwave cavity. The influence of UV illumination on the statistical spread of microwave-induced electrical breakdown at pressures up to 300 Torr, and the use of a fiber initiator to achieve breakdown above atmospheric pressure are presented. A marked decrease in the statistical spread in breakdown was observed with UV illumination, but the maximum pressure at which breakdown occurred in the cavity with and without UV illumination was the same. To initiate breakdown in gases above 1 atm, we used a Pt-coated SiC fiber. This combination takes advantage of the physical properties of a SiC fiber, and the conductivity of Pt to enhance the applied macroscopic electric field at the fiber tip. The resulting tip-emitted electrons experience the strongly enhanced electric field around the tip, and electron multiplication can occur, seeding a breakdown event. Using 8 micron diameter SiC fibers coated with a 0.2 micron thick Pt, breakdown fields were obtained with 0.25-1 ms pulses in the pressure ranges 1-3 atm for Ar, Kr and Xe. The required field at 2280 Torr with one fiber was less than that at 200 Torr without a fiber. The increase of the breakdown field with pressure is much slower than linear.

*Funded by Fusion Lighting, Fusion UV Systems and Axcelis Tech.

16:15

ET1 4 He₂* (60-100nm) and Ne₂* (80-90nm) excimer lamps pumped by low energy electron beams ANDREAS ULRICH, *Fakultät für Physik E12, Technische Universität München, Garching, Germany* JOCHEN WIESER, *Gesellschaft für Schwerionenforschung, Darmstadt, Germany* MANFRED SALVERMOSER, *Dept. of Physics, Rutgers University, Newark, NJ, USA* DANIEL E. MURNICK, *Dept. of Physics, Rutgers University, Newark, NJ, USA* Low energy (10 to 20keV) electron beams transmitted through extremely thin ceramic foils into high pressure rare gases and rare gas mixtures have been demonstrated to produce efficiently excimer radiation [1,2]. In this report, previous work has

been extended to the deep UV emission from helium and neon excimers. The localized nature of the excitation allows windowless systems to be used in a rare gas atmosphere transparent to the 60 to 100nm radiation produced. Both pulsed and cw sources can be realized with extremely high brightness possible. Because of the high energy per photon, such systems may be useful for a variety of materials modification applications. [1] J. Wieser et al. *Rev. Sci. Instrum* 68, 1360 (1997) [2] M. Salvermoser et al., *J. Appl. Phys.* 88, 453 (2000) [3] A. Ulrich et al. *Physikalische Blätter* 56, 49 (2000)

16:30

ET1 5 Pulsed microhollow cathode discharge excimer sources
MOHAMED MOSELHY, WENHUI SHI, ROBERT H. STRAK, KARL H. SCHOENBACH, *Physical Electronics Research Institute, Old Dominion University, Norfolk, VA 23529* Microhollow cathode discharges (MHCDs) are non-equilibrium, high-pressure gas discharges between perforated electrodes separated by a dielectric layer. Typical dimensions for the electrode foil thickness and hole diameter are 100 μm . Direct current experiments in xenon, argon, neon, helium, argon fluoride, and xenon chloride [1,2] have been performed. The excimer efficiency varies between 1 % and 9 %. Pulsed operation allowed us to increase the current from 8 mA (dc) to approximately 80 mA (pulsed with a pulse width of 700 μs), limited by the onset of instabilities. The total excimer power was found to increase linearly with current, however, the radiant emittance and efficiency stayed constant. Reducing the pulse duration into the nanosecond range allowed us to increase the current into the ampere range. The maximum measured excimer power was 2.75 W per microdischarge. The maximum radiant emittance was 15 W/cm^2 and the efficiency reached values of 20 %. This effect is assumed to be due to non-equilibrium electron heating in the high-pressure plasma [3]. This work was supported by the National Science Foundation under grant # CTS0078618. 1. Karl H. Schoenbach, Ahmed El-Habachi, Mohamed M. Moselhy, Wenhui Shi, and Robert H. Stark, *Physics of Plasmas* 7, 2186 (2000). 2. P. Kurunczi, J. Lopez, H. Shah, and K. Becker, *Int. J. Mass Spectrom.* 205, 277 (2001). 3. Robert H. Stark and Karl H. Schoenbach, *J. Appl. Phys.* 89, 3568 (2001).

16:45

ET1 6 Koedam Beta Factors Revisited J.E. LAWLER, *Univ. of Wisconsin-Madison* G.G. LISTER, *OSRAM-SYLVANIA INC.* D.A. DOUGHTY, *Perkin-Elmer Optoelectronics* Koedam Beta Factor (KBF) values are very useful in radiometric efficiency studies of glow discharge plasmas for lighting applications. A KBF enables one to compute the total output power in resonance radiation from a positive column using a single radiance measurement normal to an aperture in the wall, by correcting for the non Lambertian angular distribution of flux. New Monte Carlo simulations of KBF values for a variety of conditions are reported. We find KBF values in the range of 0.7 to 0.8 for a parabolic source function or fundamental mode source function, independent of optical depth with a uniform density of ground state (absorbing) atoms. These KBF values are in conflict with earlier theoretical results (typically 0.6), but are in agreement on the weak variation of KBF with optical depth or column radius. An analytic calculation is used to check the new results in the limit of low optical depth. A com-

parison of the new results to experimental KBF's (also about 0.6) requires modeling of additional effects. An analysis of the effects of reflection and lensing at the tube wall is presented. The effect of radial cataphoresis on the KBF is also explored.

17:00

ET1 7 On the importance of Coulomb collisions for the modeling of positive column plasmas* UWE KORTSHAGEN, *University of Minnesota - Dept. of Mechanical Engineering* Positive column plasmas used in discharge light sources often operate at high current densities for which Coulomb collisions may be important. There are two main influences of Coulomb collisions: (1) Electron-electron collisions may drive the electron energy distribution function towards a Maxwellian distribution. (2) Momentum transfer in electron-ion collisions may be an important contribution to the overall electron momentum transfer, affecting transport parameters such as the electron mobility. In this contribution, we study the effect of Coulomb collisions using a selfconsistent positive column model. The electron distribution function is obtained by solving the radially dependent Boltzmann equation. The ion motion is described by a fluid model accounting for mobility and ion inertia. The ambipolar electric field is determined by the solution of the Poisson equation. An efficient iterative scheme is discussed which leads to a selfconsistent solution of this set of equations.

*This work is supported by DOE under grant 54554 and by General Electric R & D.

17:15

ET1 8 Spectroscopic Identification of Novel Catalytic Reaction in Hydrogen Plasma PARESH RAY, *BlackLight Power Inc.* RANDELL MILLS, *BlackLight Power Inc.* We report a breakthrough observation of intense extreme ultraviolet (EUV) emission from incandescently heated hydrogen and a gaseous catalyst (e.g. Ar +, Ne +, Sr, Rb +, K and Cs) that generated a plasma at low temperatures and low voltage. Typically the emission of extreme ultraviolet light from hydrogen gas is achieved by a discharge at high voltage or by high power microwaves. No emission was observed with catalyst or hydrogen alone. The emission intensity of the plasma generated by the Cs or Sr catalyst increased significantly with the introduction of Ar gas only when Ar+ emission was observed, wherein Ar+ acted as a second catalyst. Mills predicts that atomic hydrogen may react with a catalyst to form a lower energy state hydrogen which further reacts to form a corresponding hydride ion. The mechanism is a nonradiative resonant energy transfer from atomic hydrogen to a catalyst of a multiple of the potential energy of atomic hydrogen (m X 27.2 eV). Exemplary catalytic reactions are: Ar + + 27.3 eV \rightarrow Ar 2+ + e-, Cs (m) + 27.05 eV \rightarrow Cs 2+ + 2e-, K (m) + 81.7 eV \rightarrow K 3+ + 3e-, Rb + + 27.28 eV \rightarrow Rb 2+ + e-, Sr (m) + 188.2 eV \rightarrow Sr 5+ + 5e-, Ne + + H + + 27.36 eV \rightarrow Ne 2+ + H The EUV spectra showed the presence of K 3+, Rb 2+, Ar 2+, Ne 2+ and Cs 2+ in hydrogen plasma which confirmed the catalysis mechanism. Predicted novel higher binding energy hydride ions were observed in our emission spectra. Further, the catalysis reaction may be highly energetic. It is very interesting to note that our EUV spectrum indicated the presence of highly ionized Ar ions [e.g. Ar (XI)] which can not be theoretically or experimentally produced with 200 V glow discharge.

**SESSION ET2: GLOWS: DC PULSED RF,
MICROWAVE, INDUCTIVE, OTHER**

Tuesday afternoon, 9 October 2001

Ballroom AB Nittany Lion Inn at 15:30

Vladimir Kolobov, CFD Research, presiding

15:30

ET2 1 Pulsed DC Magnetron Plasma: Time-Resolved Investigation A. BELKIND, *Stevens Institute of Technology* K. BECKER, *Stevens Institute of Technology* Z. ZHAO, *Stevens Institute of Technology* DC reactive sputter deposition of dielectric can be greatly effected by arcing. Observations have indicated that arcing is due to breakdown, of the dielectric (oxide) film, which grows on the surface of the metal target, as a result of positive charge accumulation. The use of pulsed-DC power has been employed to reduce or eliminate arcing. Using duty cycles, which could be varied between 10 dynamics were studied. Plasma decay during off-time and its reestablishment during on-time are investigated using time-resolved electrical and optical measurements. Plasma dynamics and its relationship with deposition process are discussed. Work supported by Advanced Energy Industries, Inc.

15:45

ET2 2 Study of the Two-Dimensional Electric Potential Structure in the Anode Region of Cylindrical Glow Discharge Plasmas STEFAN ARNDT, DIRK UHRLANDT, ROLF WINKLER, *Institut für Niedertemperatur-Plasmaphysik, 17489 Greifswald, Germany* The anode region of a cylindrical glow discharge represents the transition region between the axially homogeneous and radially inhomogeneous positive column and the equipotential anode surface. Thus, a very complex structure of the electric potential is to expect. Up to now, no detailed description of the potential structure has been performed. Previous experiments have only provided a rather restricted view. The potential has to be determined in two space dimensions because its strong axial variation in front of the anode as well as the transition from the radial space-charge confinement to the equipotential anode surface have to be taken into account. The potential structure is studied by the coupled solution of the Poisson's equation for the electric potential and the hydrodynamic equations of the electrons and ions, i.e., their particle and momentum balance equations. The transport properties of the electron component, described by the spatially varying diffusion coefficient, mobility, and mean collision frequencies of the electrons, are obtained from a strict kinetic description of the electrons in the anode region by solving the spatially two-dimensional Boltzmann equation¹.

¹S. Arndt, D. Uhrlandt, R. Winkler, *J. Phys. D: Appl. Phys.*, **34** (2001), in press

16:00

ET2 3 Selfconsistent Description of the He Plasma in an Axially Symmetric Hollow Cathode F. SIGENEGGER, R. WINKLER, *Institut für Niedertemperatur-Plasmaphysik, Greifswald, Germany* The radial variations of the electron properties, the excited atom densities and the electric field of a cylindrical helium hollow cathode discharge at pressures of some Torr and discharge currents of some mA have been theoretically investigated. An axially symmetric arrangement consisting of a central hollow cathode and two, symmetrically arranged anodes is considered which

recently has been experimentally investigated. The studies refer to the plasma around the axial center where the axial inhomogeneity can be neglected. The radial variations of the electron properties and the excited atom densities have been determined by a coupled solution of the radial-dependent electron Boltzmann equation and the particle balance equations of the excited atoms. Based on a tensorial expansion of the electron velocity distribution function a multiterm approach has been developed for the solution of the electron Boltzmann equation. The radial profile of the strongly varying radial electric field is determined from the Poisson equation which is selfconsistently coupled with the electron and excited state kinetics and the ion particle and momentum balance equations. The results evidence a distinct nonlocal behavior of the electrons in the transition from the cathode fall to the negative glow. The profiles of higher excited atoms partly show pronounced minima in the center and strongly change with the pressure.

16:15

ET2 4 Sonoluminescence, a weakly ionized plasma* DOMINIK HAMMER, *Department of Physics, The University of Texas at Austin* LOTHAR FROMMHOLD, *Department of Physics, The University of Texas at Austin* Large-amplitude ultrasonic waves in water cause cavitation. Micrometer-sized gas bubbles expand and contract (implode) synchronously with the sound for many acoustic cycles and emit a flash of light once per cycle. This is called (single-bubble) sonoluminescence (D. Hammer et al., *J. Mod. Opt.* **48**, 239 (2001)). We present numerical simulations of sonoluminescent bubbles that predominantly consist of rare gas atoms, but water vapor and chemical reactions of the dissociation products of water have also been included. Since peak temperatures of above 10,000 K are reached at densities of a few hundred amagat the gas mixture is weakly ionized. Thus we include in our model radiation due to electron-ion and electron-neutral bremsstrahlung, recombination radiation and radiative electron attachment to oxygen and hydrogen atoms. We find all of these processes to be important, yet to a varying degree, depending on the input parameters of our simulation. Spectral shapes and intensities as well as light pulse widths in good agreement with experiment are obtained.

*The support by the Welch Foundation, Grant 1346, is gratefully acknowledged.

16:30

ET2 5 Pressure Heating of Electrons by Capacitive RF Sheaths GEORGE GOZADINOS, *Dublin City University, Ireland* DAVID MILES M. TURNER, *Dublin City University, Ireland* DAVID VENDER, *Dublin City University, Ireland* High-frequency plasma discharges are often sustained by collisionless heating of electrons—the nature of these mechanisms is a central problem in the theory of such discharges. In capacitive discharges, collisionless heating occurs in the vicinity of boundaries, and is often attributed to inelastic collisions of electrons with oscillating plasma sheaths, regarded as moving rigid barriers—the “hard wall” model. We show that when current conservation is required, such heating necessarily vanishes, and we conclude that this accepted model of the heating process cannot be correct. We go on to develop an alternative view that associates the heating with acoustic disturbances in the electron fluid. An analytic model based on moments of the Vlasov equation reduces the computation of the heating effect to a quadrature, and gives results in good agreement with particle-in-cell simulations. In terms of individual particle dynamics, this acoustic heating may be interpreted as a transit-time effect.

16:45

ET2 6 Comparison of Plasma Characteristics between Electro-Positive and Electro-Negative Gases in Two-Dimensional Model SOON-YOUL SO, HIROTAKE SUGAWARA, YOSUKE SAKAI, *Hokkaido University, Sapporo 060-8628 Japan* Analysis of plasmas is necessary for high-quality electronic material processing and its general control. Study of the electro-positive and electro-negative discharges for etching and deposition is important as such analysis. For example, a one-dimensional fluid model has been developed for these discharges and their properties were compared in a previous report.¹ In this work, a two-dimensional fluid model of rf plasma was developed for a cylindrically symmetric coordinate system based on the GEC reference cell. Ar and SiH₄ are taken as electro-positive and electro-negative discharge media. The calculation was performed at 100–500 mTorr at 13.56 MHz (rf). The model is based on continuity equations for the plasma species and electron energy conservation coupled with Poisson's equation. The calculation result predicts that the plasma structures in a periodic steady state show an off-axis maximum of the plasma density due to the guard ring and dc self-bias of the powered electrode. Then, the results are compared to those of a one-dimensional. We discuss the characteristics of electro-positive and electro-negative discharges in comparison between one- and two-dimensional models.

¹N. Nakano and T. Makabe, *J. Phys. D: Appl. Phys.* **28**, 31–5 (1995)

17:00

ET2 7 Microwave excitation in large-area plasma sources without large dielectric plate IVAN GANACHEV, *Shibaura Mechatronics* YUSUKE NAKAI, HIDEO SUGAI, *Department of Electrical Engineering, Nagoya University* Large-area non-magnetized microwave plasmas have been traditionally excited along large-area dielectric walls. Still excitation through small dielectric windows in a metal wall has been found possible^{1,2} and may be sometimes advantageous. Initial interpretations^{1–3} suggested as one possible explanation surface-wave (SW) propagation along a sharp [sheath]–[bulk plasma] boundary along the metal wall. Another explanation was non-local plasma production in the volume by long-free-path electrons locally heated at the windows (this supported by the observed pressure dependence²). In the present contribution we present a theoretical analysis supporting this second explanation. Taking into account the continuous electron density profile decreasing towards the wall, we found that the SW, although indeed excited at the windows, decays dramatically within a few centimeters from them, so that the electrons can be heated only locally near the excitation windows. Multiple antenna configurations are analyzed as a means to enlarge the area where the electrons are heated. Such arrangement was found to be not critically affected by the difficult to control phase difference between the fields in the individual windows.

¹Sugai et al.: *Bul. Am. Phys. Soc.* **42** (1997) 1768.

²Morita et al.: *Jpn. J. Appl. Phys.* **37** (1998) L468

³Margot et al.: *Bul. Am. Phys. Soc.* **44** (1999) No. 4, p 70.

SESSION GW1: COLLISIONS WITH MOLECULES

Wednesday morning, 10 October 2001; Ballroom C Nittany Lion Inn at 8:00; Ann Orel, University of California, Davis, presiding

Invited Papers

8:00

GW1 1 Studies of Low-energy Positron-molecule Interactions using Trap-based Beams*C. M. SURKO,[†] *University of California, San Diego*

Study of positron interactions with matter at low energies has historically been severely hindered by the relative unavailability of intense positron sources and bright cold beams. Recently, we have developed new tools to make such measurements using positrons accumulated and cooled in a specially designed Penning-Malmberg trap. This talk presents overview of these techniques and recent measurements made with them. A state-of-the-art, trap-based cold positron beam (parallel energy spreads as low as 18 meV (FWHM), tunable from 50 meV upwards) was developed for scattering and annihilation studies [1]. A complementary technique was developed to study elastic and inelastic scattering by exploiting the magnetized orbits of positrons in a field of variable strength [2]. This technique is particularly suited to measuring integral and other absolute cross sections. Potentially, it has wider application, including studying aspects of electron scattering. The first measurements of state-specific integral cross sections for vibrational excitation of small molecules (CO, CO₂, H₂, and CH₄) [3], and for electronic excitation of atoms and molecules (Ar, N₂ and H₂) by positron impact will be described. Comparison with available theoretical predictions will be discussed. Measurement of differential cross sections, energy-resolved positron annihilation cross sections, and searches for scattering resonances [4] will also be briefly discussed, as well as plans for a colder beam based on a cryogenic positron plasma. [1] S. J. Gilbert, et al., *Appl. Phys. Lett.* 70, 1944 (1997). [2] S. J. Gilbert, R. G. Greaves and C. M. Surko, *Phys. Rev. Lett.* 82, 5032 (1999); S. J. Gilbert, et al., *Nucl. Instrum. and Meth. B* 171, 81 (2000). [3] J. P. Sullivan, et al., *Phys. Rev. Lett.*, 86, 1494 (2001). [4] J. P. Sullivan, et al., *J. Phys. B Lett.*, in press, June 2001.

*Work supported by NSF and ONR.

[†]In collaboration with J. P. Sullivan, S. J. Gilbert, S. J. Buckman, J. P. Marler and L. D. Barnes.

8:30

GW1 2 Electron-Driven Processes: From Single Collision Experiments to High-Pressure Discharge Plasmas.KURT BECKER, *Stevens Institute of Technology*

Plasmas are complex systems which consist of various groups of interacting particles (neutral atoms and molecules in their ground states and in excited states, electrons, and positive and negative ions). In principle, one needs to understand and describe all interactions between these particles in order to model the properties of the plasma and to predict its behavior. However, two-body interactions are often the only processes of relevance and only a subset of all possible collisional interactions are important. The focus of this talk is on collisional and radiative processes in low-temperature plasmas, both at low and high pressures. We will limit the discussion (i) to ionization and dissociation processes in molecular low-pressure plasmas and (ii) to collisional and radiative processes in high-pressure plasmas in rare gases and mixtures of rare gases and N₂, O₂, and H₂. Electron-impact dissociation processes can be divided into dissociative excitation and dissociation into neutral ground-state fragments. Neutral molecular dissociation has only recently received attention from experimentalists and theorists because of the serious difficulties associated with the investigation of these processes. Collisional and radiative processes in high-pressure plasmas provide a fertile environment to the study of interactions that go beyond binary collisions involving ground-state species. Step-wise processes and three-body collisions begin to dominate the behavior of such plasmas. We will discuss examples of such processes as they relate to high-pressure rare gas discharge plasmas. Work supported by NSF, DOE, DARPA, NASA, and ABA Inc.

Contributed Papers

9:00

GW1 3 A Comparison of Near-threshold Cross Sections for Electron and Positron Excitation of Atoms and Molecules*J. P. SULLIVAN, J. P. MARLER, S. J. GILBERT, S. J. BUCKMAN,[†]C. M. SURKO, *University of California, San Diego*

The application of state-of-the-art, buffer-gas accumulation and trapping techniques for the production of cold positron beams [1] has heralded a new era of high energy resolution positron scattering studies. Exploiting the properties of the magnetized positron

orbits following scattering in a high magnetic field, very high levels of absolute sensitivity can be achieved in the measurement of near-threshold positron excitation cross sections for atoms and molecules [2]. In the present study we compare cross sections (elastic scattering and excitation) for electron and positron impact for a range of atoms and molecules at energies close to threshold. The positron data, obtained using the new trapping and magnetic-field scattering techniques, is compared to electron scattering data from the literature. These comparisons illustrate some of the fundamental differences in the nature of the scattering processes between electrons and positrons and shed light on the role, if any, of resonances in positron excitation. The new techniques also have

much to offer for the measurement of near-threshold electron excitation processes which are germane to many gaseous electronic environments. [1] Gilbert et al., *Appl. Phys. Lett.* 70, 1944 (1997) [2] Sullivan et al., *Phys. Rev. Lett.* 86, 1494 (2001)

*Supported by NSF and ONR

†Permanent address, Australian National University

9:15

GW1 4 Electron-Molecule Elastic Scattering via 3D FFT Computations MERLE E. RILEY, *Sandia National Labs* A. BURKE RITCHIE, *Lawrence Livermore National Lab* Advanced computational hardware/software capabilities have changed the approach to several theoretical problems in atomic and molecular physics. We present detailed cross sections for elastic electron scattering from molecular hydrogen as a test of an iterative three-dimensional solution of the Lippmann-Schwinger equation. Variations of this direct approach are examined. The wave function is represented by a vector of 10^7 or so points in space, and fast Fourier transform (FFT) methods are used to make an iterative solution possible, even in a matter of minutes on a single processor personal computer. Singularities in the interactions and the momentum representation of the Green's function are dealt with by simple numerical patches that do not slow down the FFT usage. Although the current patches limit the overall accuracy to order of a few percent, the cross sections compare well with partial wave results. Convergence is obtained for $Z=1$ and $Z=2$ systems from less than 1eV upwards. The interesting orientation-dependent cross sections for scattering from molecular hydrogen, prior to molecular-axis averaging, will be presented.

SESSION GW2: COMPUTATIONAL METHODS FOR PLASMAS

Wednesday morning, 10 October 2001

Ballroom AB Nittany Lion Inn at 8:00

K. Nanbu, Tohoku University, presiding

8:00

GW2 1 Self-consistent model and characteristics of power dissipation mechanism for rf biased electro-negative plasma sheath YOUNG D. LEE, J. J. OH, JAI K. SHIN, *Samsung Advanced Institute of Technology* The self-consistent model for the rf-biased electro-negative plasma sheath is developed. The low pressure high density plasma conditions are assumed. The negative ion effect on the sheath boundary is separately considered in calculating the sheath properties. The time-resolved wave forms of the sheath potential and thickness are investigated with respect to the electro-negativity. The characteristics of the rf power dissipation mechanisms are also investigated. The rf power absorbed through the biased sheath is assumed to be dissipated through two channels – the first is due to ion's acceleration in sheath and the second is due to the electron heating in bulk plasma. With the equivalent circuit model from the rf power loss point of view, the sheath impedance is considered. The electro-negativity as well as the current and rf bias frequency is found to be an important factor in determining the characteristics of the rf power losses to ion and electron for the electro-negative plasma sheath.

8:15

GW2 2 Negative ion injection to a wafer in a pulsed two frequency CCP in CF_4/Ar for SiO_2 etching* K. MAESHIGE, T. YAGISAWA, T. MAKABE, *Keio University at Yokohama, Japan* A capacitively coupled plasma (CCP) with electrodes connected respectively to the rf sources for sustaining the plasma at VHF and for biasing the wafer at LF is a powerful tool for a high energy ion assisted SiO_2 etching. A time modulation of the two frequency (2f-)CCP by a pulsed-power operation will be one of the practical solutions of the next generation of etcher with the active function of a charging free plasma process for a high aspect ratio hole or trench manufacturing. We have numerically predicted the structure and functions of a pulsed two frequency CCP in $CF_4(5\%)/Ar$, under a consideration of the negative ion production from CF_3 in a high density plasma with $10^{11}cm^{-3}$. The functional separation is investigated between a plasma production by VHF (100MHz) and a bias voltage application by LF (1MHz). Alternate injections of high energy positive and negative ions to a patterned wafer are predicted during the off-phase of the pulsed 2f-CCP. It will enable us to provide a function of a local charge neutralization in the bottom of a high aspect ratio hole/trench.[2mm] *Work supported by STARC and Selete.

8:30

GW2 3 Lattice Boltzmann simulations for technological plasma discharges* RICHARD BARRETT, DECLAN DIVER, *Dept. of Physics and Astronomy, The University of Glasgow, Scotland*. Simulations of discharges in plasma reactors using the lattice Boltzmann method (LBM) are presented, and their significance for determining the uniformity of the sheath and surface processes are discussed. In previous studies [1] we successfully applied the LBM to the evolution of the neutral component of weakly ionised processing plasmas, and examined the influence of the neutrals on the charged species (modelled crudely assuming ambipolar diffusion with a collisional drag term), finding a significant effect on the sheath properties, and hence on the processing characteristics, in certain ranges of the discharge parameters. Here we extend these simulations, employing a much more realistic model for the charged species: we solve for the ion and electron densities and the potential self-consistently using an efficient, implicit scheme. The difference between this work and previous results using a similar approach is that we include the collisional coupling to the moving neutral gas (whose flow is determined using the LBM). This more accurate treatment of the plasma component allows a detailed, quantitative analysis of the plasma evolution to be made. In processing plasmas the nature of the sheath above the substrate is of crucial importance in determining the number flux and energies of ions delivered to the substrate. With this in mind we use our simulations to examine the impact of the neutral flow and other factors on the sheath characteristics and uniformity. Potential limitations of these simulations are discussed and further generalisations of this work are outlined. [1] Barrett, R.K., Wade, N.S. and Diver, D.A. (2000) *Simulating fluid flow in industrial plasma reactors*, submitted.

*Research funded by the Technological Plasma Initiative of the UK EPSRC

8:45

GW2 4 Plasma modelling in the UMIST Magnetron device R. SOBBIA, J. BRADLEY, P.K. BROWNING, *UMIST, Manchester, UK* M. COPPINS, D. ZDRAVKOVIC, *ICSTM, London, UK* We have simulated particle trajectories in the configuration of a magnetron device at UMIST (supplied by Gencoa Ltd) using an adap-

tive stepsize Runge-Kutta algorithm, focusing on secondary electrons emitted from the cathode. Magnetic fields are determined from the external permanent magnets, using spline interpolation to evaluate fields at all points, electric fields by fitting smooth polynomials to measured potentials in the bulk plasma, joined to a cathode sheath. We consider a particle ensemble to investigate the Hall currents and the effect of the ratio of the Larmor radius to the Debye length on the fraction of electrons lost collisionlessly. Natural extensions would be to incorporate neutral gas collisions and to calculate electric fields self-consistently. We have thus developed a 1D PIC-MC model of the region near the racetrack where the magnetic field is parallel to the electrodes. Magnetic effects on the sheath are investigated. Next we will incorporate electrode pulsing, shown experimentally greatly to improve the properties of surface coatings, and determine its effects on the electron energy distribution.

9:00

GW2 5 Four Dimensional Fokker-Planck Solver for Electron Kinetics in Gas Discharges* VLADIMIR KOLOBOV, *CFD Research Corp.* H.Q. YANG, *CFD Research Corp.* ROBERT ARSLANBEKOV, *CFD Research Corp.* We have developed a four-dimensional Fokker-Planck (FP) solver coupled to electromagnetic, chemistry and other modules in a multi-disciplinary software CFD-ACE+ to enable simulations of kinetic problems for a variety of applications. In this paper we will describe the design and numerical implementation of the kinetic module and its application to electron kinetics in gas discharges. For electron kinetics, the FP equation is derived from the Boltzmann transport equation using the two-term spherical harmonic expansion in velocity space. We apply the FP solver to self-consistent simulations of positive column of a direct current glow discharge, two-dimensional simulations of low pressure inductively coupled plasmas, and kinetic simulations of capacitively coupled discharges. The spatially resolved electron energy distribution functions (EEDF) will be compared to available experimental data. Specifics of non-local electron kinetics in these systems will be discussed. The range of applicability of the FP approach to electron kinetics as well as its relationship to statisti-

cal (Monte Carlo) methods and simple (semi-analytical) models will be addressed.

*Supported by NSF SBIR Program

9:15

GW2 6 Results from the numerical modelling (for various laser pulsewidths) of laser-induced ablation and the subsequent plasma expansion S. LAVILLE, F. VIDAL, M. CHAKER, T.W. JOHNSTON, B. LE DROGOFF, *INRS Energie et matériaux - QC - CANADA* O. BARTHELEMY, J. MARGOT, *Universite de Montreal - QC - CANADA* M. SABSABI, *IMI - QC - CANADA* To study Laser Induced Plasma Spectroscopy (LIPS) for quantitative analysis of materials, we have developed a self-consistent one-dimensional Lagrangian fluid model using a fractional solid-angle spherical geometry. We have modeled both the (i) laser ablation of an aluminum target and (ii) the subsequent plasma expansion in ambient air. Various laser fluences and several pulse durations (from femtoseconds to nanoseconds) were considered. The calculated ablation depth and the ablation threshold fluence are in good agreement with experiments. The integrated absorption coefficient in aluminum for the laser pulse is constant for pulsewidths of 10 picoseconds or less and is a maximum for pulsewidth of a few hundred picoseconds. The greatest ablation efficiency is obtained for pulsewidths less than picoseconds, in agreement with experiments. The model also shows that the separation of the ablated material occurs via the unstable Van Der Waals pressure instability and is accompanied by the formation of droplets ejected from the target. The model indicates that the ablated plasma in air expands to a distance of a few millimetres and stops expanding after about 10 microseconds. The axial profiles of temperature and density are strongly inhomogeneous and the maximum radiation emission occurs in the outer region of the plasma. The model also shows that, at late times, the spatially integrated values of temperature and electron density do not depend on the laser pulse duration for a given fluence, and this is also in agreement with experiments. In addition, experimental results are in reasonable agreement with the condition of local thermodynamic equilibrium, which is an important assumption in the model.

SESSION HW1: FOUNDATIONS OF GASEOUS ELECTRONICS

Wednesday morning, 10 October 2001; Ballroom C Nittany Lion Inn at 10:00; Tim Gay, University of Nebraska, presiding

10:00

HW1 1 Giving Electrons an Honourable Discharge: Measuring their Cross Sections.

BILL MCCONKEY, *University of Windsor*

A quantitative knowledge of the appropriate electron collision processes has always been a pre-requisite for a proper understanding of electrical discharges. Over the years the interests of the GEC community has changed (lamps, lasers, plasma etching and displays etc), fuelling the need for electron collision data on more and different species. The interaction between those who produce cross section data and those who need them has been a fruitful one. An attempt will be made to provide an overview of this field highlighting both the successes and the challenges.

SESSION JWP: POSTER SESSION II
 Wednesday afternoon, 10 October 2001
 Board Room Nittany Lion Inn at 13:15

JWP 1 ENVIRONMENTAL APPLICATIONS AND
 INNOVATIVE APPLICATIONS

JWP 2 PFC Abatement in Capacitively-Coupled Plasma Reactor P.I. PORSHNEV, *ESPD, Applied Materials* M. ALAOU, *ESPD, Applied Materials* STELA DIAMANT, *ESPD, Applied Materials* TERRY FRANCIS, *ESPD, Applied Materials* SEBASTIEN RAOUX, *ESPD, Applied Materials* MIKE WOOLSTON, *ESPD, Applied Materials* A low-pressure plasma reactor, was developed to reduce PFC emissions of dielectric etch tools, is a point-of-use environmentally and economically sound solution. Generally, local electric fields in capacitively-coupled (CC) plasmas are higher than in inductively-coupled (IC) plasmas. As a result, electron energy distributions in CC plasmas have more pronounced high-energy part compared to the ones in IC plasmas. This is particularly important for effective breaking of the strong C-F bonds, which dissociation potentials are observably higher than the average electron energy. CC plasma in the Pegasys (Plasma Exhaust Gas Abatement SYStem) reactor was found to be in so-called g-regime, in which ionization is provided with secondary emission electrons. Though in these plasmas, the majority of electrons still reside in plasma bulk, the most important discharge characteristics, in particular, the abatement efficiency, are determined by highly-energetic electrons from sheath zones. With water being added to the incoming gas mixture, better than 95% destruction removal efficiency of the PFCs has been achieved for all dielectric etch applications. CC plasma-based abatement significantly differs from existing abatement methods, especially combustion and catalytic oxidation, which are much less environmentally friendly and economically viable.

JWP 3 NO Removal in High Pressure Plasmas of N₂/H₂O/NO Mixtures* F. FRESNET, G. BARAVIAN, L. MAGNE, S. PASQUIERS, C. POSTEL, V. PUECH, A. ROUSSEAU, *LPGP, Universit Paris-Sud / CNRS, France* Influence of H₂O on NO removal has been studied using a homogeneous photo-triggered discharge with a time resolved LIF measurement of the NO density, in N₂/H₂O/NO mixtures at 460 mbar. The H₂O maximum concentration was 2.5 was between 70 and 160 J/l. Measurement of NO density has been performed up to 180 s after the current pulse excitation of short duration, 50 ns. Kinetic analysis has been made using a self-consistent 0D-discharge model. NO is in great part dissociated, in N₂/NO, through collisions with the excited singlet states of N₂. We have previously shown that addition of ethene induces

de-excitation of these states, leading to a decrease of the NO removal¹. Similar processes take place when C₂H₄ is replaced by H₂O. The value of the rate constant for collision of singlet states with water, $3.10^{-10} \text{ cm}^3 \text{ s}^{-1}$, is obtained from our study.

*Work supported in part by GIE : PSA Peugeot-Citron / RENAULT, ECODEV-CNRS, and ADEME.

¹F. Fresnet, G. Baravian, L. Magne, S. Pasquiers, C. Postel, V. Puech, A. Rousseau, *Appl. Phys. Lett.*, 77 (2000) 4118.

JWP 4 Benzene Dissociation in DC Atmospheric Pressure Air Glow Discharges CHUNQI JIANG, ROBERT H. STARK, KARL H. SCHOENBACH, *Physical Electronics Research Institute, Old Dominion University* By using a micro-hollow cathode discharge (MHCD) as an electron source to lower or eliminate the cathode fall voltage, a glow discharge could be operated in a dc atmospheric pressure air [1]. The effect of this glow discharge plasma on VOC (Volatile Organic Compound) remediation, particularly, benzene remediation, has been studied. A higher than 90 % destruction rate has been obtained by flowing a 300 ppm benzene/ dry air mixture through the plasma filament. The plasma is confined by a dielectric to a cross-section of 1 mm by 1.5 mm and extends over a depth of 0.8 mm. With a flow rate of 100 sccm, the residence time of the gas in the plasma column is 0.7 ms. A destruction efficiency of more than 0.5 L/kJ has been measured. The energy efficiency is 0.9 g/kWh which is comparable to that achieved by low pressure glow discharges in benzene/ noble gas mixtures [2]. References: [1] R. H. Stark and K. H. Schoenbach, "Direct Current Glow Discharges in Atmospheric Air," *Appl. Phys. Lett.* 89, 3568 (2001). [2] D. L. McCorkle, W. Ding, C. Ma and L. A. Pinnaduwa, "Dissociation of Benzene and Methylene Chloride Based on Enhanced Dissociative Electron Attachment to Highly Excited Molecules," *J. Phys. D: Appl. Phys.* 32, 46 (1999). Acknowledgments: This work is supported by the Air Force Office of Scientific Research.

JWP 5 A wet plasma scrubber for removal of sulfur dioxide SHIRSHAK DHALI, *Southern Illinois University* SREERAM SEETAMSETTY, BAKUL DAVE, *Southern Illinois University** We have modified the dielectric barrier discharge to create a discharge in a gas, liquid and solid medium. The electric discharge takes place in the gas bubbles formed in this mixture. The discharge behaves like a partial discharge in voids. It is excited with a 2- 5 kHz high voltage source. In this paper, we present some basic characteristics of the wet plasma scrubber followed by removal of SO₂. The configuration is a cross flow reactor with the water coming down and the gas moving up. It consists of a glass dielectric cylinder with the inside filled with glass pellets. The inner electrode is a stainless steel rod and the outer electrode is a conducting film on the outer surface of the dielectric. The plasma is created in the gas and liquid mixture between the beads. This produces a heterogeneous medium and enhances the removal rate considerably. The removal efficiency of SO₂ was studied under various conditions. It was found to work better compared to dry plasma techniques. The power requirements were less by a factor of 5 compared to dry reactors. The addition of water in the reactor causes enhanced production of OH radicals, which improves the

removal efficiency. In addition, the water removes H₂SO₄ from the discharge and prevents regeneration of SO₂. Due to the relative changes in gas and dielectric capacitance, it was found that the power coupled to the discharge decreases due to water flow.

*This research was partially supported by funds from the National Science Foundation.

JWP 6 Rf-magnetron plasma for co-sputtering deposition of bioactive calcium phosphate coatings for biomedical application J.D. LONG, S. XU, N. JIANG, K. OSTRIKOV, C.H. DI-ONG, *Plasma Processing Laboratory, NIE/NTU, 637616 Singapore* The Rf-magnetron plasma sputter system has been successfully applied for the development of bioactive Ca - P - Ti thin film on Ti6Al4V substrates. The plasma sputter system shows excellent controllability in the deposition process. The synthesis processes have been monitored by means of *in-situ*, high resolution (0.023nm) optical emission spectroscopy (OES). The OES spectra show that the emission of CaO is dominant and the CaO, PO and CaPO species, which affect the composition and microstructure of Ca - P film, are strongly related to the deposition conditions. The coating layers have been characterized using XRD, XPS, and FTIR techniques. The XRD pattern suggests that crystalline Ca - P thin film can directly form in the sputter deposition process and the Ca - P thin films are of crystalline calcium oxide phosphate (4CaO · P₂O₅) with preferred orientation of (130). The XPS results show that the films are composed of O (53.8%), Ca (26%), P (12.8%) and Ti (3.4%), Ca/P ratio is 2.03. These results approximate an expected stoichiometric value of HA. The XPS and FTIR data reveal the formation of O - H, and O = P groups and hybridization of O - Ca - P. It is seen that the introduction of Ti element during deposition provide stable interface between bio-inert substrates Ti6Al4V and bioactive HA coating. The *in-vitro* cell culture shows that the Ca - P thin films have good biocompatibility.

JWP 7 CAPACITIVE PLASMAS

JWP 8 Effects of Secondary Electron Emission in High Pressure Capacitively Coupled Plasma Discharges G. I. FONT, W. L. MORGAN, *Kinema Research, L.L.C.* Simulation of capacitively coupled discharges at high pressure is made difficult by the presence of secondary electron emission from the electrodes. The secondary electrons require special treatment in the simulation since a single energy distribution function is not adequate to describe the secondary electron population, which may be at 100 eV, and the thermalized population which is typically below 10 eV. The high energy electrons are normally dealt with by using a second fluid species or a discrete particle model. These treatments, however, add complexity and require additional computational time to converge. In this study, the difficulties associated with the second electron population are circumvented by modeling them as an ionization source term derived from particle studies of glow discharges. The applicability to industrial rf discharges is evaluated and comparisons with experiments are presented.

JWP 9 Behaviors of Charged Particles in Narrow Gap Capacitively Coupled RF Discharge YASUNORI OHTSU, *Department of Electrical and Electronic Engineering, Saga University* HIROHARU FUJITA, *Department of Electrical and Electronic Engineering, Saga University* Capacitively coupled radio frequency (RF) glow discharges are widely used for material processing such as plasma chemical vapor deposition (CVD) and etching techniques. Recently, high quality preparation of thin film has been performed in narrow gap capacitively coupled RF plasma (NGCCP) at high-pressure or high driving frequency. However, the basic characteristics in NGCCP have not almost been clarified. In this work, we present the experimental results on plasma parameters such as temperature, density and energy distribution of electrons in NGCCP. The effects of electrode gap and gas pressure on plasma parameters were investigated in NGCCP. It was found that with decreasing the gap the temperature and density of electrons increased and decreased, respectively. Electron temperature decreased remarkably at $0.2 < p < 1$ Torr and then gradually with increasing gas pressure p . Electron density increased drastically with increasing gas pressure p at $0.2 < p < 1$ Torr and then saturated. It was found that in the pressure of 0.2 Torr, high-energy component of electrons with the energy of 20-30 eV existed. Since this value was in good agreement with the estimation of hard-wall model of RF discharge, which ascribed the electron acceleration with moving RF sheath. In the pressure of 2 Torr, electron energy distribution was almost Maxwellian.

JWP 10 COMPUTATIONAL METHODS

JWP 11 Monte Carlo and Boltzmann Equation Study of the Spatiotemporal Electron Relaxation DETLEF LOFFHAGEN, ROLF WINKLER, *Institute of Non-Thermal Plasma Physics, Greifswald, Germany* ZOLTAN DONKO, *Research Institute for Solid State Physics and Optics, Budapest, Hungary* Recently the complex spatiotemporal relaxation of electrons in non-isothermal inert gas plasmas acted upon by electric fields has been investigated by solving the spatially one-dimensional, time-dependent kinetic equation for the electron velocity distribution function in two-term approximation. To confirm these Boltzmann equation studies by a completely independent method, now results for inhomogeneous column-anode plasmas of glow discharges between plane electrodes are compared with corresponding ones obtained by Monte Carlo simulations. In the framework of the relaxation model, argon plasmas acted upon by a constant electric field and sustained by a continuous injection of electrons at the cathode side of the plasma with an isotropic angular distribution and a Gaussian energy distribution are considered. Starting from steady-state at a given field, the spatiotemporal electron relaxation is triggered by an instantaneous change of the electric field strength and is traced until the associated steady-state is reached. For electric fields typical of glow discharges the macroscopic quantities and the distribution functions obtained by both approaches agree well during the transient process and in steady-state.

JWP 12 Multiterm Treatment of the Electron Kinetics in Cylindrical Hollow Cathodes F. SIGENEGER, R. WINKLER, *Institut für Niedertemperatur-Plasmaphysik, Greifswald, Germany* In order to analyse the radial variations of the electron kinetic properties in cylindrical hollow cathodes a multiterm method for solving the radially inhomogeneous Boltzmann equation has been developed. The studies are initiated by recent experimental investigations of an axially symmetric hollow cathode discharge. Because of its symmetric setup an one-dimensional radial description becomes possible around the axial center. Since existing multiterm solution methods have been developed for plane cathodes they are not applicable to the cylindrical geometry of the hollow cathode. To solve the problem, an expansion of the electron velocity distribution function in symmetric and irreducible tensors has been used. The resultant hierarchy for the tensorial expansion coefficients involving complex tensor operations has been adapted to cylindrical coordinates and rotational symmetry. Finally, it could be deduced that in each truncation order of the hierarchy a reduced set of tensor components and corresponding partial differential equations remains which represents the relevant subsystem of the kinetic problem. The number of these relevant components non-linearly increases with the truncation order. Typical applications lead to differences, e.g. in the ionization rate, of up to a factor two between the 2- and 4-tensor-term approximation and to nearly convergent results if using 6 tensor-terms.

JWP 13 Simulation of breakdown in He-Xe gas mixtures and comparison with experiment* YURIY SOSOV, CONSTANTINE THEODOSIOU, *University of Toledo* Breakdown curves for pure He and Xe were calculated for a simple 1D plasma display panel cell and compared with experiment. Good agreement is found with measurements. The necessary for the calculations values of secondary electron emission coefficients for excited and ionized atoms of He and Xe on brass were obtained through a combination of calculations and the breakdown experimental data. They are consistent with similar experimental data available in the literature. Using these secondary emission coefficients and assuming their applicability to gas mixtures, the breakdown curves for HeXe mixtures are calculated and compared with the experimental ones. Our results indicate that two-term expansions in the Boltzmann equation solution are inaccurate for mixtures like HeXe with large differences in the ionization thresholds of the constituent gases.

*Work supported by NSF Grant ECS9896103

JWP 14 Ion mass effects in the modelling of a RF driven, capacitively coupled GEC reference cell* ELM COSTA I BRICHA, CHARLES M.O. MAHONY, PHILIP G. STEEN, WILLIAM G. GRAHAM, *Queen's University of Belfast* In many previous PIC code modelling studies a reduced ion mass has been used to reduce the calculating time. Here the consequences of doing this are discussed. A two-dimensional Particle In Cell (PIC) code is used to model a RF driven, capacitively coupled GEC reference cell. The present code is based on XOOPIC³, which was developed by the UC Berkeley group. Ion masses of 1, 2, 4, and 8 a.m.u. are used in the simulation to compare with experimental measurements in Ar (40 a.m.u.). It is found that the predicted electron density in the plasma is lower and the temperature somewhat higher if lower masses are used. The effect becomes

less pronounced as the ion mass increases. However it is possible to obtain a simple calibrating relationship. The ion mass also effects the sheath and associated phenomena. ³<http://www.ptsg.eecs.berkeley.edu/xoopic/xoopic.html>

*Supported by EU BRITE

†Present address: N.I.B.E.C., University of Ulster at Jordanstown, Northern Ireland

JWP 15 DISTRIBUTION FUNCTIONS

JWP 16 Effect of Electron Reflection at the Anode on Ionization Coefficient AKIHIDE TAKEDA, *Shikoku Univ.* NOBUAKI IKUTA, *Chiba Inst.Tech.* The ionization coefficient α is determined with the gradient of $\log(I)$ (ionization current) versus gap length d assuming the energy equilibrium over full gap space. However, the equilibrium in full space is difficult as well known. The α values in H_2 reported by Haydon[1] and Satoh[2] show sudden breaking of increase with increase of reduced electric field E/p_0 at less than $200 \text{ Vcm}^{-1}\text{Torr}$. The relaxation of electron energy distribution in H_2 is much slower than that in other gases due to the low values of inelastic cross sections in particular in high-energy range, accordingly in high E/p_0 condition. Hayashi pointed out[3,4] that the breaking is due to the runaway of electrons. Many electrons are lost from the anode without sufficient ionization collisions with H_2 . In such a situation, it is found that the electron reflection at the anode, the ratio is considerably large in practice, gives large increase in the measured values of αd . The effect of reflection on the values of αd in H_2 with the change of E/p_0 and $p_0 d$ will be reported. [1]S. C. Haydon and H. M. Stock: *Aust. J. Phys.* 24 pp.527-42(1966). [2]K. Satoh, T. Kudoh, T. Miki, M. Kawashima, H. Itoh and H. Tagashira: *T. IEEE Jpn.* 119-A pp.1136-41(1999) [3]M. Hayashi, M. Ohoka and A. Miwa: *18th ICPIC* pp.14-15(1987) [4]M. Hayashi: *4th ICDG Vol.1* pp.195-198(1976)

JWP 17 Impact of the Electron-Electron Interaction on the Spatial Relaxation of Plasma Electrons DETLEF LOFFHAGEN, ROLF WINKLER, *Institut für Niedertemperatur-Plasmaphysik, Institute of Non-Thermal Plasma Physics, Greifswald, Germany* The spatial relaxation of electrons in weakly-ionized plasmas under the action of an electric field and the inherent complex relaxation mechanisms have comprehensively been studied in recent years¹. The investigations were based on the analysis of the space-dependent electron Boltzmann equation taking into account the action of an electric field as well as the impact of elastic and inelastic collisions of the electrons with the neutral gas particles. In particular, it was found that pronounced, spatially periodic relaxation processes are stimulated in some inert gases at medium electric field strengths which are characterized by very large relaxation lengths. But, the impact of the collisions between electrons has been neglected so far. By implementing the nonlinear electron-electron interaction into the space-dependent kinetic equation, now it became possible to estimate the additional impact of the collisions between electrons on the spatial relaxation process. The analysis reveals an unexpectedly large impact of the

electron-electron collisions on the damping behavior and a significant decrease of the relaxation lengths with increasing intensity of the collisions between electrons already at relatively low ionization degrees of the plasma.

¹R. Winkler et al., *Plasma Sources Sci. Technol.* 6 (1997) 118.

JWP 18 The Structure of Double-Peaked EVDF of Electron Swarms in N_2 H. SUGAWARA, *Hokkaido University, Japan* K. SATOH, *Muroran Institute of Technology, Japan* Y. SAKAI, *Hokkaido University, Japan* The electron velocity distribution function (EVDF) of electron swarms in N_2 has two peaks at E/N around 200 Td. We analyzed the structure of the double-peaked EVDF using a propagator method and a Monte Carlo simulation. The valley between the two peaks of the EVDF appears over the electron energy range in which the vibrational excitation collision cross section q_v lies. Thus, the valley has been explained from the barrier effect of q_v that prevents the acceleration of slow electrons. Our simulation confirmed this explanation, and also suggested assistance of elastic collision for vibrational excitation. The elastic collision cross section q_e takes its maximum near the electron energy for the q_v maximum, and the q_e maximum also has a barrier effect although the energy loss at elastic collision is negligible. Then, the q_e maximum does not induce the double-peaked EVDF by itself alone, however, it affects the formation of the valley in collaboration with q_v . The q_e maximum holds slow electrons in a low-speed region of velocity space, that gives the electrons more opportunity of vibrational excitation collisions. We discuss the barrier effect of the q_v and q_e maxima through a simulation of single electron motion around the valley and an evaluation of the electron flow in velocity space.

JWP 19 INDUCTIVELY COUPLED PLASMAS

JWP 20 Characteristics of a new high frequency inductively coupled plasma source DONG SEOK LEE, *KAIST YONGKWAN LEE, KAIST HONG-YOUNG CHANG, KAIST* We suggest a new very high frequency ICP source with a modified resonance antenna in parallel [S.S. Kim et al., *Appl. Phys. Lett.* Vol. 77, 492(2000)]. We can control the plasma uniformity and achieve high electron density and low electron temperature that are important plasma properties especially for oxide etching. Many researchers have reported that low electron temperature is needed for oxide etching selectivity and our studies were focused to achieve low electron temperature without losing good plasma characteristics. Electron temperature decreases to 1.8 eV as driving frequency increases up to 100 MHz and the plasma uniformity by controlling current of the outer antenna connected to the capacitor is achieved within 5

JWP 21 Electron energy distribution functions, plasma parameters and optical emission in low-frequency inductively coupled plasmas of Ar , N_2 , and CH_4 gas mixtures. EREKLE TSAKADZE, KOSTYA OSTRIKOV, ZVIADI TSAKADZE, NING JIANG, SHUYAN XU, *Plasma Processing Laboratory, NIE, Nanyang Technological University, 1 Nanyang Walk, 637616*

Singapore Electron energy distribution functions, plasma parameters, and optical emission in low-frequency inductively coupled plasmas (LFICPs) of Ar , N_2 , and CH_4 mixtures have been studied. An Rf-compensated cylindrical Langmuir probe has been used to investigate the electron/ion number densities, plasma potential, effective temperature and energy/probability distribution functions (EEDF/EPPF) of the plasma electrons. The dependence of the global plasma parameters on Rf power and the feedstock gas composition and pressure is presented as well. It is revealed that the EEDFs in $Ar + N_2 + CH_4$ discharges sustained in low-frequency (~ 500 kHz) ICP source appear to be non-Maxwellian. As compared with a typical Maxwellian EEDF, the measured EEDF peaks are shifted towards higher of electron energies, which is peculiar to Dryuvestein-like EEDFs. Using the EEPF, optical emission, and reaction threshold data, the electron population responsible for the major dissociation/ionization reactions in $Ar + N_2 + CH_4$ gas mixture, has been computed. It is shown that knowledge of EEDFs and composition of the ionic/radical/molecular species in LFICPs is instrumental in optimizing film deposition processes.

JWP 22 Investigation of Electronegativity in a RF Xe/SF₆ Inductively Coupled Plasma using a Langmuir probe T. KIMURA, K. OHE, *Nagoya Institute of Technology* SF₆ content and power dependences of plasma parameters such as the electronegativity, the electron density and the effective electron temperature were investigated in a RF Xe/SF₆ inductively coupled plasma (ICP), with keeping the total pressure for discharge-off at 2.5 mTorr. We used the two ways to estimate electronegativity; one way is to use the detected peak of the second derivative of the probe current with respect to the probe bias voltage, and the other way is to use the ratio of the negative saturation current to the positive ion one measured for negative bias of -30 - -50 (V) far from the plasma potential. The electronegativity (the ratio of negative ion to electron densities) is between 5 and 10 in a RF Xe/SF₆ inductively coupled plasma, where the electron density is in the order of 10^{16} (m^{-3}) and the electron and negative ion temperatures are about 3.5 - 5 (eV) and 0.4 (eV) respectively. The electronegativity does not strongly depend on SF₆ content, while it decreases gradually with the increase of electron density. This work was partially supported by Grant-in-Aid from Japan Society for the Promotion of Science.

JWP 23 Mass spectrometric investigations of ionic species in rf biased inductively-coupled discharges in CF₄/Ar and SF₆/Ar YICHENG WANG, AMANDA GOYETTE, MARK SOBOLEWSKI, *National Institute of Standards and Technology* We report the measured ion fluxes and ion energy distributions (IED) in radio-frequency (rf) discharges in CF₄/Ar and SF₆/Ar mixtures as a function of rf bias voltage and gas pressure. A Gaseous Electronics Conference rf reference cell with an inductively-coupled plasma source was used to produce the discharges, with the lower electrode covered by a Si wafer. Ions were sampled through a 10 μ m diameter orifice and analyzed with an electrostatic energy selector in tandem with a quadrupole mass spectrometer which was mounted to a side port of the cell. The total ion fluxes were measured using a Faraday cup. The two most abundant ions in CF₄/Ar (50%:50%) discharges at 200 W are CF₃⁺ and Ar⁺. The CF₃⁺ fraction increases while the Ar⁺ fraction decreases with increasing discharge pressure from 0.67 Pa to 5.3 Pa. The dominant Si-containing ion in CF₄/Ar is SiF₃⁺, which increased consistently over the pressure range when a 200 V rf voltage at 10 MHz was

applied. Surprisingly, the relative ion fluxes in SF₆/Ar (25%:75%) discharges at 200 W, from 0.67 Pa to 5.3 Pa were observed to change little when the rf bias voltage was increased from 0 to 200 V, despite a dramatic change in the IED. The dominant F-containing ion in SF₆/Ar is SiF₃⁺, with its fraction increasing with increasing pressure from 0.67 Pa to 5.3 Pa.

JWP 24 A Computational Study of CF, CF₂ and SiF_x Densities in C₂F₆ and Ar/C₂F₆ Inductively Coupled Plasmas* SANGHOON CHO, *University of Illinois* The spatial distributions of CF, CF₂ and SiF_x in low pressure, inductively coupled plasmas (ICPs) are of interest with respect to optimizing the uniformity of fluxes for microelectronics fabrication. To investigate these distributions the Hybrid Plasma Equipment Model (HPEM) was used to model ICPs sustained in C₂F₆ and Ar/C₂F₆. Parametric studies in 2-dimensions were performed as a function of inductive power, gas mixture, pressure and biases for discharges sustained in the GEC Reference Cell. Comparisons will be made to experiments [G. A. Hebner, *J. Appl. Phys.* 89, 900 (2001)] for densities of radicals such as CF, CF₂ and SiF. A recent improvement to the HPEM has enabled more accurate inclusion of electron-electron collisions in the Electron Monte Carlo Module. The transition from two-temperature to single-temperature distributions will be discussed by examining electron energy distributions as a function of position.

*Work supported by NSF (CTS99-74962)

JWP 25 Prediction of Device Damage in Plasma Processing D NAKAGAWA, K MAESHIGE, T MAKABE, *Keio University at Yokohama, Japan* Charging damage from plasma etching to gate oxide has become an important issue for the fabrication of integrated semiconductor device. The damage is caused by a topographically dependent charging during etching. As a result, ULSI will introduce the decrease in performance. Successive modeling of the plasma process from plasma structure to device damage is one of the solutions to these problems. Previously we proposed a tool to predict the plasma damage to the device, VicAddress¹. In this work, we develop the VicAddress, in order to estimate the charging damage to an ultra thin gate oxide in a contact hole etching, by considering the local charge accumulation in a 2D trench. We investigate the spatiotemporal damages during etching, those are dependent both on an etching pattern and on the arrangement of the device element. The device damage is estimated in terms of tunneling current and the integrated charge through the element. A correlation between the etching pattern and the device damage will be discussed.

¹T.Makabe, J.Matsui and K.Maeshige, *Sci. and Technol. of Adv. Materials* (in press).

JWP 26 Experiment & Model Comparisons in an Ar/Cl₂ ICP C.M.O. MAHONY, C.N. ESCOFFIER, P.D. MAGUIRE, *NIBEC, University of Ulster, Northern Ireland* C.S. CORR, S. GOMEZ, E. COSTA I BRICHA, W.G. GRAHAM, *Queen's University, Belfast, Northern Ireland* Cl & Cl⁻ densities measured in a 13.56 & 14MHz Ar/Cl₂ inductively coupled processing plasma are compared with results from a kinetic model. The experiments used powers up to 200W, pressures of 0.5 to 12Pa and Cl₂ fractions up

to 50%. Atomic Cl was measured by laser induced fluorescence and Cl⁻ by probe based photo-detachment. A compensated Langmuir probe was used to measure electron energy distribution functions (EEDFs) and other parameters. From these EEDFs, which were often non-Maxwellian, we calculated the rate coefficients for electron-heavy particle reactions and thus equilibrium particle balance equations. For 5% Cl₂ the modelled Cl density rises as power or pressure is raised, and the Cl⁻ fraction drops as power is raised, all in agreement with experiment. The measured Cl⁻ fraction drops as pressure is raised whilst the model predicts little change, possibly due to the wall sticking and recombination coefficients used. Altering these values changes the above trend and is being studied. UK EPSRC & EU IST Microtrans supported.

JWP 27 Instabilities in a Low-Pressure Inductively Coupled Oxygen Plasma CORMAC CORR, PHILIP STEEN, *Affiliation WILLIAM G. GRAHAM, Queen's University Belfast* A previously reported[1,2], reproducible instability has now been observed and studied in a low-pressure 13.56 MHz inductively coupled GEC rf cell operating in oxygen without a Faraday shield. It's magnitude observed in the form of periodic oscillations in the output of a photodiode and an unbiased Langmuir probe can be as high as 30 percent. The instability is observed in a pressure and power regime where both the capacitive and inductive modes can exist. This pressure window coincides with the pressure regime where the time-averaged negative ion fraction reaches a maximum in both modes. Time resolved measurements of the electron energy distribution functions and negative ion densities indicate that at all phases of the instability, the plasma parameters resemble those of the normal inductive mode. The instability appears linked to the spatial movement of the plasma suggesting minor fluctuations in the charge particle spatial distribution. It does not appear to be a transition between capacitive and inductive modes. 1. M. Tuszewski, *J. Appl. Phys.* 79, 8967 (1996) 2. M.A. Lieberman, A.J. Lichtenberg, and A.M. Marakhtanov, *Appl. Phys. Lett.* 75 23, 3617 (1999)

JWP 28 The effect of pressure and gas species on electron cyclotron resonance (ECR) heating and the radial density profile change at the ECR condition in weakly magnetized inductively coupled plasma CHINWOOK CHUNG, *KAIST* S.S. KIM, *Kyoto University* S.J. YOU, *KAIST* H.Y. CHANG, *KAIST* Last conference, we suggested the existence of electron cyclotron resonance heating (ECR) in weakly magnetized planar inductively coupled plasma (ICP). As a continuous study, electron energy distribution functions (EEDFs) in the ICP were measured at various conditions (pressure and gas species). The effect of ECR heating on the EEDF weakens when pressure increases. For Helium gas, the effective heating of low energy electrons in the EEDF at the ECR condition do not clearly appear while it is distinctly observed in Argon. This is mainly attributed to Ramsauer effect. The calculated EEDFs from the kinetic theory at the ECR condition are compared with the experimental EEDFs for Argon and Helium. They well agree each other. Radial electron density profiles are significantly near the ECR condition. This can be explained by considering magnetic field confinement and the ECR heating.

JWP 29 GLOWS: DC, PULSED, RF, MICROWAVE, INDUCTIVE, OTHER

JWP 30 Hollow Cathode Magnetrons with Gas Injection through Target Y. ARANDA GONZALVO, J.W. BRADLEY, *UMIST* DC magnetrons are well-known sputtering sources. Introducing a groove in the cathode target, which acts as a hollow cathode, and feeding the gas through this groove modifies the plasma properties in these magnetrons. It is observed that this allows the magnetron to operate at lower pressures, or with higher discharge current in comparison with the conventional planar target¹. Experiments have been performed for different groove dimensions (1.5 and 3 mm), different pressures (0.033 to 0.53 Pa) and different target materials (Cu, Ti). Comparison between planar and hollow cathode target will be given for the I-V characteristics found while operating both types. Differences in the plasma parameters T_e , n , V_p and V_f , measured using a Langmuir probe system, will be shown. The energy distribution of ions and neutrals in the plasma has been measured by an energy-resolving mass spectrometer and confirms that for the grooved target at low pressures the density of Cu neutrals and Ar ions in the plasma is larger, making these magnetrons more efficient. Explanation for the observed data will be given to some detail.

¹J.W. Bradley et al., *J. Vac. Sci. Technol. A* **17** (6) pp 3333 (1999)

JWP 31 A RF Discharge in Argon at Atmospheric Pressure SHIRSHAK DHALI, *Southern Illinois University* NAVIN MUTHUSWAMY, BAKUL DAVE, *Southern Illinois University** A dual chamber discharge is used to create an atmospheric pressure plasma in Argon. The discharge consists of two chambers: one at low pressure (few Torr) and the other at atmospheric pressure. The chambers are separated by fused silica window. A RF source (13.56 MHz) is used to create a discharge first in the low pressure chamber which is filled with Xenon. As the RF power is increased, a glow discharge is created in the atmospheric pressure chamber. Without the low pressure chamber, no discharge is obtained at atmospheric pressure. The UV radiation from the low pressure chamber, which is coupled to the high pressure chamber through the quartz window, initiates the discharge in the high pressure region. We will report the electrical characteristics of the discharge. The self bias voltage is about -2.0 V for a power input of 25 W. The dissociation of hydrogen in an argon/hydrogen mixture was studied by monitoring the hydrogen H-beta line.

*This research was partially supported by funds from the National Science Foundation.

JWP 32 Experimental Investigation of Submillimeter Plasmas of High Power Density THOMAS MATHIEU, HANNS-PETER POPP, *Lichttechnisches Institut, Universität Karlsruhe, 76131 Karlsruhe, Germany* To study plasma phenomena in submillimeter dimensions microwave generated discharges in capillaries with diameters between 0.2 and 1.0 mm are investigated. For this purpose a special cavity had to be constructed to guarantee impurity free operation in spite of the small diameters. The supplied filling gases were Xenon, Krypton, Argon and Neon. Typical discharge conditions of this investigation were pressures ranging from 100 to 10000 Pa and an average power between 5 and 13 W. The plasma

was characterised by means of optical emission spectroscopy. With specific combinations of both pressure and diameter the generation of a plasma consisting only of spectral lines of ions could be achieved. Calculations, based either on the Boltzmann distribution or the so-called corona model, yielded good agreement with the experimentally determined population of the energy levels. Financial support supplied by the Deutsche Forschungsgemeinschaft (Po 190/9-1).

JWP 33 Multi-dimensional model for parallel plate rf plasma simulation accelerated by spline function Poisson equation solver TAKUMA SUZUKI, *Hokkaido Institute of Technology* KAZUTAKA KITAMORI, *Hokkaido Institute of Technology* IKUYA HORIE, *Hokkaido Institute of Technology* KOUICHI MARUYAMA, *Hokkaido Institute of Technology* Plasma simulation by Monte Carlo (MCS) method provide the advantage of clearly reproducing 1d3v (one dimensional displacement with three velocity components) or 2d3v models with little approximation. Brute force implementations of 2d3v models require large calculation times for decent statistics. MCS with LPWS and parallelized technique can be used to reduce CPU time. In 1d3v models Poisson's equation is not a limiter as analytic solutions can be imposed. 2d3v (and 3d3v) models are challenging in that the whole system must be solved numerically. Poisson's equation solver method expressed by the bi-cubic spline function coupled with LPWS as an acceleration technique is proposed in this article for 2d3v. The results of "1d3v" and "2d3v" for parallel plate rf discharge are discussed.

JWP 34 Gas Temperatures of XeCl Microwave Plasmas* SCOTT ANDERSON, *University of Michigan, Ann Arbor, MI 48109* MICHAEL DELANEY, *University of Michigan, Ann Arbor, MI 48109* COREY COLLARD, *University of Michigan, Ann Arbor, MI 49109* MARY BRAKE, *University of Michigan, Ann Arbor, MI 48109* In this work, an Asmussen microwave resonant cavity, operating in the TM012 cavity mode, is used to excite a XeCl excimer discharge. A CW microwave power supply operating at 2.45 GHz delivering 50W-150W of absorbed power is used to excite the discharge at pressures up to an atmosphere. The plasma is contained within a quartz tube that runs along the center of the resonant cavity with Xe:Cl₂ ratios ranging from 1:2 to 10:1. Coupling efficiencies from the microwave supply to the discharge are typically greater than 80% as high as 94% discharges play an important role in the disassociation of the excimer molecule. High temperatures can greatly increase the disassociation of molecules and thus reduce the efficiency of UV production. Rotational structures of XeCl 308nm (B-X transition) molecular bands are difficult to resolve. In order to calculate rotational temperatures, trace amounts of N₂ gas are added to the XeCl discharge. >From previous work, we have shown that the N₂ rotational temperatures are a good estimate of bulk gas temperatures. These gas temperatures are compared to optical output as a function of pressure, the amount of forced cooling of the tube, and discharge volume as viewed with a CCD detector. [1] M.L. Passow, et al. "Microwave Resonant-Cavity-Produced Air Discharges," *IEEE Transactions on Plasma Science*, Vol. 19, No. 2, pp. 219-228, 1991.

*supported by Naval Research Labs

JWP 35 Production of Charge Donor Molecules in a Resonant Microwave Cavity Discharge G. M. BROOKE, L. VUŠKOVIĆ, S. POPOVIĆ *Department of Physics, Old Dominion University, 4600 Elkhorn Ave., Norfolk VA 23529* Our study of charge transfer reactions at thermal energies is based on the selective ion flow tube which requires a clean and efficient source of charge donor molecules such as H_3O^+ and O^+ . For efficient charge transfer, it is necessary to produce a charge donor molecule which matches the resonant energy of the molecule being studied. Previously we have investigated a hollow cathode discharge and a capacitively coupled discharge, but contamination and inefficient impedance matching circuits have hindered their use. We will be presenting the results of a custom built resonant microwave cavity (RMC) ion source to produce various charge donor molecules. Since the RMC source is electrodeless, the discharge is not contaminated by the presence of a cathode or filament. Additionally, impedance matching is accomplished by simply adjusting the cavity length. We will also present the results of a comparative study conducted on several gas mixtures at pressures ranging from 50 to 500 mTorr. Finally, we will be presenting results of charge transfer reactions using the new RMC ion source with the flow tube in order to measure the rate coefficients of exotic molecules.

JWP 36 PLASMA INTERACTIONS WITH SURFACES

JWP 37 Study of surface reactions in plasma etching using mass-analyzed ion beams KAZUHIRO KARAHASHI, *Semiconductor Technology Research Department Association of Super-Advanced Electronics Technologies (ASET)* HIDEO TSUBOI, YOSHIKAZU YAMAOKA, KAZUAKI KURIHARA, MAKOTO SEKINE, MORITAKA NAKAMURA, We have constructed a new mass-analyzed low-energy ion beam etching apparatus (MALIEA) for investigate desorption products from silicon or silicon dioxide surfaces during CF_x^+ ($x=1-3$) ion bombardments. In this paper, we describe this newly developed ion beam apparatus, and results of CF_3^+ ion bombardment experiments. The apparatus consists of an ion beam source, an ultra high vacuum (UHV) process chamber, and a detector chamber. As there are three differentially pumping stages between the source and process chamber, the process chamber was maintained at UHV condition during all experiments. Therefore, experiments were not affected by contaminations from the ion source. Pure ion beams such as F^+ , CF^+ , CF_2^+ and CF_3^+ , were obtained with good mass resolutions by a 90 mass-selecting electromagnet. The sample is mounted on a manipulator, located at the foci of a hemispherical energy analyzer and x-ray sources to allow chemical analysis of irradiated surfaces. The desorption products and scattered ions were detected by a rotatable differentially pumped quadrupole mass spectrometer (QMS). In experiments of CF_3^+ irradiation on silicon dioxide surface @ 1000eV, etching rate was about 1.1 atoms/ion, and silicon fluorides for etching products were detected by QMS. Therefore, it is possible to investigate the interaction between silicon or silicon dioxide surfaces and low-energy CF_x^+ ($x=1-3$) ions with a well-defined energy. This work was supported by NEDO.

JWP 38 Influence of Fluorocarbon Polymer Film Deposited on Aluminum Electrodes on Breakdown Voltage of Nitrogen* C. BILOIU, I. A. BILOIU, *Hokkaido University, Japan, on leave from Faculty of Physics, Bucharest University, Romania* Y. SAKAI, H. SUGAWARA, Y. SUDA, *Hokkaido University, Japan* M. NAKAJIMA, *Fuji Electric Co., R&D Ltd., Japan* In the present work, fluorocarbon polymer films (FCP) were fabricated on Al electrodes by plasma enhanced chemical vapor deposition (PECVD), and the influence of these films on the breakdown voltage of nitrogen gas were examined. The electrodes were made of aluminum with sphere shape of 40 mm diameter. FCP films with a thickness from a few tens of nm up to a few μm have been obtained in 13.56 MHz C_8F_{18} vapor plasma. The XPS analysis of the films showed the successful formation of FCP due to the presence of the characteristic chemical bonds components: C-C at 285 eV, C- CF_x at 287.3 eV, CF at 289.5 eV, CF_2 at 292.1 eV, and CF_3 at 294 eV. The breakdown voltage was measured in nitrogen gas in the pressure range between 0.2 and 10 Torr, for gap lengths between 1 and 2 cm. The result revealed that the breakdown voltage increased approximately 365 V for a case of FCP film thickness of 10 μm .

*This work was performed under the auspices of Grant-in-Aids for Scientific Research (B), for Encouragement of Young Scientists (A), and for JSPS postdoctoral fellows.

JWP 39 Atomic Oxygen Density Profiles and Sticking Coefficients for 5 Different Surfaces in an Inductively Coupled Plasma* SERGI GOMEZ, WILLIAM G. GRAHAM, *Queen's University of Belfast* There is increasing interest in inductively coupled plasmas (ICPs) for material processing. Here the effect of 5 substrate materials on atomic oxygen density profiles in a low pressure oxygen plasma has been investigated. Stainless steel (SS), aluminium (Al), SiO_2 , Si and polypropylene (PP) samples were placed on the lower electrode of an ICP Gaseous Electronic Conference (GEC) reactor. Operation in capacitive and inductive mode is contrasted by spatially resolved TALIF measurements of atomic oxygen at pressures from 1.67 Pa to 66 Pa, and input powers from 25 to 300 W. Densities range from 10^{12} to 10^{14} cm^{-3} in capacitive mode, and from 5×10^{13} to $5 \times 10^{14} \text{ cm}^{-3}$ in inductive mode. The measured profiles allow the determination of the oxygen sticking coefficients on the surfaces (α). For all materials the measured values increase with decreasing pressures and when changing from capacitive to inductive mode. In capacitive mode the highest values correspond to SS (0.02-0.5), then to PP, Si, and finally to Al and SiO_2 (0.009-0.2).

*Work supported by the EU BRITE programme.

JWP 40 Low Temperature Plasma Nitriding Of Stainless Steel In $N_2/H_2/Ar$ LFICP Discharges S. XU, W. LUO, N. JIANG, K.N. OSTRIKOV, *Plasma Processing Laboratory, NS/NIE, Nanyang Tech. Univ., 637616 Singapore* A low frequency, high density, inductively coupled plasma (LF ICP) source has been developed and used for nitriding of AISI stainless steels. A series of experiments has been conducted in a low temperature (320-400 °C), low pressure $N_2/H_2/Ar$ gas mixture discharges. The results show that the nitriding process is very fast, $\sim 45 \mu\text{m/hr}$ for AISI 304 and $\sim 90 \mu\text{m/hr}$ for AISI410, even at a low nitriding temperature. After nitriding, the micro hardness of the nitrided layer is increased by a factor of 7 and the free corrosion potential is also improved. The pin-on-disc measurement indicates that the wear resistance improved more than 10 times. The microstructure and

composition of the nitrated surface layers characterised using scanning electron microscopy/energy dispersive x-ray diffraction and x-ray diffraction reveal that the nitrated layer has crystalline structure with various phases. The distribution of the nitrogen content varies sharply: high in the nitrated layer and almost zero elsewhere. The content of Cr, however, remains constant over the entire substrate/nitrated layer.

JWP 41 Experimental Investigations of the Thermal Expansion of Solid SF₆ and CHCl₃ IVAN SARWAR, *Cherkassy Institute of Engineering and Technology, 18006, Cherkassy, Bul'var Shevchenko 460, Ukraine* The absolute dilatometric study of the thermal expansion is carried out for the high temperature phase of solid SF₆ and CHCl₃ in the temperature range 85 - 170 K by the laser Michelson interferometric dilatometer. Experimental technique is described. From the comparison of results for the investigated samples and the solid xenon the quality analysis was carried out to investigate the influence of the phonon-rotational interaction in molecular crystals with different spherical symmetry to check performance of low corresponding states. Received results are in the good agreement with existing structure analysis X-ray data for SF₆ [1]. It is found that with the temperature increase due to the growth of liberation amplitudes the additional effect has take place in comparison with solidified rare gases. Grunisen's constants for the solid SF₆ were calculated. It is shown that these constants are the same as for solidified rare gases and weakly raise with the temperature in accordance to Max Born theory.

JWP 42 Influence of Orientational Motion of Molecules in the Process of Heat Transfer in the Solid CHCl₃ and C₆H₆ IVAN SARWAR, NICK ZHOLONKO, *Cherkassy Institute of Engineering and Technology, 18006, Cherkassy, Bul'var Shevchenko 460, Ukraine* The isobaric thermal conductivity of solid CHCl₃ and C₆H₆ have been studied at high temperatures. It has been found that with a temperature increase the isobaric thermal conductivity CHCl₃ and C₆H₆ decrease more rapidly than $\lambda \sim T^{-1}$ law. The isobaric data recalculation on fixed molar volume was done. The contribution of phonon-phonons (Umclapp - processes) and phonon-rotations interactions to full thermal resistance are calculated.

JWP 43 Isobaric Thermal Conductivity of Solid SF₆ in the Plastic Phase: The Influence of the Hindered Molecular Rotation and the Sound Velocity Decrease IVAN SARWAR, NICK ZHOLONKO, *Cherkassy Institute of Engineering and Technology, 18006, Cherkassy, Bul'var Shevchenko 460, Ukraine* The high temperature phase investigations of the isobaric thermal conductivity of solid SF₆ in the temperature range 90 - 220 K has been studied by a flat stationary method. The experimental technique and work for sample growth and thermal conductivity measuring is described. It has been found the temperature increase causes the isobaric thermal conductivity decrease as $\sim 1/n$ where $n \geq 1$, as against isohoric researches, where the thermal conductivity grows. The thermal conductivity behaviour of molecular crystals is discussed depending on temperature within the framework of representations about additional influence on a phonon flow of the molecular orientational movement. The received results discussed in connection with the found out influence of changes of speed sound due to increase of temperature on heat transport of the crystal

lattice in equilibrium samples of solid SF₆. The relation between the temperature dependence of the thermal conductivity and the influence of the orientation motions of the molecules on heat transport is considered in connection with the existent isochoric thermal conductivity data also.

JWP 44 PLASMA DIAGNOSTICS II

JWP 45 Plasma Diagnostics on a Pulsed Argon ICP Source* C. A. DEJOSEPH, JR., *Air Force Research Laboratory, Wright-Patterson AFB, OH* WEI GUO, *Innovative Scientific Solutions, Inc., Dayton, OH* A planar inductively coupled plasma (ICP) source is characterized using current and voltage probes, a commercially-built Langmuir probe system, and a fast photomultiplier with narrow band filter. The rf supply operates at 13.56 MHz and can be 100% power modulated to allow pulsed operation of the source. By digitally recording long current and voltage waveforms and using accurate phase correction for the electronics, time resolved rf power and complex impedance are measured during a pulse. With the Langmuir probe operated in boxcar mode, time resolved electron and ion densities along with electron temperatures are also measured. Data will be presented for rep rates between 1 KHz and 10 KHz and duty cycles of 10% and 25% with average powers (during a pulse) from 50 to 500 watts. It will be shown from the behavior of the complex impedance that the discharge is capacitively coupled at the beginning of a pulse and later becomes inductively coupled. During a single pulse the plasma exhibits a sharp peak in power loading which is also seen in the photomultiplier signal and the plasma density. Peak plasma densities on the order of 10^{12} cm^{-3} have been measured.

*This work supported by Air Force Office of Scientific Research.

JWP 46 Time resolved measurements for mass identified, neutral particles sampled from a plasma. J.A. REES, *Hidden Analytical Limited* T.H. RUSSELL, P.J. HATTON, I.D. NEALE, *Hidden Analytical Limited* It is of interest to study for processing plasmas the time dependence of the abundances and energies of both neutral species and ions arriving at the surface of a target, particularly when the targets electrical bias is pulsed or when the plasma itself is dependent on variations with time of parameters such as the gas pressure or composition. We consider here the response of the ionisation source of a quadrupole mass spectrometer to sudden changes in its operating parameters and the implications of these observations in the study of mass-identified neutral species generated, for example, by laser ablation from a surface, or sampled from a pulsed plasma. It is shown that for a well-designed source, resolution times of better than 40 microsec are possible. (The resolution time is defined as the time taken for the number density of ions in the mass spectrometers source to be reduced, when the generation of ions is suddenly stopped, to below 1/original steady state value). The time observed represents the time taken for the ion population in the source to collapse to a value representing the new operating parameters and may be taken as setting the limit of the time-dependent changes observable for

the plasma process under examination. The response times are a factor of more than 5 better than those of a more conventional mass spectrometer source. The sensitivity of the source and the linearity of its output as a function of its electron emission current, are also discussed. The energy distributions of the ions created were examined using the electrostatic energy analyser incorporated in the instrument. Typical data are outlined.

JWP 47 Time resolved measurements for mass identified ions sampled from an R.F. Plasma. J.A. REES, *Hidden Analytical Limited* D. MILLS, C.L. GREENWOOD, I.D. NEALE, *Hidden Analytical Limited* It is increasingly popular for R.F. processing plasmas to be pulsed in some manner, typically by pulsing the applied R.F. power itself, or by applying time-varying potentials to the target substrate. To understand the beneficial effects obtained when etching or coating target surfaces in this way, it is useful to have available measurements of the energy distributions of the ions incident on the target, particularly if the energy distributions can be measured at intervals during the pulsing cycle. To illustrate the profound changes in ion energy distributions which can occur, we describe here measurements for a capacitively-coupled argon plasma operated at 13.6MHz between plane-parallel electrodes, in which the R.F. power could be applied to either electrode. The electrode not connected to the R.F. supply could be D.C. biased. The energy distributions of the Ar⁺ and other ions formed in the plasma were measured at the surfaces of the two electrodes using a Hidden EQP instrument. In the first series of measurements the ions were sampled as they arrived at the R.F. electrode, when the counter-electrode was pulsed with a 200 Hz, square-wave, signal of between 0 and 50 volts. The energy distributions were measured as a function of time using a sample window of 20 microsecs. scanned across the whole period of the 200Hz signal. The data show clearly the adjustment in the potential of the plasma to the A.C. bias applied to the counter electrode and the decay of the energy distribution during the 0 volt-period of the A.C. bias. The effects of varying the frequency and amplitude of the A.C. signal and the gas pressure are shown. The data are contrasted with those obtained when the connections to the two electrodes were exchanged, and illustrate the marked changes in the distributions to be expected when applying pulsed voltage waveforms to target surfaces exposed to an R.F. plasma.

JWP 48 Energy and Angular Distribution of Ions Extracted from a Large Hole in Contact with a Plasma* DEMETRE ECONOMOU, *University of Houston* CHANG-KOO KIM, *Novellus Inc.* The energy and angular distribution of ions extracted from a hole in contact with a low-temperature plasma have been measured for both argon and deuterium plasmas. A single hole is thought to be a well-defined system for understanding the interaction of a plasma with a biased grid. Such plasma-grid interaction finds applications in neutral beam etching, ion sources, satellite thrusters, neutron generators, etc. The plasma parameters (Debye length or sheath thickness), hole diameter and thickness, determine the characteristics of the ions (and fast neutrals) extracted through the hole. The energy distribution of ions showed distinctly different behavior according to the ratio of the hole diameter to the sheath thickness (d/L). The angular distributions of ions depended both on the ratio of the hole diameter to the sheath thickness and the aspect ratio of the hole. Plots showing the angular distribution of ions as a function of the d/L were derived for both argon and deuterium plasmas.

*Work supported by Sandia National Labs and NSF

JWP 49 Investigation of the LAPPS Ion Flux to a Surface Biased with an Arbitrary High Frequency Waveform* DAVID BLACKWELL,[†] SCOTT WALTON,[‡] DARRIN LEONHARDT, DONALD MURPHY, RICHARD FERNSLER, ROBERT MEGER, *Naval Research Laboratory, Plasma Physics Division Washington, DC 20375* Materials etching using accelerated ions has become a widely used procedure in the semiconductor industry. Typically the substrate is biased with high frequency voltage waveforms, which cause the substrate to acquire a negative DC voltage to accelerate the ions. However, the ions do not reach the substrate as a monoenergetic beam. The ion energy distribution function (IEDF) is profoundly influenced by the frequency and shape of the applied waveform. At NRL, we have been experimenting with electron-beam produced plasmas as an alternative to radiofrequency (RF) driven discharges. The most promising of these sources is the hollow cathode driven Large Area Plasma Processing System. This source is designed to produce large area ($> 1 \text{ m}^2$), high density, uniform sheets of plasma. In this presentation we will show measurements of the ion energy distribution function (IEDF) from continuous and pulsed electron beam plasmas produced in 20-30 cm wide \times 1 cm thick sheets by a 2 kV hollow cathode. The IEDF is obtained using a gridded energy analyzer incorporated into a biasable stage. The surface flux and IEDF as a function of the waveform input to the stage will be investigated by using various types of pulse functions and variable frequency RF voltages. Typical operating conditions are 15-20 millitorr of argon, oxygen, or nitrogen, and 150-200 Gauss magnetic field.

*work supported by the office of Naval Research

[†]NRL/NRC Postdoctoral Research Associate

[‡]SFA, Inc., Landover MD 20785

JWP 50 Effect of Electron Energy Distribution Function on Spectroscopic Characteristics of Microwave Discharge Argon Plasma HIROSHI AKATSUKA, RYOUJI KASHIWAZAKI, *Research Laboratory for Nuclear Reactors, Tokyo Institute of Technology* In this paper we discuss effects of electron energy distribution function (EEDF) on number densities of excited states of Ar sci in a microwave discharge argon plasma at pressure range 0.1 - 10 Torr. The argon discharge was generated by a rectangular waveguide and a quartz tube (26 mm i.d.) with an adjustable short-circuited plunger. The microwave frequency was 2.45 GHz and the output power was 300 W. We carried out single probe measurement and found the electron temperature $T_e \approx 5 - 12 \text{ eV}$ and density $n_e \approx (1 - 4) \times 10^{11} \text{ cm}^{-3}$, respectively. We also measured EEDF by the second derivative of the measured $V-I$ characteristics, which revealed the EEDF to be not a Maxwell but almost a Druyvesteyn distribution, with large uncertainty, since the EEDF was determined by numerical averaging operation. We also measured the number densities of some excited states by spectroscopic examination. The experimental results were compared with calculations with the collisional radiative (C-R) model. The calculated results agreed well with the present experiments when we adopted the Druyvesteyn distribution as the EEDF, whereas the Maxwell distribution gave poor results.

JWP 51 Thomson Scattering Measurement of Electron Density and Temperature in a Microwave Plasma for Diamond Deposition S. NARISHIGE, S. KITAMURA, K. TEII, K. UCHINO, K. MURAOKA, *Kyushu University, Japan* T. SAKODA, *Kitakyushu Nat. College Tech., Japan* The composition and fluxes of gaseous species in a reactive plasma are highly affected by behavior of electrons. The detection of electrons in a microwave plasma operating at pressures as high as 10-100 Torr is known to be difficult. For example, the small mean-free path obstructs the use of electrostatic probes. In this study, electron density (n_e) and temperature (T_e) in a microwave CH_4/H_2 plasma for diamond deposition were measured by laser Thomson scattering spectroscopy. This method can provide the local density and temperature without perturbing the discharge condition. A Nd:YAG laser at a frequency doubled wavelength of 532 nm was injected into the chamber. The scattered light was passed through a double-monochromator and the output signal was detected by a photomultiplier tube. With a pure H_2 plasma at 20 Torr, $n_e = 3 \times 10^{17} \text{ m}^{-3}$ and $T_e = 1.7 \text{ eV}$ were obtained. However, with a 10% CH_4 -90% H_2 plasma, the scattering spectrum confirmed that the component of rotational Raman scattering of molecules originated from CH_4 were overlapped on the Thomson scattering spectrum. It was found that the use of a Nd:YAG laser at fundamental wavelength of 1064 nm was suitable to suppress the component of the Raman scattering since the scattering intensity is inversely proportional to the 4th power of wavelength.

JWP 52 Thomson Scattering Observation of Non-Maxwellian EEDF and the Effect of Local Electron Heating A. KONO, H. FUNAHASHI, *Nagoya University, Nagoya 464-8603, Japan* Laser Thomson scattering measurements were carried out to study electron energy distribution function (EEDF) of inductively coupled plasmas using $\text{C}_4\text{F}_8/\text{Ar}$ and CF_4/Ar mixture gases. The plasma was produced using a one-turn coil antenna immersed in the plasma at a total pressure of 25 mTorr. A specially designed triple-grating spectrometer was used, which produces Thomson spectra on the output focal plane with the interfering Rayleigh and stray components highly suppressed; an ICCD camera operated in the photon-counting mode was used for multichannel detection of the spectrum. At a RF (13.56 MHz) input power of 300 W in the case of pure Ar plasma, EEDF was Maxwellian with an electron density $> 10^{12} \text{ cm}^{-3}$. Upon mixing of C_4F_8 as well as CF_4 , decrease in the electron density and upward bend of the plot of the Thomson spectrum (energy vs. logarithmic scattering intensity) at energies around 5 eV was observed. The mechanism for producing this bend was studied via Monte-Carlo particle simulation. The results indicate that electron heating in a uniform electric field does not lead to upward bend; electrons should be heated locally near the antenna surface where the RF electric field is strong and cooled in other part of the plasma by inelastic collisions.

JWP 53 Investigation of a Microwave Discharge by Electric Field Measurements D. LUGGENHÖLSCHER, U. CZARNETZKI, H.F. DÖBELE, *Institut für Laser- und Plasmaphysik, Universität GH Essen, D-45117, Germany* A microwave discharge is investigated by laser spectroscopic electric field measurements. Both microwave fields and plasma generated microfields are measured. The field strengths range between 10 V/cm and about 100 V/cm. The microfields are a measure of the plasma density. The electric field distribution in the discharge is investi-

gated by fluorescence dip-spectroscopy in atomic hydrogen. This laser spectroscopic technique allows the determination of low electric field strengths down to 5 V/cm with high spatial and temporal resolution by probing the splitting of Rydberg states ($n = 14 - 30$). The microwave plasma source is a commercial device with a plasma volume of 16 cm diameter and a length of 50 cm. The plasma is generated in a central region of 6 cm height. The microwave frequency is 2.45 GHz and the discharge is operated either cw or pulsed (typ. 20 Hz - 200 Hz) at peak powers in the range between 1 kW and 2 kW. The operating gas is mainly argon with a 10 % admixture of hydrogen. The ignition phase and the afterglow phase as well as parameter dependencies are investigated in detail.

JWP 54 Electric Field Measurement Methods based on Stark Effects in Xenon Atoms MARK BOWDEN, BRAM VISSER, GERRIT KROESEN, *Eindhoven University of Technology, The Netherlands* The electric field in a plasma is an important quantity but in-situ measurement is often difficult due to the lack of suitable measurement techniques. This is particularly true for measurement in lighting plasmas such as discharge lamps and plasma display panels. In this paper, we report the development of a method for the measurement of electric fields in glow discharge plasmas, based on Stark spectroscopy of xenon atoms. A key feature of the method is that the electric field is determined by matching experimentally obtained absorption spectra to theoretically calculated spectra. Measurements of Stark spectra are made in the sheath region of a glow discharge using laser optogalvanic spectroscopy and laser induced fluorescence spectroscopy. These measurements are compared with theoretical spectra, calculated by solving the Schrodinger equation for the case of a xenon atom in the presence of an electric field. In this paper, results of preliminary spectra will be presented and the suitability of different excitation schemes will be discussed.

JWP 55 Towards measurement of the electric field distributions around structures immersed in a plasma: calibration of electric field induced energy level shifts in Argon G. A. HEBNER, *Sandia National Laboratories* The characteristic of the plasma sheath around structures immersed in plasma is of fundamental interest. In particular, the details of the sheath structure in the presheath region or around objects immersed in flowing ion fields are not well characterized. A key aspect of this work is obtaining the required spatial, temporal and electric field sensitivity. Argon is a commonly used rare gas in a number of discharges. As such it is an ideal candidate for spectroscopic based electric field measurements within the sheath and bulk discharge regions. This poster shows the use of an atomic beam system combined with pulsed laser spectroscopy to directly calibrate the electric field induced shift of high lying energy levels. In addition, data on very high lying argon levels, up to the 20 F manifold, were obtained. Comparison of our electric field induced energy level shift calibration curves with previous work will be shown. The possibility of using this system to calibrate energy level shifts in other gases of technological interest to the microelectronics and lighting industry will be discussed.

JWP 56 LIGHTING AND DISPLAYS

JWP 57 Vacuum Ultraviolet Emission Dynamics of a Surface Discharge type PDPs WOO-GEUN LEE, MAY SHAO, MIKE BROWN, JEFF GOTTSCHALK, ALVIN D. COMPAAN, *University of Toledo* JERRY SCHERMERHON, *Electro Plasma Inc.* DEPARTMENT OF PHYSICS, UNIVERSITY OF TOLEDO, TOLEDO, OH TEAM, ELECTRO PLASMA INC., MILLBURG, OH COLLABORATION, We report nanosecond time-resolved measurements of the vacuum ultraviolet (VUV) emission and current waveforms for a planar, surface-discharge plasma display electrode in Xe/Ne mixtures. The 173nm excimer emission is separately resolved from the overall VUV emission by a removable fused silica filter. The time difference between the maximum of excimer emission and that of resonant atomic emission is measured at high Xe concentration. The decay time of the overall VUV emission decreases abruptly as the Xe concentration increases. The relative efficiency of VUV emission increases strongly from 4 but only a marginal increase in VUV emission efficiency occurs at 30 emission efficiency drops with increasing driving voltage. supported by Electro Plasma Inc.

JWP 58 Radiative lifetimes, branching fractions, and atomic transition probabilities for Tb II J.E. LAWLER, E.A. DEN HARTOG, J.A. FEDCHAK, M.E. WICKLIFFE, *Univ. of Wisconsin* Rare-earth salts are used in many commercial metal-halide high intensity discharge lamps. Terbium is known to enhance the blue region of the spectra from metal-halide lamps. Accurate atomic transition probabilities are needed in the models used for lamp design and for diagnostics. We have determined accurate radiative lifetimes for 40 odd-parity levels and 36 even-parity levels of Tb II using time-resolved laser-induced fluorescence on a slow beam of Tb ions. Tb II branching fractions have been determined from emission spectra taken with the 1.0 m Fourier transform spectrometer (FTS) at the National Solar Observatory and the 2.0 m FTS at NIST. These are combined with the radiative lifetimes to produce 195 accurate transition probabilities for Tb II. This work is supported by NSF grant AST-9819400. J. E. L. is a guest observer at the NSO on Kitt Peak, AZ.

JWP 59 Excimer radiation from pulsed micro hollow cathode discharges ISFRIED PETZENHAUSER, UWE ERNST, KLAUS FRANK, *Physikalisches Institut I, Univ. Erlangen-Nuremberg, 91058 Erlangen, Germany* Since several years d.c. microhollow cathode discharges (MHCDs) are under investigation as efficient sources of VUV excimer radiation [1]. Up to now overall efficiency and the radiation power of the MHCDs are too low to compete e.g. with silent discharges. Substantial improvement in these parameters would make by its simple geometry MCHDs attractive for a wide range of applications. Experiments and simulations show that the efficiency of MCHDs is substantially reduced by high gas temperatures beyond 1500 K. Measurements in pure nitrogen showed that the gas temperature can be reduced about 40. The actual experiments are with Xe and Ar bands in the VUV and the results of radiation output under d.c. and pulsed operation for different pulse duration and repetition rates are presented. [1] A. El-Habachi, K.H. Schoenbach, *Appl. Phys. Lett.* 73(7), pp.

885-887 (1998) [2] U. Ernst, "Emissionsspektroskopische Charakterisierung von Hochdruck-Mikrohohlkathodenentladungen," Ph. D thesis, Univ. of Erlangen-Nuremberg, 2001 This work was supported by DFG under the contact FR 1273-1

JWP 60 Mercury Excited State Density Measurements in an Inductively Coupled Low Pressure Discharge PHIL MOSKOWITZ, *OSRAM SYLVANIA* The inductively coupled low pressure Hg rare gas discharge forms the basis of several fluorescent lighting products, including OSRAM SYLVANIA ICETRON [TM] lamp. In this work, the Hg(3P1) resonance level population has been measured in a discharge cell resembling the ICETRON lamp, but with flat end windows for laser access. Using CW dye laser absorption spectroscopy at 435nm, the on-axis density was acquired for a range of rare gas pressure (50-600 milli Torr), mercury cold spot temperature (20-50C), and discharge current (3-10A). Using curve of growth analysis and taking advantage of the lasers high spectral resolution to probe a single isotopic and hyperfine component, access to the linear portion of the growth curve was achieved. Data are presented for discharges with argon and krypton as buffer gas. Saturation in the population density is observed at these current levels, with densities in the range of 10^{12} cm⁻³. On-axis gas temperature, extracted from the Doppler width of the absorption profile, ranges from 450-850K, and will be compared with previously published results on the Philips QL lamp (1). (1) J. Jonkers et al., *J. Phys. D* 30, 1928 (1997).

JWP 61 Laser Thomson Scattering Diagnostics of a PDP Micro Discharge Plasma Y. NOGUCHI, T. HONDOU, K. UCHINO, K. MURAOKA, *Kyushu University, Japan* In order to improve efficiency of the PDP, much effort is being made to understand the structure of the micro-discharge plasma. However, because its size is extremely small, no direct measurements of electron density (n_e) and electron temperature (T_e) have been reported. In this study, we applied the laser Thomson scattering method to a micro-discharge plasma for the direct measurement of n_e and T_e . For this measurement, there are following difficulties. First, the size of the plasma in a single PDP cell is about 0.2 mm, and so the scattering volume size should be below 0.1 mm. This may result in a very small Thomson scattering signal. Second, the stray laser light may be very strong because the wall of the discharge cell is close to the scattering volume. In order to overcome these difficulties, we used the photon counting method, and fabricated a spectrometer which had a stray light rejection of 10^{-8} . Then, we have successfully performed measurements at the distance of $Z=0.1$ mm from the electrode substrate surface. In this experiment, the discharge gas was a Ne-Ar (10%) mixture at a pressure of 200 Torr. Values of n_e and T_e were $(0.2-3) \times 10^{19}$ m⁻³ and 1.6-3.4 eV, respectively, depending on the time from the beginning of the pulsed discharge and the measuring position. Experimentally measured distributions of n_e and T_e are used to discuss about the structure of the micro-discharge.

JWP 62 Stepwise Ionization of Xenon in RF Plasma Display Panels* C. PUNSET, L.C. PITCHFORD, J.-P. BOEUF, *CPAT, Universit Paul Sabatier & CNRS, Toulouse, France* The efficiency for conversion of electrical energy to visible photons in typical Plasma Display Panels (PDP's) conditions (3-10% Xe in Ne, 100's of kHz, 500 torr, 100 microns) is low (about 1 lumen/watt). The main factor limiting the efficiency is the energy lost in heating ions in the sheaths. RF excitation (10's of MHz) would therefore be

more efficient, and investigations of RF PDP's are underway. We present here a study of the role electron-impact ionization of the xenon metastable atoms on the ionization balance in RF PDP's. In this study, rate equations for the resonance, R, and metastable, M, atoms are coupled to our fluid model of PDP's. Cascading from and excitation to the higher excited states are included via one parameter. Uncertainties in the excitation transfer rates and branching ratios for cascading to R and M preclude a more precise treatment. For 3%Xe in Ne, 400 torr, and 40 MHz, direct ionization dominates the ionization balance. Stepwise ionization is important for low discharge powers and high xenon concentrations.

*supported in part by LG Electronics

JWP 63 SURFACE PROCESSING

JWP 64 Implantation of Iron Ions into Silicon by Ablation Plasma Ion Implantation BO QI, RONALD GILGENBACH, Y. Y. LAU, MARK JONSTON, JIE LIAN, LUMING WANG, *Intense Energy Beam Interaction Lab, Nuclear Eng. and Rad. Sciences Dept., University of Michigan, Ann Arbor, MI 48109-2104* GARY DOLL, A. LAZARIDES, *Advanced Materials Research and Development, Timken Research, The Timken Corporation, Canton, OH, 44706-0930* Experiments have confirmed the acceleration and implantation of ions generated by KrF laser ablation of solid iron targets. [1] Optical diagnostics have shown plasma electron temperatures of 12 eV immediately following the laser pulse, cooling to the eV level on a microsecond timescale. Silicon substrates are pulse-biased to voltages of about -10 kV. Ion implantation into substrates has been verified by Transmission Electron Microscopy (TEM) and X-Ray Photoelectron Spectroscopy (XPS). TEM data show that for zero applied voltage, the deposited films consist of an amorphous iron silicide layer on the silicon with an overlying, nanocrystalline Fe layer. When -10 kV is applied to the substrate the samples also exhibit a damage layer extending 7.6 nm below the original Si surface, demonstrating Fe implantation. This damage layer depth is slightly less than TRIM code calculations for a maximum, effective ion energy of about 8 keV. XPS data on implanted structures confirm Fe implantation into Si covered by amorphous layers of iron silicide and the top layer of Fe. [1] B.Qi, et al., *Appl. Phys. Lett.*, 78 3785 (2001) Research funded by the National Science Foundation

JWP 65 The Simulation of Neutral Beam Source for Nanoscale Etching Technology* S.J. KIM, *Affiliation* H.S. LEE, *Affiliation* M.S. HUR, *Affiliation* H.J. LEE, *Affiliation* J.K. LEE, *Department of Electrical Engineering, Pohang University of Science and Technology, Pohang 790-784, S. Korea* PLASMA APPLICATION MODELING GROUP TEAM, Hyperthermal neutral beam has been proposed as a prime candidate to overcome the plasma process induced damage that is a serious problem in the fabrication of semiconductor device. We have performed the simulation of a neutral beam made from ion-surface neutralization. The simulation is composed of two parts: 1) Ion-gun and 2) neutral beam transport. For the simulation of ion-gun, XOOPIE (Object Oriented Particle-in-Cell) code is utilized. By the variation of ion-gun geometry and grid voltage, we find the optimized condition of

high flux that is used as an ion source for low-pressure neutral-beam etching. For neutral transport simulation, the XOOPIE and DEGAS2 code have been modified to include particle-surface interaction and various collision reactions. In addition, we use TRIM (Transport of Ions in Matter) code to find reflection characteristic of ion which is applied to modified codes as input data. The reflection coefficient is about 0.3 with incident ions of 100eV on the silicon, and the average energy of reflected neutrals is 30 and ion current are optimized to obtain high flux and uniform neutral beam. The larger neutral flux is obtained at low angle of incident ions around 5.

*Work supported by Korea Ministry of Science and Technology, 21st C Frontier R&D Project.

JWP 66 Microtrench/oxide island reduction with electron beam irradiation in high aspect ratio oxide etching M. WATANABE, D. M. SHAW, G. J. COLLINS, *Department of Electrical Engineering, Colorado State University, Fort Collins, CO 80523* During high aspect ratio oxide etching, the feature surface charges up and deflects the subsequent ion trajectories to the sidewalls due to local electric field, which results in microtrenching at the feature edges. At the etch end point, the microtrench reaches the conducting underlayer, which does not accumulate charge, and an oxide island remains at the center if no overetching is used. An electron beam source [1] is developed to neutralize the positive charge buildup at the feature bottom during etching. SEM images of the etch profiles show that the microtrench/oxide island formation is reduced with the electron beam irradiation. The electric field and ion trajectories within an etch feature are calculated, indicating that the reduction of the microtrench/oxide island formation is achieved by electron beam charge neutralization at the feature bottom. [1] D. M. Shaw, M. Watanabe, G. J. Collins, and H. Sugai, *Jpn. J. Appl. Phys.* 38, 87 (1999).

JWP 67 Ion Energy Distribution of Pd and Ni Positive Ions in DC and Pulsed DC Plasma Discharge Sputtering RAVIPRAKASH JAYARAMAN, LAWRENCE J. PILIONE, HSIN-PAI HSEUH, RUSSELL MESSIER, ROBERT T. MCGRATH, *Pennsylvania State University* Palladium and its alloys have long been known to adsorb hydrogen spontaneously when exposed to hydrogen containing ambient. Adsorption of hydrogen results in changes in the physical, electrical and optical properties of the metal and these phenomena can be utilized in sensing hydrogen gas. To date, no systematic investigation of the relationships between deposition condition, film morphology and sensor performance have been carried out. In this work, we present IEDFs measured in Ar driven sputter discharges used for deposition of Pd/Ni alloy thin films. Changes in the ion energy distributions of Pd⁺, Ni⁺ and Ar⁺ with power, pressure, pulsing frequency and pulsing width used in the deposition condition are presented and will be correlated to the morphology of the alloy film deposited. For pulsed DC source operation with both Pd and Ni targets IEDFs measured show two narrow, Gaussian shaped, peaks. One is centered at around 65 eV with an energy half width of about 5 eV and the second, equally narrow peak is centered near 5 eV. For DC discharge operation under identical conditions, a single IEDF peak near 0 eV is observed. Plasma and sheath responses to the drive voltage pulse shapes that produce the observed IEDFs will be discussed along with control procedures for producing Pd/Ni alloy films that have the desired composition and morphology.

JWP 68 Hydrogen plasma treatment of Si(100), (110), and (111) surfaces monitored by in situ infrared spectroscopy MASANORI SHINOHARA, TAKAYUKI KUWANO, YASUO KIMURA, MICHIO NIWANO, *Research Institute of Electrical Communication, Tohoku Univ. Sendai, 980-8577, Japan* Hydrogen plasma pre-treatment of Si crystal surfaces is widely used in depositing Si and diamond thin films on Si. It is known that the chemical state of the plasma-treated surface have a great influence on the quality of deposited thin films. However, there are few reports on the chemical state of Si surface during plasma treatment. In this study, therefore, we investigate the chemical state of Si(100), (110) and (111) surfaces during hydrogen plasma treatment, using in situ infrared absorption spectroscopy (IRAS) in the multiple internal reflection (MIR) geometry. We found that at initial stages of plasma treatment hydrogen atoms are abstracted from the surface hydride species. With further plasma treatment, the surface is covered with hydrogen again. We also found that hydrogen plasma treatment produces hydrogen-terminated Si vacancies (VH_x) in the vicinity of the surface. The surface concentration of VH_x strongly depends on the crystallographic orientation of the Si surface; it increases in the order: Si(111) < Si(100) < Si(110).

JWP 69 Atmospheric pressure glow discharge (APG) for thin film deposition RÜDIGER FOEST, FLORIAN SIGENEGER, MARTIN SCHMIDT, *Institut für Niedertemperatur-Plasmaphysik, 17489 Greifswald, Germany* Surface treatment by APG avoids expensive vacuum equipment. This contribution treats the deposition of thin films in an APG in He (30 sccm) with small admixtures (10^{-4}) of HMDSO. The powered (100 kHz) plane electrode ($80 \cdot 15 \text{ mm}^2$) is covered by a glass insulator and is positioned about 2 mm above the grounded Al-sheet substrate. Power absorption of the discharge ($\approx 2 \text{ W}$) and gap voltage ($U_{pp} \approx 1.2 \text{ kV}$) are determined by measuring sustaining voltage ($V_{pp} \approx 2 \text{ kV}$) and current wave forms ($j \approx 1 \text{ mA cm}^{-2}$). The gas composition is studied by mass spectrometry, film deposition rate is measured by weighing ($10^{-7} \text{ g cm}^{-2} \text{ s}^{-1}$). The thin film is characterized by the contact angle, the corrosion resistance against NaOH, and its chemical structure (XPS, FTIR). The reduced electrical field strength E/p in the gap varies between 5 and 15 V Torr $^{-1} \text{ cm}^{-1}$. The electron velocity distribution function has been determined by solving the stationary and homogenous Boltzmann equation. Using these results thin film deposition is discussed in relation to the ionization rate of the precursor molecules and the current density. Supported by BMBF No.13N7351/0.

JWP 70 Lattice Gas Model Based Optimization of Plasma-Surface Processes for GaN-Based Compound Growth KIYOHIDE NONOKAWA, *Hokkaido Institute of Technology* TAKUMA SUZUKI, *Hokkaido Institute of Technology* KAZUTAKA KITAMORI, *Hokkaido Institute of Technology* TAKAYUKI SAWADA, *Hokkaido Institute of Technology* Progress of the epitaxial growth technique for GaN-based compounds makes these materials attractive for applications in high temperature/high-power electronic devices as well as in short-wavelength optoelectronic devices. For MBE growth of GaN epilayer, atomic nitrogen is usually supplied from ECR-plasma while atomic Ga is supplied from conventional K-cell. To grow high-quality epilayer, fundamental knowledge of the detailed atomic process, such as adsorption, surface migration, incorporation, desorption and so forth, is required. We have studied the influence of growth conditions on the flatness of the growth front surface and the growth rate using

Monte Carlo simulation based on the lattice gas model. Under the fixed Ga flux condition, the lower the nitrogen flux and/or the higher the growth temperature, the better the flatness of the front surface at the sacrifice of the growth rate of the epilayer. When the nitrogen flux is increased, the growth rate reaches saturation value determined from the Ga flux. At a fixed growth temperature, increasing of nitrogen to Ga flux ratio results in rough surface owing to 3-dimensional island formation. Other characteristics of MBE-GaN growth using ECR-plasma can be well reproduced.

JWP 71 POST-DEADLINE ABSTRACTS

JWP 72 Detection of Rydberg Levels of Ar Atoms in a Plasma by Laser-Induced Fluorescence-Dip Spectroscopy K. TAKIZAWA, K. SASAKI, K. KADOTA, *Department of Electronics, Nagoya University, Japan* Low-temperature plasmas are utilized for various material processing, such as reactive ion etching, sputtering, plasma immersion ion implantation (PIII), etc. In these material processing using plasmas, ions are accelerated by electric field in a sheath. Consequently, to optimize the material processing, the distribution of the electric field must be controlled accurately. We have attempted to measure the electric field in a reactive plasma by detecting Stark splitting of Rydberg levels of Ar atoms. We detected them by laser-induced fluorescence-dip (LIF-Dip) spectroscopy, which has been applied to a hydrogen plasma and allows the sensitive measurement of weak electric fields close to 5 V/cm.¹ We applied this method to metastable Ar atoms. The measurement was carried out in an inductively coupled plasma (ICP) at a low gas pressure below 100 mTorr by using two visible tunable lasers. We have succeed in detecting highly-excited Rydberg states having principal quantum numbers up to $n = 58$. The sensitive detection of electric field may be possible by measuring the Stark splitting of the highly-excited Rydberg state.

¹U. Czarnetzki, D. Luggenhölscher, and H. F. Döbele, *Phys. Rev. Lett.* **81**, 4592 (1998).

JWP 73 Determination of 2p Excitation Transfer Rate Coefficients In Neon Gas Discharge D.J. SMITH, *University of Strathclyde* R.S. STEWART, *University of Strathclyde* We will discuss our theoretical modelling and application of an array of four complementary optical diagnostic techniques for low-temperature plasmas. These are cw laser collisionally-induced fluorescence (LCIF), cw optogalvanic effect (OGE), optical emission spectroscopy (OES) and optical absorption spectroscopy (OAS). We will briefly present an overview of our investigation of neon positive column plasmas for reduced axial electric fields ranging from $3 \times 10^{-17} \text{ Vcm}^2$ to $2 \times 10^{-16} \text{ Vcm}^2$ (3-20 Td), detailing our determination of five sets of important collisional rate coefficients involving the fifteen lowest levels, the 1S0 ground state and the 1s and 2p excited states (in Paschen notation), hence information on several energy regions of the electron distribution function (EDF). The discussion will be extended to show the new results obtained from analysis of the argon positive column over similar reduced fields. Future work includes application of our

multi-diagnostic technique to more complex systems, including the addition of molecules for EDF determination. array of four complementary optical diagnostic techniques OGE L C I F determination of five sets of important collisional rate coefficients

JWP 74 Optical Emission Detection of SO₂ by Microfabricated Inductively Coupled Plasma (mICP). OLGA MINAYEVA, JEFFREY HOPWOOD, *Northeastern University* In this work a microfabricated ICP is used to optically detect trace amounts of SO₂. An mICP system consists of a planar microfabricated plasma source and miniature aluminum chamber and operates at 1-10 torr pressure and 0.7-3.5 W of 493 MHz RF power. An SO₂ fraction as low as 2 ppm was measured using the intensity of atomic sulfur emission at 469.5 nm. The detection limit, however, depends on power and pressure, and is as low as 190 ppb. As power increases from 1 W to 3.5 W, the detection limit improves from 400 ppb to 190 ppb due to the increase in electron density. Improvement of detection limits from 300 ppb to 190 ppb was achieved by increasing the pressure from 2.5 to 5.6 torr. In addition, this miniature ICP has the ability to excite the entire SO₂ molecule, which is a desirable feature as compared to large-scale plasma spectrometry systems, where triatomic molecules generally get destroyed due to extensive dissociation in the plasma. Therefore, unlike large-scale ICP-OES, which is traditionally used for atomic detection, this mICP-OES is also a promising molecular detection tool.

JWP 75 A Plasma Technique for Functionalization of Carbon Nanotubes BISHUN KHARE, NASA Ames M. MEYYAPPAN, NASA Ames Carbon nanotubes (CNTs) are receiving much attention recently for their potential in composites, sensors, probes and other applications. Some of these applications require attachment of molecular groups to the ends or sides of the nanotubes which is called functionalization. Typically this is done by treating CNTs with the appropriate wet chemical or exposing them to the vapor of the chemical. We have developed an elegant, simple, and clean process to achieve functionalization through the use of glow discharges. A microwave cavity is used to generate the plasma that contains the needed molecular group. A novel arrangement has been used to filter out the deleterious effects of the plasma photons. The current demonstration focuses on attaching atomic hydrogen to CNTs. In-situ FTIR analysis clearly shows a band at 2940 cm⁻¹ which is characteristic of C-H stretching mode. The approach can be used to attach other groups such as N, NH, F etc.

JWP 76 Ion Energy and Ion Flux Distributions of CF₄/Ar/O₂ inductively coupled plasmas in a GEC cell M.V.V.S. RAO, BRETT CRUDEN, Elore SURENDRA SHARMA, MEYYA MEYYAPPAN, NASA Ames Research Center, Moffett Field, CA 94035 Knowledge of ion kinetics in plasma processing gas mixtures, such as CF₄:Ar:O₂, is important for understanding plasma assisted etching and deposition of materials. Ion energies and ion fluxes were measured in this mixture for 80:10:10, 60:20:20, and 40:30:30 mixture ratios in the pressure range of 10-50 mTorr, and at 200 and 300 W of RF power. Ions from plasma, sampled through a 10 microns orifice in the center of the lower plane electrode, were energy and mass analyzed by a combination of electrostatic energy and quadrupole mass filters. CF_x⁺ (x = 1 - 3), F₂⁺, F⁺, C⁺ from CF₄, Ar⁺ from Ar, and O₂⁺ and O⁺ from O₂, and by-product ions SiF_x⁺ (x = 1 - 3) from etching of quartz

coupling window, COF_x⁺ (x = 1 - 3), CO⁺, CO₂⁺, and OF⁺ were detected. In all conditions ion flux decreases with increase of pressure but increase with increase of RF power. Ar⁺ signal decreases with increase of pressure while CF₃⁺, which is the dominant ion at all conditions, increases with increase in pressure. The loss mechanism for Ar⁺ and increase of CF₃⁺ is due to large cross section for Ar⁺ + CF₄ → Ar + CF₃⁺ + F. Ion energies, which range from 15-25 eV depending on plasma operating conditions, are nearly Gaussian. By-product ion signals are higher at lower pressures indicating stronger plasma interaction with quartz window.

JWP 77 Langmuir Probe Measurements of inductively coupled plasmas in CF₄/Ar/O₂ mixtures M.V.V.S. RAO, BRETT CRUDEN, Elore SURENDRA SHARMA, MEYYA MEYYAPPAN, NASA Ames Research Center, Moffett Field, CA 94035 Inductively coupled plasmas of CF₄:Ar:O₂, which have been of importance to material processing, were studied in the GEC cell at 80:10:10, 60:20:20, and 40:30:30 mixture ratios. Radial distributions of plasma potential (V_p), electron and ion number densities (n_e and n_i), electron temperature (T_e), and electron energy distribution functions (EEDFs) were measured in the mid-plane of plasma across the electrodes in the pressure range of 10-50 mTorr, and RF power of 200 and 300 W. V_p, n_e and n_i, which peak in the center of the plasma, increase with decrease of pressure. T_e also increases with pressure but peaks toward the electrode edge. Both V_p and T_e remain nearly independent of RF power, whereas n_e and n_i increase with power. In all conditions the EEDFs exhibit non-Maxwellian shape and are more like Druyvesteyn form at higher energies. They exhibit a broad dip in the energy range 0-10 eV suggesting an electron loss mechanism, which could be due to via resonance electron attachment processes producing negative ions in this rich electronegative gas mixture. This behavior is more prominent towards the electrode edge.

JWP 78 Spectrally Filtered Raman/Thomson Scattering Measurements in High Pressure Plasmas LEE WONCHUL, LEMPERT WALTER, Depts. of Chemistry and Mechanical Engineering Ohio State University Recent advances in solid state laser technology have enabled a variety of new optical diagnostic techniques based on the use of atomic/molecular vapor filters as narrow bandwidth "notch" filters and/or as spectral discriminators. In this poster we will present new results obtained using a rubidium vapor filter in combination with a diode laser injection-seeded, titanium:sapphire laser at 780 nm. The emphasis will be to use the rubidium vapor filter as an ultra narrow band (1-2 GHz) pre-absorption filter in order to attenuate elastic and/or molecular Rayleigh scattering, there by facilitating low wave number inelastic scattering diagnostics, such as pure rotational Raman and Thomson scattering. In particular, we shall compare and contrast the results of two approaches for reduction of residual broad band output of the injection seeded laser. The first approach is to incorporate a "prism monochromator," consisting of a series of twenty equilateral dispersing prisms and a spatial filter. The second is the incorporation of a phase conjugate stimulated Brillouin scattering cell. We shall show that use of both approaches, in series, provides more discrimination than the product of each when used alone. Finally, proof of concept measurements will be presented in order atmospheric pressure mixtures of nitrogen and/or argon.

JWP 79 Optically Enhanced E-Beam Sustained Air Plasmas PETER PALM, ELKE PLOENJES, *Department of Mechanical Engineering, The Ohio State University* IGOR V. ADAMOVICH, *Department of Aerospace Engineering and Aviation, The Ohio State University* VISH V. SUBRAMANIAM, J. WILLIAM RICH, *Department of Mechanical Engineering, The Ohio State University** Time resolved electron density measurements in electron beam sustained cold atmospheric pressure air plasmas were used to study the effect of vibrational excitation of the diatomic air species on electron removal processes, notably dissociative recombination and attachment to O₂. Vibrational excitation of the diatomics was efficiently produced by optical pumping of CO seeded into the air and subsequent vibration-vibration energy transfer within and between the vibrational modes of CO, O₂, and N₂. From the electron density decay after an e-beam pulse upper limits for the electron recombination rate and the electron attachment rate in these plasmas were determined. Compared to equilibrium cold air, electron recombination and electron attachment in vibrationally excited cold air were found to be reduced by one and three orders of magnitude, respectively.

*This research was supported by the Director of Defense Research and Engineering (DDR&E) within the Air Plasma Ramparts MURI Program managed by AFOSR. Partial support from the Ohio Board of Regents Investment Fund is gratefully acknowledged.

JWP 80 Numerical Simulation of an Optically Pumped CO/Argon Plasma DOUG DIETZ, VISH V. SUBRAMANIAM, *The Ohio State University* SHASHI M. AITHAL, *Novellus Systems, Inc.** Volumetrically diffuse plasmas can be produced in some gas mixtures by optical pumping. Low-lying vibrational modes ($v < 10$) of CO can be excited by resonance absorption of CO laser radiation. Population of very high vibrational levels occurs by vibration-vibration exchange collisions, leading to a highly non-Boltzmann distribution in the vibrational populations. Ionization in these types of plasmas occurs by an associative mechanism in collisions between two highly vibrationally excited molecules. We present 2-D axi-symmetric modeling calculations of an optically pumped, flowing CO/Ar gas mixture, with the aim of predicting steady-state spatial distributions of electron densities. The multi-dimensional model accounts for state-specific vibration-vibration and vibration-translation energy transfer processes as well as associative ionization processes, and examines the variation of electron density in such an electrodeless discharge. In addition to the gas phase Boudouard reaction ($\text{CO}(v) + \text{CO}(w) \rightarrow \text{C} + \text{CO}_2$) and vibration to electronic transfer from the ground electronic state ($X^1\Sigma$) to an excited state ($A^1\Pi$) are included in the model. Coupling of the flow with vibrational kinetics and associative ionization processes is examined.

*This research was supported by NASA Glenn Research Center and by the DDR&E Air Plasma Ramparts MURI Program managed by AFOSR.

JWP 81 Electron-Mediated Vibration-Electronic (V-E) Energy Transfer in Optically Pumped Plasmas ELKE PLOENJES, PETER PALM, J. WILLIAM RICH, IGOR V. ADAMOVICH, *The Ohio State University** Energy transfer from high vibrational states of the CO electronic ground state to electronically excited states is investigated in optically pumped CO-Ar or CO-N₂ plasmas, with and without O₂ and NO additives. Ionization in these strongly nonequilibrium plasmas occurs by an associative

ionization mechanism in collisions of two highly vibrationally excited CO molecules. Removal of the electrons from the optically pumped plasmas using a saturated Thomson discharge results in substantial reduction of UV/visible radiation from the plasma (CO 4th positive bands, NO γ bands, CN violet bands, and C₂ Swan bands). On the other hand, deliberate electron density increase by adding small amounts of O₂ or NO to the optically pumped CO-Ar plasmas produces substantial increase of the UV/visible radiation intensity, which correlates with the electron density. The present experiments strongly suggest that the V-E energy transfer process $\text{CO}(X^1\Sigma \rightarrow A^1\Pi)$, and, possibly, analogous processes populating radiating excited electronic states of NO, CN, and C₂, in optically pumped plasmas, may be mediated by the presence of electrons. Detailed kinetics of the processes will be presented.

*Support by the AFOSR Space Propulsion and Power Program, the NSF and the Ohio Board of Regents is gratefully acknowledged.

JWP 82 Single-Walled Carbon Nanotube Synthesis in CO Laser Pumped Carbon Monoxide Plasmas ELKE PLOENJES, KRAIG FREDERICKSON, PETER PALM, G. BABU VISWANATHAN, IGOR V. ADAMOVICH, VISH V. SUBRAMANIAM, WALTER R. LEMPERT, HAMISH L. FRASER, J. WILLIAM RICH, *The Ohio State University** Single-walled carbon nanotubes (SWNTs) are synthesized in a gas-phase thermally non-equilibrium plasma process. The carbon producing CO disproportionation reaction is driven very efficiently at low temperatures in a flow reactor, in which extreme vibrational mode disequilibrium of the carbon monoxide is maintained by using a carbon monoxide laser. In the presence of metal catalysts, the vibrationally excited CO reacts to form CO₂ and SWNTs. The CO laser photodissociates the carbonyls that form metal clusters in situ. Ropes of SWNTs with a high degree of alignment have been observed in the deposits. The flow reactor employed allows access for spectroscopic studies of the kinetic processes involved in the SWNT formation. The vibrational distribution function of the CO and the gas temperature are monitored using FTIR emission spectroscopy. Fe and C₂ are observed with UV-Vis emission spectroscopy and the carbon atom concentration is determined using VUV absorption spectroscopy.

*This research was partially supported by the DDR&E Air Plasma Ramparts MURI Program managed by AFOSR, the AFOSR Space Propulsion and Power Division, and the Ohio Board of Regents.

JWP 83 Enhancement of CO₂ in Reactions with Vibrationally Excited Gas Phase CO Over Surfaces K. ESSENHIGH, J. W. RICH, U. OZKAN, *The Ohio State University* We study the reaction of cool, vibrationally excited gas phase carbon monoxide, produced in an optically pumped discharge, with a CuO surface. The surface reaction produces gas phase CO₂. We perform spectroscopic absorption measurements of the CO₂ produced by this reaction. These measurements are compared with CO₂ production for the thermally equilibrium oxidation reaction for the same surface in a furnace at two different temperatures. The CO₂ production rate with the vibrationally excited reactant is greatly increased over the thermal rate at the same temperature.

JWP 84 Electron Impact Ionization of C_2F_6 IONE IGA, IVANA PEREIRA SANCHES, *Department of Chemistry, Universidade Federal de São Carlos*, SANTOSH KUMAR SRIVASTAVA, *Jet Propulsion Laboratory, CIT¹* Besides CF_4 , perfluoroethane, C_2F_6 , is also one of the fluorocarbon compounds most frequently used in plasma processing applications. Consequently, the knowledge of the ionization properties of C_2F_6 is clearly of interest in order to model the plasma-chemical reactions. Nevertheless, only few partial ionization-cross-section measurements [1,2] for this molecule were reported in the literature. Also, the energy range covered in these studies was very limited (below 120 eV). Recently, we have studied these properties. More specifically, partial ionization cross sections (PICS) for the fragments: C^+ , F^+ , CF^+ , CF_2^+ , CF_3^+ and $C_2F_5^+$, produced by electron impact on C_2F_6 , were measured in a single-collision condition from near ionization

threshold to 1000 eV. In addition, total ionization cross sections (TICS) are also obtained by summing up the PICS's. The comparison of our measured PICS and derived TICS with available data [1-4] will be presented during the Conference.

[1] H. U. Poll, J. Meischner, *Contrib. Plasma Phys.* **27**, 359 (1987).

[2] C. Q. Jiao, A. Garscadden, P. D. Haaland, *Chem. Phys. Lett.* **310**, 52 (1999).

[3] H. Nishimura, W. M. Huo, M. A. Ali and Y-K. Kim, *J. Chem. Phys.* **110**, 3811 (1999).

[4] L. G. Christophorou and J. K. Olthoff, *J. Phys. Chem. Ref. Data* **27**, 1 (1998).

¹This research is supported by FAPESP, CNPq and CNPq-NSF International Programs.

SESSION KW1: PLASMAS FOR NANOSTRUCTURED MATERIALS

Wednesday afternoon, 10 October 2001; Ballroom C Nittany Lion Inn at 15:30; Mark Horn, The Pennsylvania State University, presiding

Invited Papers

15:30

KW1 1 Synthesis of Highly Oriented Microcrystalline Silicon Films in Pulse-Time-Modulated Ultrahigh-Frequency Silane Plasmas.

MASARU HORI, * *Dept. of Quantum Eng., Nagoya University, Japan*

Microcrystalline silicon (c-Si) and polycrystalline silicon (poly-Si) thin films grown on the glass substrate temperature (<450) have been investigated extensively for their application in low cost solar cells and thin film transistors (TFTs) since these films exhibit a high mobility and a low dark conductivity compared with hydrogenated a-Si thin films. The direct deposition of these films using plasma-enhanced chemical vapor deposition (PECVD) potentially has a great advantage to form films over a large area at a low temperature. These films have usually random crystalline orientations, which lead to decrease in the carrier mobility since the carrier transport is strongly dependent on the film structure such as trap states at grain boundaries. The preferentially oriented growth is the most effective way to decrease the traps. Recently, we have synthesized c-Si thin films with precisely controlled crystalline orientation on a glass substrate using the pulse-time-modulated ultrahigh frequency (UHF) plasma employing silane/hydrogen (SiH_4/H_2). The ratio of (111) to (220) intensity in the X-ray diffraction spectra was increased with decreasing pulse duty ratio or pulse frequency at substrate temperatures below 300 and conversely the ratio of (220) to (111) intensity was increased at 400. The behaviors of absolute densities of hydrogen (H) atoms and silicon (Si) atoms in the pulse-modulated-plasma are clarified by using vacuum ultraviolet absorption spectroscopy (VUVAS) and ultraviolet absorption spectroscopy (UVAS), respectively. The ratio (Si/H) was closely related with the preferential crystalline orientation. An overview on recent results on gas phase and surface reactions of radicals for the mechanism of preferentially oriented c-Si film growth will be presented.

*Co-author: Toshio Goto.

16:00

KW1 2 Plasma production of nanocrystalline silicon particles. A new route for nanostructured silicon thin films.

P. ROCA I CABARROCAS, *Laboratoire de Physique des Interfaces et des Couches Minces (UMR 7647 CNRS), Ecole Polytechnique, 91128 Palaiseau Cedex, France*

The study of silane plasma deposition processes is important due to the large number of large area devices based on amorphous silicon. When transferring research results to production, deposition rate and uniformity are key issues. Also, production facilities must avoid powder formation which could reduce device yield. The study of square-wave modulated discharges revealed that silicon nanocrystals (powders precursors) can be intentionally produced even at room temperature. This result has motivated for the work on plasma conditions near the onset of powder formation. Our aim is to produce better-structured silicon thin films using plasma conditions close to the formation of powder, in which silicon clusters, nanoparticles, and crystallites are formed in the plasma and contribute to the deposition. Among the nanostructured materials we produced thus far, most work has focused on polymorphous silicon films because they share the high optical absorption of a-Si:H while having improved transport properties. In this presentation we review our recent work on the production, the characterization, and the study of devices based on this new material¹. Even though the detection

of nanometer size silicon particles in the plasma is a challenging problem, new techniques such as cavity ring down and impedance measurements have emerged as useful guides to control the size and the density of nanoparticles. Moreover, these growth studies were used to determine and control the thermophoretic force acting on particles in order to intentionally promote or inhibit nanoparticles motion towards or away from the substrate. These studies have unambiguously demonstrated the importance of the nanocrystallites and/or clusters in pm-Si:H deposition. In conclusion, low pressure silane plasmas are an interesting way of producing nanocrystalline silicon particles. The precise control of the size and concentration of nanocrystalline silicon particles in the plasma opens the way to the nanoelectronics field in which the plasma-produced nanocrystallites can be passivated, coated,* and incorporated into devices such as non-volatile memories. This is in our opinion an important challenge for the plasma community in the next few years.

¹P. Roca i Cabarrocas, J. of Non Cryst. Solids 266-269 (2000) 31.

Contributed Papers

16:30

KW1 3 A coupled chemistry and particle growth model to study nanoparticle formation in silane plasmas* UPENDRA BHANDARKAR, UWE KORTSHAGEN, STEVEN GIRSHICK, *University of Minnesota - Dept. of Mechanical Engineering* Particle generation in processing plasmas has long been considered harmful. However, in a recent development it was discovered that nanoparticles in the 2-10 nm range embedded in aSi:H films improved the performance of solar cells. This result has further spurred research efforts to study particle growth in silane plasmas. We have developed a zero dimensional plasma model to study particle nucleation and growth in such plasmas. This model consists of a chemistry module developed previously coupled to a particle growth module that accounts for coagulation and surface growth of particles. The coagulation module is based on a sectional approach that divides the entire volume range into sections on a logarithmic scale. The coagulation and chemistry modules are coupled via the nucleation and surface growth terms. Particle charging is calculated using the orbital motion limited theory. Plasma properties are calculated self-consistently by considering plasma quasineutrality and global positive ion balance. The effect of various parameters such as gas pressure, gas temperature, input power and dilution ratios on the nucleation and growth process were studied. We will present results obtained from these calculations.

*This work is supported by NSF under grant ECS-9731568

16:45

KW1 4 Plasma CVD of Carbon Nanotubes LANCE DELZEIT, *NASA Ames Research Center* IAN MCANINCH, *NASA Ames Research Center* BRETT CRUDEN, *Eloret Corporation* M. MEYYAPPAN, *NASA Ames Research Center* Carbon nanotubes (CNT) have created much excitement recently in the research community about their potential in electronics, computing, sensor and structural applications. Realization of these applications critically depends on the ability to control the properties (such as diameter, chirality) as well purity. We have investigated CNT growth in an inductively coupled plasma (ICP) reactor using hydrocarbon feedstock. The catalyst required for nanotube growth consists of thin sputtered layers of aluminum and iron (10 nm each), and aligned carbon nanotubes have been obtained. The nanotubes have been examined using SEM, TEM, EDAX, and Raman spectroscopy. The alignment of nanotubes appears to be better than that possible from thermal CVD done in our laboratory.

Optical emission diagnostics of the plasma has been undertaken to understand growth mechanisms. This presentation will discuss growth characteristics under various pressure, power and feedgas compositions and our understanding from plasma diagnostics.

17:00

KW1 5 Modeling of Carbon Nanotube Growth in Inductively Coupled Plasma Reactors DAVID HASH, M. MEYYAPPAN, *NASA Ames Research Center* Carbon nanotubes (CNT) exhibit extraordinary mechanical and unique electronic properties and hence have been receiving much attention recently for applications in nanoelectronics, sensors, scanning probes, high strength composites, and many more applications. Critical issues at present in realizing these applications involve control of nanotube diameter, vertical alignment of nanotubes, and patterned growth. We have recently built an inductively coupled plasma (ICP) reactor and used it to grow CNTs with a methane/hydrogen mixture feed gas. In this presentation, we report results from our complementary modeling efforts which consist of both 0-d and 2-d analysis of the plasma. The 0-d model is used to sort out the extensive hydrocarbon chemistry into a manageable set for use in the 2-d model entitled SEMS (Semiconductor Equipment Modeling Software). SEMS consists of a comprehensive fluid model which couples the plasma and neutral gas transport and heat transfer in a self-consistent manner by solving a coupled set of equations including mass conservation for each species, a total momentum equation, and thermal energy conservation equations for the neutrals and electrons.

17:15

KW1 6 Carbon nanostructure Growth in an ICP-GEC Reference Cell COREY COLLARD, *University of Michigan* SARA BERNAL, *University of Michigan* MARY BRAKE, *University of Michigan* SUSAN SONG, *Michigan State University* VIRGINIA AYRES, *Michigan State University* MARTY CRIMP, *Michigan State University* Carbon nanostructures are grown in a modified GEC reference chamber that is run in an inductive mode, using Ar, CH₄, and H₂ as the fill gasses and using a 50/50 mixture of CH₄ and H₂. Ar is added to sustain the inductive mode. Well aligned, dense nanostructures are grown on a silicon substrate. The substrate is prepared by sputter coating a silicon wafer with 10 - 20 nm of iron. Iron acts as a growth catalyst for nanostructures such as nanotubes. Samples are analyzed using SEM, which show nanostructures of about 20 nm wide and microns long. High Resolution Transmission Microscopy, Raman Spectroscopy and Surface Enhanced Raman Spectroscopy are also used to characterize the samples. Initial Raman spectroscopy analyses on these samples gives the same results as those found for carbon nanotubes. Opti-

cal emission spectroscopy shows that the major species in the discharge are C2 and CH, along with neutral argon. Nitrogen is added to system to obtain rotational temperatures. The rotational temperature of the nitrogen indicates the gas temperatures around 750 K. This is lower than is what is usually used for carbon

nanotube growth. When a bias is applied to the lower electrode, different substrate growth morphology is observed compared to cases where a bias is applied to the lower electrode. A comparison of the growths of bias versus no bias plasmas will be discussed as well as the different types of morphologies grown on the samples.

SESSION KW2: ELECTRON COLLISIONS WITH METAL VAPORS

Wednesday afternoon, 10 October 2001; Ballroom AB Nittany Lion Inn at 15:30; S.J. Buckman, Australian National University, Canberra, presiding

Invited Papers

15:30

KW2 1 Spin-resolved electron scattering from heavy metal atoms.

G. FRIEDRICH HANNE, *Physikalisches Institut, Universität Münster*

More sophisticated experimental methods to study electron-atom collisions include polarization-correlation measurements such as generalized *STU* parameters, spin asymmetries with polarized targets, optical methods (integrated Stokes parameters, laser-excited targets, electron-photon coincidences and stepwise electron-photon excitation), triple differential cross section (*e,2e*) measurements and study of electron dichroism. Sources of polarized electrons with a polarization of $P > 0.5$ and currents of up to several microamps have been developed with which such investigations can be performed successfully. Spin effects in elastic and inelastic collisions of electrons with atomic targets can be explored on the most fundamental level in such experiments. In this talk some recent experimental work on spin-resolved electron scattering from heavy metal atoms is reviewed with the main emphasis on recent results for elastic collisions from Mn atoms and electron-photon coincidences from Hg and Pb atoms. In the experiment with Mn atoms electron exchange is observed directly, whereas in the electron-photon-coincidence experiment propensity rules for angular momentum orientation effects are studied. We can extract the orientation of the target electrons from measurements of the circular polarization. For *s-p* transitions there exists a propensity rule that states that the orientation of a charge cloud is positive for scattering of unpolarized electrons by small angles. The experiments and calculations show that this propensity rule not valid for collisions where the electron spin is initially down. This can be explained by a quantum mechanical interference effect caused by intermediate coupling of the target states.

16:00

KW2 2 Calculation of electron scattering from metal vapors using the convergent close-coupling method.

DMITRY FURSA, *Flinders University, Australia*.*

A review of the present status of theoretical calculations for electron scattering from metal vapours will be given. We have used convergent close-coupling method to perform calculation of electron scattering from Mg, Ca, Zn, Sr, Ba, and Hg. The model of two active electrons above frozen Hartree-Fock core has been used for all considered atoms. For lighter atoms (Mg, Ca, Zn, Sr) the nonrelativistic approximation proves to be adequate, however for a number of transitions in Ba and Hg the semirelativistic approximation has to be used. The calculations have been performed in the incident electron energy range of 1 to 1000 eV. Integrated cross sections for elastic scattering and excitations for a selected set of transitions will be presented, including scattering between excited states. Good agreement was found with available measurements for resonance transitions. The primary aim of these calculations is to provide reliable set of cross sections for use in applications, particularly in the lighting industry.

*In collaboration with Igor Bray, Murdoch University, Australia.

16:30

KW2 3 Hybrid modeling network for argon glow discharges with copper cathode sputtering.

ANNEMIE BOGAERTS, *University of Antwerp, Dept. of Chemistry*

An application of glow discharges that is not so well-known is in analytical chemistry, as spectroscopic sources for the analysis of (mainly) solid samples. The material to be analyzed is used as the cathode, and is sputtered by energetic plasma species. The sputtered atoms arrive in the plasma and can be detected, after ionization or excitation, by mass spectrometry or optical emission spectrometry. For good analytical practice, an insight in the glow discharge processes is desirable. We try to obtain this by modeling. A set of 2D models has been developed for the various species in an argon glow discharge with copper cathode. The fast electrons are simulated with a Monte Carlo model. The slow electrons are described with a fluid model, in combination with the argon ions and Poisson's equation for a self-consistent electric field. The argon ions are also followed with a Monte Carlo model in the cathode dark space, as well as the fast argon atoms

created from collisions of the argon ions. Argon atoms in 64 excited levels are described with a collisional-radiative model. The sputtering of copper atoms is calculated with an empirical formula. Once the atoms are sputtered, they are rapidly thermalized by collisions, which is described with a Monte Carlo model. Their further behavior, the ionization and excitation of the atoms, and the behavior of the various excited copper atom and ion levels, is described with a collisional-radiative model. Finally, the copper ions in the cathode dark space are also treated with a Monte Carlo model. All the models are coupled due to the interaction processes between the species, and they are solved iteratively until final convergence is reached. Typical results of the models include the densities, fluxes and energy distributions of the various plasma species, information about collisions and sputtering, the potential distribution, optical emission spectra, etc. The modeling results are compared with experimental data, and the reasonable agreement tells us that the models present a realistic picture of the glow discharge.

Contributed Papers

17:00

KW2 4 Electron-Impact Excitation Cross Sections for Metal Vapors YONG-KI KIM, *NIST** Two simple scaling methods to generate integrated cross sections from plane-wave Born cross sections for dipole-allowed excitations of metal vapors by electron impact¹ are shown to produce cross sections comparable in accuracy to those obtained by more sophisticated collision theories, such as the convergent close-coupling method. The scaled cross sections σ_{BE} and σ_f are: $\sigma_{BE} = \sigma_{PW} \times [T/(T + B + E)]$, $\sigma_f = \sigma_{PWsc} \times (f_{mc}/f_{sc})$, where σ_{PW} =unscaled plane-wave Born cross section, T =incident electron energy, B =binding energy of the target electron, E =excitation energy, f_{mc} and f_{sc} are the dipole f -values calculated from multiconfiguration wave functions and single-configuration wave functions, respectively. The two scalings can be used consecutively. The scaled cross section for the 4s-4p excitation of Cu is in excellent agreement with the experiment by Ismail and Teubner.² Many examples of resonance transitions of atoms, including Ag, Au, and Hg, will be presented.

*Work supported in part by the Office of Fusion Energy Sciences, DOE.

¹Y.-K. Kim, *Phys. Rev. A*, **64**, in print.

²M. Ismail and P. J. O. Teubner, *J. Phys. B* **28** 4149 (1995)

17:15

KW2 5 R-matrix with Pseudo-States Calculations for Electron Collisions with Cesium Atoms. K. BARTSCHAT, Y. FANG, *Drake University** We present results of cross sections, spin asymmetries, and Stokes parameters for elastic and inelastic electron collisions with Cs atoms. These results were obtained in a conver-

gent R-matrix with pseudo-states (RMPS) close-coupling-type calculation, with relativistic effects accounted for by the one-electron terms of the Breit-Pauli hamiltonian. The success of the model for elastic collisions [1] and comparison with recent experimental data [2,3] provides confidence in the accuracy of the results, indicating their potential to assist in the interpretation of ongoing experiments. [1] K. Bartschat and Y. Fang (2000), *Phys. Rev. A* **62** 052719. [2] G. Baum (2001), private communication. [3] V. Karaganov and P.J.O. Teubner (2001), private communication.

*Work supported by the NSF under grant PHY-0088917.

17:30

KW2 6 Second-Order Effects in Ionization and Ionization-Excitation of Calcium Y. FANG, K. BARTSCHAT, *Drake University** We have extended our recent work on electron-impact ionization and ionization-excitation of helium [1-3] to the calcium target. The calculations were performed using a second-order perturbative model for a "fast" incident projectile together with a convergent R-matrix with pseudo-states (RMPS) close-coupling-type model for the initial bound state and the scattering of a "slow" ejected electron in the field of the ion. We compare the results obtained in perturbative and non-perturbative approaches, with particular emphasis on second-order effects. Preliminary results indicate that these effects are much stronger in calcium than in helium for comparable kinematic situations. [1] Y. Fang and K. Bartschat, *J. Phys. B* **34** (2001). [2] Y. Fang and K. Bartschat, *J. Phys. B* **34** (7/2001), in press. [3] Y. Fang and K. Bartschat, *Phys. Rev. A* **64** (8/2001), in press.

*Work supported by the NSF under grant PHY-0088917.

SESSION LRI: MATERIALS PROCESSING

Thursday morning, 11 October 2001

Ballroom C Nittany Lion Inn at 8:00

Ravi Jayaraman, The Pennsylvania State University, presiding

8:00

LR1 1 Optical characterization of etch damage in GaN produced by inductively coupled and electron cyclotron resonance plasmas D.K. GASKILL, O.J. GLEMOCKI, V. SHAMAMIAN, D. KOLESKE, R. HENRY, *Naval Research Laboratory, Code 6862, Washington, DC 20375, USA* Plasma processing of semiconductors and semiconductor device structures, the preferred industrial tool, utilizes energetic ions in combination with reactive gases. This results in the large throughputs that are required in the semiconductor industry. The energies of the ions ($>100\text{eV}$), however, are significantly in excess of the surface binding energies, which are typically tens of volts. This leads to not only the removal of surface atoms, but also to the displacement of subsurface atoms. This type of structural damage invariably manifests itself in modified electronic and optical properties of the material, which is often deleterious to device performance. In this paper, we report on the nature of the etch induced damage in GaN. We have used both photorefectance (PR) and photoluminescence (PL) to study the damage. The PR measurements allow us to ascertain the near surface damage, while the PL measurements probe subsurface damage. We find that in inductively coupled plasmas composed of 90sensitive to ion energies. We find that ion energies as small as 40eV can produce substantial surface damage, which is insensitive to further increases in ion energy. Conversely, subsurface damage is observed to increase with energy, for energies above 75eV. Our measurements indicate that the etch induced subsurface damage is similar to the defects found in as grown GaN. We will compare ICP to ECR and discuss methods of reducing the damage.

8:15

LR1 2 A comparison of nitride film etching in fluorocarbon plasmas HELEN HWANG, *NASA Ames Research Center* JONG SHON, *Lam Research Corp.* Large-scale memory device fabrication involves nitride hard mask etching. Self-aligned contact (SAC) etching, for example, typically relies on complicated gas mixtures containing fluorocarbons, which consequently leads to selectivity issues of the nitride hard mask to photoresist. We will present computational and experimental results for fluorocarbon etching of silicon nitride films. Using a plasma reactor model along with double Langmuir probe measurements, plasma properties such as ion fluxes, neutral fluxes, and species distribution functions, can be generated. These quantities are then used by a level set based simulation (SPELS) for etching. The overall etch rates are obtained using a modified surface site balance model, which includes a generalized expression for fluorocarbon deposition and F atom diffusion. We will present comparisons of simulated and measured etch rates and feature profiles of structures containing silicon oxynitride and nitride films, as well as photoresist. We will also show initial results for temperature dependent etch rates.

8:30

LR1 3 Sputter-Etching Characteristics of BST and SBT using a Surface-Wave High-Density Plasma Reactor. L. STAFFORD, J. MARGOT, *Groupe de physique des plasmas, Université de Montréal, Montréal, Qc* S. DELPRAT, M. CHAKER, *INRS-Energie et Matériaux, Varennes, Qc* D. QUENEY, *Groupe de physique des plasmas, Université de Montréal, Montréal, Qc* In the context of the integration of ferroelectric capacitors such as FeRAMs and DRAMs, the dry etching of pulse laser deposited barium-strontium-titanate (BST) and bismuth-strontium-tantalate (SBT) is investigated using a non-reactive surface-wave high-density argon magnetoplasma. The etching characteristics of rf-biased thin films are evaluated as a function of the self-bias voltage, the magnetic field intensity and the gas pressure. It is found that high etch rates with a good selectivity over resist can be achieved without any plasma chemistry provided the plasma is operated in the mtorr regime. For BST, etch rates as high as $1000 \text{ \AA} / \text{min}$ with a selectivity of 0.6 over HPR504 photoresist are obtained for self-bias voltages lower than 150 V. Both BST and SBT present similar sputter-etching characteristics, SBT being however etched faster than BST.

8:45

LR1 4 Noble-Gas-Modified Reactive Ion Energy Distributions in Inductively Coupled Plasma Enhanced and Ion Beam Enhanced Reactive Sputtering of Thin Film Compounds CHRIS MURATORE, JOHN MOORE, *Advanced Coatings and Surface Engineering Laboratory (ACSEL), Colorado School of Mines, Golden, CO 80401-1887* J. ALAN REES, *Hidden Analytical Limited, 420 Europa Boulevard, Warrington, WA5 5UN England* DAN CARTER, GREG ROCHE, *Advanced Energy Industries, 1625 Sharp Point Drive, Fort Collins, CO 80525* Through the use of a plasma mass spectrometer coupled with an energy filter, the authors have observed that reactive ion energy distributions can be modified by mixing a noble gas to the reactive gas prior to excitation by the reactive plasma source for both ion beam- and inductively coupled plasma- enhanced reactive sputtering deposition processes. These modified IED's are useful in that they have a remarkable effect on the micro-structure and properties of both oxide and nitride thin films. Preliminary measurements of electron energy distributions suggest that the addition of helium for example, increases the most probable electron energy in the reactive plasma. Metastable noble gas species are also presumed to make a contribution to the modified IED's.

9:00

LR1 5 Plasma Diagnostics For The Investigation of Silane Based Glow Discharge Deposition Processes DIMITRIOS MATARAS, *Plasma Technology Laboratory - Department of Chemical Engineering - University of Patras* ELEFATHERIOS AMANATIDES, DIMITRIOS RAPAIOULIAS, In this work is presented the study of microcrystalline silicon PECVD process through highly diluted silane in hydrogen discharges. The investigation is performed by applying different non intrusive plasma diagnostics (electrical, optical, mass spectrometric and laser interferometric measurements). Each of these measurements is related to different plasma sub-processes (gas physics, plasma chemistry and plasmasurface interaction) and compose a complete set, proper for the investigation of the effect of external discharge parameters on the deposition processes. In the specific case these plasma diagnostics are applied for prospecting the optimal experimental conditions from the c-Si:H deposition rate point of view. Namely, the main characteristics of the effect of frequency, dis-

charge geometry, power consumption and total gas pressure on the deposition process are presented successively. Special attention is given to the study of the frequency effect (13.56 MHz 50 MHz) indicating that the correct way to compare results of different driving frequency discharges is by maintaining constant the total power dissipation in the discharge. The important role of frequency in the achievement of high deposition rates and on the optimization of all other parameters is underlined. Finally, the proper combination of experimental conditions that result from the optimal choice of each of the above-mentioned discharge parameters and lead to high microcrystalline silicon deposition rates (7.5 /sec) is presented. The increase of silane dissociation rate towards neutral radicals (frequency effect), the contribution of highly sticking to the surface radicals (discharge geometry optimum) and the controlled production of higher radicals through secondary gas phase reactions (total gas pressure), are presented as prerequisites for the achievement of high deposition rates.

9:15

LR1 6 Synthesis And Characterization of Al-C-N Films Using Inductively Coupled Plasma Assisted DC Magnetron Sputtering N. JIANG, S. XU, Z.L. TSAKADZE, E.L. TSAKADZE, J.D. LONG, K.N. OSTRIKOV, *Plasma Processing Laboratory, NIE/NTU, 1 Nanyang Walk, Singapore 637616* This work reports on the synthesis of novel aluminum modified carbon nitride Al-C-N thin film using a low frequency inductively coupled plasma (LF ICP) assisted DC magnetron sputtering system. During the synthesis, Al target atop of a magnetron electrode is sputtered in Ar+N₂CH₄ gas mixture discharge. Al-C-N thin film is then deposited on Si substrate by bonding Al, C and N atoms together. Optical emission spectroscopy (OES) and Langmuir probe are used for *in-situ* diagnostics. The as-deposited thin films are characterized *ex-situ* by x-ray photoelectron spectroscopy (XPS) and x-ray diffraction spectroscopy (XRD). The OES spectra show that single C-N bond is formed in the plasma state. The binding states of C-Al, sp²C-N and sp³C-N are investigated using XPS narrow scan technique. C composition increases with the CH₄/N₂ flow rate ratio, and saturates at higher CH₄/N₂ value. The dominant component in the film is c-AlN (111), which is mixed with Al₄C₃ and AlCN ternary compound. The results demonstrate that the LF ICP is a powerful tool in synthesis of novel materials.

SESSION LR2: ENVIRONMENTAL APPLICATIONS AND THERMAL PLASMAS

Thursday morning, 11 October 2001

Ballroom AB Nittany Lion Inn at 8:00

Bing Ji, Air Products and Chemicals, presiding

8:00

LR2 1 Kinetic of the OH-radical in high pressure plasmas of N₂/H₂O/hydrocarbons mixtures* G. BARAVIAN, F. FRESNET, L. MAGNE, S. PASQUIERS, C. POSTEL, V. PUECH, A. ROUSSEAU, *LPGP, Universit Paris-Sud / CNRS, France* Kinetic of the OH-radical has been studied in homogeneous plasmas achieved in a photo-triggered discharge device, in N₂/H₂O with C₂H₄ or C₃H₆, at 460 mbar with 1.2 concentration and a deposited energy in the plasma equal to 92 J/l. Hydrocarbon concentration ranged from 50 ppm up to 1000 ppm. Using the same technique as

for NO kinetic studies¹, a time resolved LIF diagnostic has been performed to measure the OH-radical density up to 180 s after the short current pulse excitation, 50 ns. At fixed deposited energy, the LIF signal rapidly decreases when hydrocarbon concentration increases. Measurements have been compared to predictions of a self-consistent 0D-model which takes into account a detailed kinetic scheme, including oxidation reactions of hydrocarbons by the radical which are important processes in flue gas non-thermal plasma treatment. Results are discussed.

*Work supported in part by GIE : PSA Peugeot-Citron / RENAULT, ECODEV-CNRS, and ADEME.

¹F. Fresnet, G. Baravian, L. Magne, S. Pasquiers, C. Postel, V. Puech, A. Rousseau, *Appl. Phys. Lett.*, 77 (2000) 4118.

8:15

LR2 2 Plasma Remediation of NO_x in the Presence of Hydrocarbons Using Dielectric Barrier Discharges: Microstreamer Discharge Dynamics* RAJESH DORAI, MARK J. KUSHNER, *University of Illinois* Plasma remediation is being investigated for removal of NO_x from automotive exhausts. Previous investigations using global kinetic models for simulated diesel exhausts containing N₂, O₂, CO₂, H₂O and ppm levels of NO, CO, H₂ and unburned hydrocarbons (UHCs) showed that the remediation process is primarily oxidative and most of the NO is converted to NO₂. In actual devices, the plasma consists of an assembly of filamentary microdischarges. The resulting nonuniformities in production rates of radicals and the depletion of feedstocks initiate convection which ultimately produces mixtures of reactants which are quantitatively different than uniform excitation. To study these processes, a radially dependent microdischarge model the plasma chemistry of simulated automotive exhaust, including UHCs, has been developed. The model includes a full accounting of the humid-air plasma chemistry, ambipolar charged particle transport and solution of the Navier-Stokes equations. Results will be discussed for the radial transport of reactive species and the consequences on NO_x remediation when including UHCs.

*Work supported by Ford Motor Company and NSF (CTS99-74962)

8:30

LR2 3 Characteristics of Parallel Streamer Discharges between Wire and Plane Electrodes in Water SUNAO KATSUKI,* *Old Dominion University* AMR ABOU-GHAZALA, *Old Dominion University* KARL SCHOENBACH, *Old Dominion University* HIDENORI AKIYAMA, *Kumamoto University* Streamer discharges in tap water and distilled water have been generated by applying a voltage pulse from 120 to 175 kV amplitude and 500 ns duration to a wire-plane electrode configuration immersed in water. A fast ICCD camera was employed to observe their temporal behavior in detail under several different conditions. With the wire serving as anode, multiple, parallel streamer discharges were generated. The number density of these streamers along the wire decreases with decreasing the electric field on the surface of the wire, which is determined by applied voltage and electrode geometry. The dependence of the streamer density on electric field indicates the role of field enhancement at inhomogeneous microstructure along the wire as streamer initiation mechanism. With the wire serving as cathode, only a weak light emission from the area close to the wire, and streamer did not appear under the same voltage amplitude as positive polarity. The appearance of the discharge was different for tap and distilled water. However, the average streamer propagation velocities from the wire anode to

the grounded plane electrode, measured as 32 mm/s, were independent of the conductivity of the water and the applied voltage. This suggests the existence of a self-sustained electric field at the streamer head. This work supported by a grant from AFOSR.

*On leave of absence from Kumamoto University

8:45

LR2 4 Application of Concentrated Electron Beams in Extra-Vacuum Technologies OLEG GORSHKOV, A. A. ILIIN, A. S. LOVTSOV, R. N. RIZAKHANOV, *Keldysh Research Center, Moscow, Russia* At present time the rise in development of the technology with using the concentrated electron beams in gas with atmospheric pressure is observed. Besides the technologies, which are usually carried out in vacuum and connected with surface modification by the concentrated energy flows (welding, cutting, metal surface hardening), at present time the plasma chemical processes become of greater interest. These are processes with using the beam of fast electrons to initiate the plasma chemical reactions. One of such technologies is gas cleaning of the toxic impurities (nitrogen oxides and sulfur oxides and etc.) The electron-beam gas cleaning of the toxic impurities (for example Ebara-process) is based on radiation-enhanced combining of toxic impurities. The disadvantage of this method are high level of consumed power during the gas cleaning and difficulties in devices development for the output of electron beam with megawatt unit power with foil outlet, as the facilities of this very power are necessary for the real industrial application. These problems can be solved by using the devices with concentrated electron beam output into the atmosphere. In this case the beam is transported into the dense gas through the system of lock chambers, independently pumped. But unlike the beam, output through the foil window, the concentrated electron beam is characterized by the noticeable spatial irregularity in distribution of temperature, plasma concentration and area of radiation. This paper is devoted to consideration of using the concentrated electron beams in extra-vacuum technologies.

9:00

LR2 5 Study of supersonic plasma technology jets SVETLANA SELEZNEVA, *University of Sherbrooke* DENIS GRAVELLE, *University of Sherbrooke* MAHER BOULOS, *University of Sherbrooke* RICHARD VAN DE SANDEN, *Eindhoven University of Technology* DC SCHRAM, *Eindhoven University of Technology* CRTP COLLABORATION,*ETP COLLABORATION,† Recently some new techniques using remote thermal plasma for thin film deposition and plasma chemistry processes were developed. These techniques include PECVD of diamonds, diamond-like and polymer films; a-C:H and a-Si:H films. The latter are of especial interest because of their applications for solar cell production industry. In remote plasma deposition, thermal plasma is formed by means of one of traditional plasma sources. The chamber pressure is reduced with the help of continuous pumping. In that way the flow is accelerated up to the supersonic speed. The plasma expansion is controlled using a specific torch nozzle design. To optimize the deposition process detailed knowledge about the gas dynamic structure of the jet and chemical kinetics mechanisms is required. In the paper, we show how the flow pattern and the character of the deviations from local thermodynamic equilibrium differs in plasmas generated by different plasma sources, such as induction plasma torch, traditional direct current arc and cascaded arc. We study the effects of the chamber pressure, nozzle design and carrier gas on the resulting plasma properties. The analysis is performed by means of numerical modeling using commercially

available FLUENT program with incorporated user-defined sub-routines for two-temperature model. The results of continuum mechanics approach are compared with that of the kinetic Monte Carlo method and with the experimental data.

*University of Sherbrooke

†Eindhoven University of Technology

SESSION MR1: INDUCTIVELY-COUPLED PLASMAS AND MAGNETICALLY-ENHANCED PLASMAS

Thursday morning, 11 October 2001

Ballroom C Nittany Lion Inn at 10:00

Ivan Ganashev, Nagoya University, presiding

10:00

MR1 1 Charged Species Dynamics in an Inductively Coupled Ar/SF₆ Plasma S. RAUF, P.L.G. VENTZEK, *Motorola Inc.* G.A. HEBNER, I.C. ABRAHAM, J.R. WOODWORTH, *Sandia National Laboratories* Inductively coupled SF₆ discharges are commonly used for materials processing in the microelectronics industry. Because of the presence of a large number of positive (SF_x⁺, x=1-5) as well as negative (SF_x⁻, SF₅⁻, F⁻) ions, the electrodynamic behavior of SF₆ plasmas is quite complex. In this paper, we utilize a 2-d computational model of an inductively coupled discharge in conjunction with diagnostic measurements in the GEC reference cell to understand charged species dynamics in the Ar/SF₆ plasma. The computational model is based on the Hybrid Plasma Equipment Model from the University of Illinois. The SF₆ plasma chemical mechanism considers electron impact dissociation, ionization and attachment processes for SF₆ and SF_x (x=1-5) radicals produced in the discharge. Experimental measurements include mass resolved positive ion flux at the wafer, as well as electron and negative ion density determined through microwave interferometry and laser photo-detachment. Results will be used to highlight similarities and differences between the model and experiments.

10:15

MR1 2 Numerical Study of Gas Heating in Commercial ICP Reactors* NING ZHOU, VLADIMIR KOLOBOV, *CFD Research Corp* VLADIMIR KUDRIAVTSEV, *CFD Canada* It is known that there is significant gas heating during etch/deposition processes in ICP reactors. Yet, most simulation models assume isothermal conditions. In this study, we describe coupled models of plasma/flow/chemistry/heat transfer for commercial ICP reactors. The spatial distribution of temperature is found by solving transport equation for enthalpy for systems containing gas/solid/liquid materials with different thermal properties. The gas heating due to chemical reactions and ion kinetic energy release at walls of the reactor are taken into consideration. The numerical study is performed for a commercial ICP reactor using SiH₄/O₂/Ar mixture at gas pressures 5-10 mtorr, flowrates of 0.8-1.5 slm and RF power of 3000-5000 W. The entire reactor including low pressure chamber, cooled chuck, ceramic liner, and an atmospheric pres-

sure case, is modeled. Simulations show considerable temperature increase (in excess of 1000K) for process conditions without active cooling. Results demonstrate strong influence of thermal balance on plasma density, species distributions and SiO₂ deposition.

*Work supported by NSF SBIR Phase-I Project DMI-0060283

10:30

MR1 3 A unified simulation of bulk plasma and sheath scales in a high density plasma discharge DEEPAK BOSE, *Eloret Corp.* T.R. GOVINDAN, M. MEYYAPPAN, *NASA Ames Research Center* Given the current availability of computational resources and fully implicit numerical techniques, it is now possible to simultaneously resolve widely disparate length scales in a multidimensional plasma discharge simulation. In a high density inductively coupled plasma, the bulk and the non-collisional sheath length scales span over 4 orders of magnitude. It is essential to use a fully implicit time marching technique since the CFL condition becomes extremely stringent in the sheath due to a high ion speed and a small mesh spacing. We will present high density, inductively coupled plasma simulation results showing improvements in quantities such as ion flux, plasma potential, electric field, etc. We will emphasize on obtaining accurate sheath density and potential profiles and their sensitivity to the form of electron boundary condition used and the order of accuracy of the numerical scheme. In this level of spatially detailed model, resolving the rf time scale remains a challenge. Hence, we will also propose physical models that can be used to obtain ion impact energy distributions and non-collisional sheath heating of electrons.

10:45

MR1 4 "Evaporative cooling" of electrons in the afterglow of low pressure plasmas* ANTONIO MARESCA, KONSTANTIN ORLOV, UWE KORTSHAGEN, *University of Minnesota - Dept. of Mechanical Engineering* Electron energy distribution functions were measured in the afterglow of an inductively coupled plasma using a cylindrical Langmuir probe. A surprising behavior of the time scale of "electron temperature" decay - the so called energy relaxation time - is found. The measured energy relaxation times are by orders of magnitude different from those to be expected for energy dissipation via electron-atom collisions. In addition, the measured variation of the energy relaxation time with pressure is opposite to that for collisional energy relaxation: The energy relaxation slows down with increasing pressure. This behavior can be interpreted as "evaporative cooling of electrons." The measured electron distribution functions indicate that the dominant energy loss mechanism is the escape of energetic "hot" electrons from the confining ambipolar potential well to the wall, while low-energy "cold" electrons remain confined in the plasma. A simple model based on this picture yields reasonable predictions of the measured energy relaxation times. Our experimental observations are consistent with the recent theoretical predictions of Arslanbekov *et al.* [Phys. Rev. E **64**, 016401 (2001)].

*This work is supported in part by NSF under grant ECS-9713137 and DOE under grant ER 54554

11:00

MR1 5 Warm plasma effect on the power deposition in inductively-coupled chlorine plasmas M. SHIOZAWA, K. NANBU, *Institute of Fluid Science, Tohoku University, Japan* Ohm's law is valid in higher gas pressure, i.e., when collisional electron heating is dominant. The gas pressure is less than 20 mTorr for a typical operating condition of inductively-coupled plasma sources. For such a low gas pressure the electron mean free path becomes longer and hence the electron comes into a region having an electric field at other locations. This nonlocal (kinetic or warm plasma) effect invalidates Ohm's law at low pressure. The warm plasma effect on the power deposition in inductively-coupled chlorine plasma is examined for pressures of 0.5, 1.0, and 2.0 Pa. These are the total pressures of a gas mixture of Cl₂ and Cl, where the number densities of Cl₂ and Cl are set equal. The plasma reactor consists of the quartz cylinder with diameter of 200 mm and height of 385 mm and the diffusion chamber. Eight-turned coils are wound on the cylinder. By using the electron current density J directly sampled in the Monte Carlo simulation, the azimuthal electric field E is obtained for a constant coil current of 6 A. Let P be the total power deposition resulting from J and E , and P_{cold} be that from J_{ohm} and E , where J_{ohm} is the current density given by Ohm's law. The ratio P/P_{cold} increases with decreasing the chlorine pressure. It is 0.96 at 2 Pa, 1.40 at 1.0 Pa, and 1.87 at 0.5 Pa.

11:15

MR1 6 ECR Plasma Production by a Multi-Slotted Antenna Applied to Rectangular Substrates AKIRA SUGIYAMA, TAKAMITSU TADERA, TATSUSHI YAMAMOTO, SATORU IZUKA*, NORIYOSHI SATO*, SHARP CORP. COLLABORATION, *GRAD. SCHOOL OF ENG. TOHOKU UNIV. COLLABORATION, High density plasma sources such as a microwave-excited plasma source have attracted much interest these days, as the electronic device production demands higher process speed for a large substrate. However, precise control of such plasma sources is still one of the obstacles to be overcome, before they are installed into production sites. Now we propose a new ECR plasma source suitable for rectangular substrates. It has following features. 1) An efficient and compact waveguide to transmit microwave power. It consists of several folded structures, which dimensions are determined by computer simulation. 2) A set of plural slotted antennas for radiation intensity distribution control. 3) A magnetic circuit with permanent magnets, which enables efficient plasma excitation by electron cyclotron resonance (ECR) and good plasma confinement with the enclosed magnetic field structure. This developed antenna has high efficiency of power transmission more than 99 percent, and has been able to generate a high density plasma.

11:30

MR1 7 Effects of Boundary Conditions on the Inherent Ion Heating in a Helicon Plasma J. L. KLINE, *West Virginia University* E. E. SCIME, *West Virginia University* R. F. BOIVIN, *West Virginia University* M. M. BALKEY, *Naval Research Lab* Initial ion temperature measurements in The Hot hELIXon eXperiment (HELIX) helicon source showed that the ion temperature is non-negligible and can be as high as 1 eV. The measurements also showed that the ion temperature scales with magnetic field strength and that the ion temperature is anisotropic with respect to

the magnetic field. The perpendicular ion temperature increases with increasing magnetic field strength while the parallel ion temperatures remain the same. Further investigation by Balkey et al. [Plasma Sources Sci. and Tech., 10, 284(2001)] has shown that the increase in ion temperature is correlated with the lower hybrid frequency. After replacing the Pyrex chamber with a hybrid cham-

ber, part Pyrex and part stainless steel, the ion temperature no longer increases with magnetic field strength nor is it anisotropic. A comparison of the boundary effects on ion temperature for different plasma parameters and three different plasma boundaries will be presented. Internal wave field measurements, both electrostatic and magnetic, will also be presented.

SESSION MR2: FLUOROCARBON PLASMAS

Thursday morning, 11 October 2001; Ballroom AB Nittany Lion Inn at 10:00; John Tron, Applied Materials, presiding

Invited Papers

10:00

MR2 1 Investigations in Fluorocarbon Plasmas using Planar Laser-Induced Fluorescence.

KRISTEN STEFFENS, *National Institute of Standards and Technology*

Fluorocarbon plasmas are used within the semiconductor industry for processing applications including selective etching of SiO₂ and Si₃N₄, fabrication of MEMS structures, etching of low-k dielectrics, and post-CVD chamber-cleaning. The complex chemistry in fluorocarbon plasmas is dependent on many factors including precursor gas and plasma conditions. Although the mechanisms are still not completely understood, reactive radicals such as CF and CF₂ are known to be critical participants in the plasma chemistry. Measurements of these reactive species under a variety of relevant plasmas conditions are important for gaining a better understanding of the plasma chemistry and to aid in process development and plasma model validation. Planar laser-induced fluorescence (PLIF) is a valuable tool for the measurement of two-dimensional maps of reactive species in plasmas. In this presentation, our most recent results using PLIF to measure reactive species distributions in fluorocarbon plasmas in the capacitively-coupled Gaseous Electronics Conference rf Reference Cell will be discussed. A variety of plasma conditions have been investigated including different precursors, plasmas with and without a wafer present, and various pressures, plasma powers, and electrode gaps.

10:30

MR2 2 Diagnostics of inductive and capacitive plasmas in fluorocarbon gases.

JEAN-PAUL BOOTH, *Laboratoire de Physique et Technologie des Plasmas, Ecole Polytechnique, France*

Plasmas in fluorocarbon-based gas mixtures are widely used for selective anisotropic etching of sub-micron features in SiO₂ thin films. Whereas inductively-coupled plasmas have become the industry standard for etching of Si and metals (using Cl₂-based chemistries), their use for SiO₂ etching has been abandoned in favor of dual-frequency capacitive sources. This has been for a number of reasons, including process drift issues. A range of diagnostic techniques has been used to probe the physico-chemical mechanisms occurring in fluorocarbon plasmas in both types of source. Laser-induced fluorescence has been previously used to probe the production and loss kinetics of CF and CF₂ radicals in 13.56 MHz capacitively-coupled plasmas, and has notably shown the importance of surface production of CF_x species due to the back-scattering of neutralized C_xF_y⁺ ions. Similar measurements in a pure CF₄ ICP also show that CF_x concentrations are maximal adjacent to the reactor surfaces. LIF of the CF radical was used to measure gas temperature profiles, and has shown that the temperature in the center of an ICP reactor is very high (up to 1000 K). Inductively-coupled plasmas in CF₄ also exhibit inductive-to-capacitive mode instabilities over a wide range of operating conditions. These two phenomena may be related to the processing problems encountered in fluorocarbon ICP systems. Wide-band UV absorption spectroscopy was used to probe the concentrations of free radicals present in an industrial dual-frequency capacitive source containing Ar/C₄F₈/O₂ mixtures. The species CF, CF₂, C₂, C₃, SiF₂ were detected. The ion mass distribution was also measured in Ar/C₄F₈/O₂ mixtures but using single-frequency excitation. The principal ions are C₃F₅⁺, C₂F₄⁺, CF₃⁺, CF⁺ and Ar⁺.

11:00

MR2 3 Flux-balance control for the selective etching of dielectric materials.

TETSUYA TATSUMI, *ASET plasma laboratory*

Fluorocarbon plasmas have been widely used for the etching of dielectric materials as part of the fabrication of ultra-large-scale integrated circuit (ULSI) devices. However, it is necessary develop further techniques for fabricating various structures and materials (including low-k materials) to make ULSIs with higher speed and lower power consumption. To do this requires a quantitative understanding of the mechanism of etching by fluorocarbon plasmas. To facilitate such understanding, we used a parallel-plate type reactive ion etching system (RIE) with various in situ measuring tools to analyze the relationship between the external parameters and the reactive species in the bulk plasma. The relationship between SiO₂ etch rates and the incident flux of reactive species in a dual-frequency parallel plate system was evaluated by using various in-situ measurements tools, such as infrared laser absorption spectroscopy (IRLAS), quadruple mass

spectroscopy (QMS), and optical emission spectroscopy (OES). The thickness and composition of a fluorocarbon (C-F) polymer layer on the etched SiO₂ surface was also measured by X-ray photoelectron spectroscopy (XPS). A surface reaction model for etch rate calculation was proposed. By considering the formation of steady-state polymer and the effect of the polymer on the surface reaction probability, we were able to quantitatively predict the etch rate. We found that the optimum etching condition could be obtained below the "critical point," where the total C flux became equivalent to total O flux. The differences between the etching process-windows for each low-k material such as SiO_xC_yH_z could also be predicted using the same model. This work was supported by NEDO.

Contributed Papers

11:30

MR2 4 Detection of Chamber Conditioning by CF₄ Plasmas in an Inductively Coupled GEC Cell BRETT A. CRUDEN, M V V S RAO, *Eloret Corporation, NASA Ames Research Center* SURENDRA P. SHARMA, M MEYYAPPAN, *NASA Ames Research Center* During oxide etch processes, buildup of fluorocarbon residues on reactor sidewalls can cause run-to-run drift and will necessitate time for conditioning and cleaning of the reactor. Various measurements in CF₄ and Ar plasmas are made in an attempt to identify a metric useable to indicate the chamber condition. Mass spectrometry and a Langmuir probe shows that the buildup of fluorocarbon films on the reactor surface causes a decrease in plasma floating potential, plasma potential, and ion energy in argon and CF₄ plasmas. A slight rise in electron density is also observed by probe, ion flux and impedance measurements in the argon plasmas. Because the change is seen in an argon plasma, it is indicative of altered physical, not chemical, plasma-surface interactions. Specifically, the insulating films deposited on metal surfaces alter the electromagnetic fields seen by the plasma, affecting various parameters including the floating potential and electron density. The optical emission of several species is also monitored for changes in density resulting from the buildup of film on the chamber wall. Changes in the optical emission spectrum are comparable to the noise levels in their measurement.

11:45

MR2 5 Control of Electron Temperature by Mixing Rare Gases in Fluorocarbon Plasmas TATSUO ISHIJIMA, MASAMI IKEDA, HIDEO SUGAI, *Nagoya University, Japan* Low pressure and high density fluorocarbon plasmas have been needed for high-selectivity etching of dielectric materials in the next generation LSI manufacturing. Production rate of each radical and the radical composition strongly depend on electron temperature. Thus, control of electron temperature has been one of challenges in current plasma processing. We report here how the electron temperature varies with rare gas species (Xe, Kr, Ar, Ne, He) used for a source gas (C₄F₈) dilution. The bulk electron temperature is controlled from 1.7 eV in xenon to 6.4 eV in neon at 20 mTorr ICP discharge, thus decreasing with increasing the ionization potential of rare gas species. Such differences in the electron temperature gives rise to different radical compositions. The quadrupole mass analysis revealed that the Xe dilution shows the least dissociation of C₄F₈ and the highest density of ratio CF_x to F radicals. An exception was found in electron temperature control: helium gives lower electron temperatures than neon, in spite of its higher ionization potential. This result is attributed to metastable atom contribution in helium plasma. A global model calculation shows that ionization from the metastable state strongly affects the electron temperature in the case of helium plasma.

SESSION NR1: PLASMA DIAGNOSTICS III

Thursday afternoon, 11 October 2001

Ballroom C Nittany Lion Inn at 13:15

Alex Goodyear, Open University, presiding

13:15

NR1 1 Submillimeter Absorption Spectroscopy of the ICP-GEC Reference Cell ERIC BENCK, GUERMAN GOLUBYATNIKOV, GERALD FRASER, *National Institute of Standards and Technology* Millimeter and submillimeter (100 GHz to 1 THz) absorption spectroscopy is being developed as a sensor for measuring radical densities and temperatures in processing plasmas for microelectronics. Most molecules, radicals, and ions have transitions suitable for detection at these frequencies and the necessary spectroscopic data is available in the literature for determining the absolute radical densities. In addition, the narrow linewidths of < 10 kHz of these continuous-wave sources are suitable for measuring rotational, vibrational and translational temperatures of radicals. Initial measurements are being conducted with a backward-wave-oscillator (BWO) source and a liquid-He-cooled bolometer detector. Radical density measurements have been made in an ICP-GEC Reference Reactor. At frequencies around 100 GHz, absorption signals have been observed for CHF₃, CF₂, CF, COF₂, CO, and SiF₂. Molecular dissociation of CHF₃ in a pure CHF₃ plasma is >90% the translational temperature of CHF₃, probably due to the large volume of cool gas surrounding the plasma. Extension of these measurements to 500 GHz or higher are expected to yield more than 25 times increase in the sensitivity of the absorption measurements.

13:30

NR1 2 Negative Ion Detection Using Laser Thomson Scattering Combined with Laser Photodetachment A. KONO, J. OHNO, H. FUNAHASHI, *Nagoya University, Nagoya 464-8603, Japan* A purely optical technique for detecting negative ions in plasmas has been demonstrated where laser-photodetached electrons are detected via laser Thomson scattering. The technique allows one to obtain high spatial resolution (difficult to obtain using microwave techniques) without using a Langmuir probe. The plasma was irradiated by frequency-quadrupled (266nm) and frequency-doubled (532 nm) Nd:YAG laser beams originating from the same laser oscillator; the 266 nm beam causes photodetachment, while the 532 nm beam serves as the light source for Thomson scattering. It was so arranged that the 266 nm laser pulse irradiates the plasma 10 ns (> laser pulse width) earlier than the 532 nm laser pulse and, in the observation region, the focused thin 532 nm beam forms the coaxial core of the unfocused 266 nm beam. A specially designed triple-grating spectrometer was used, which produces Thomson spectra on the output focal plane with the interfering Rayleigh and stray components highly suppressed; an ICCD camera operated in the photon-counting mode was used

for multichannel detection of the spectrum. Measurements for inductively coupled $\text{NF}_3(5\%)/\text{Ar}$ and $\text{SF}_6(5\%)/\text{Ar}$ plasmas at 25 mTorr with electron densities of $\sim 10^{11} \text{ cm}^{-3}$ indicated that the negative ion density is of comparable magnitude to the electron density.

13:45

NR1 3 Laser Thomson scattering in Ar and N_2 gas plasmas. CATHERINE THOMPSON, PHILIP STEEN, GARY CRAIG, TOM MORROW, BILL GRAHAM, *Dept. of Pure and Applied Physics, Queen's University Belfast, Northern Ireland.* Laser Thomson scattering is now being used in low density ($\sim 10^{11} \text{ cm}^{-3}$) laboratory plasmas. Here the second harmonic of a Nd:YAG laser was used to perform Thomson scattering in an inductively coupled GEC cell, with an ICCD as detector. Thomson scattering measurements have been made in argon and nitrogen plasmas between 5-250mTorr and 10-300W. The electron densities and temperatures determined are shown to compare reasonably with Langmuir probe measurements in similar conditions. However the EEDF's derived from the Thomson scattering measurements show the presence of low energy electrons ($\leq 3\text{eV}$) not seen in the probe measurements. This potentially important finding is now being investigated more closely. In nitrogen the analysis is further complicated by factors such as Raman scattering and complex plasma emission.

14:00

NR1 4 Time-resolved Thomson Laser Scattering Measurements in Argon Plasma Jets GIANLUCA GREGORI, *Dept. of Mechanical Engineering, University of Minnesota* UWE KORTSHAGEN, *Dept. of Mechanical Engineering, University of Minnesota* JOACHIM HEBERLEIN, *Dept. of Mechanical Engineering, University of Minnesota* EMIL PFENDER, *Dept. of Mechanical Engineering, University of Minnesota* In this paper we present time-resolved Thomson laser scattering measurements in argon plasma jets. Argon plasma jets typically exhibits strong fluid dynamic fluctuations and characteristic values derived from scattering data averaging over longer time period are influenced by these fluctuations. To increase signal-to-noise ratio, several spectra are selectively accumulated. In contrast to previous measurements where single spectra were added together irrespective of the local plasma conditions in the jet, in this work data accumulation is performed only when similar plasma properties, as measured from local broad band visible light emission in the scattering volume, are reproduced from one single line-shape to another. In addition, strong electron-ion collision effects and the weakly non-ideal behavior characterized by the presence of a few electrons in the Debye sphere could considerably dampen the spectrum of the electron density correlations, and must be considered during data processing. A phenomenological approach based on the memory function formalism is proposed in order to better describe the effects of electron collisions and plasma non-ideality in the dynamic structure of the density correlation.

14:15

NR1 5 Plasma Etch Endpoint and Fault Detection Along with UV-Vis Absorption Spectroscopy from a Single Compact Solid State Detector. HAROLD ANDERSON, *Dept. of Chemical and Nuclear Engineering, University of New Mexico.* STEVE GUNTHER, *CETAC Technologies* BOB FRY, *CETAC Technologies* Array detector based systems with statistical analysis capability integrated with real-time data acquisition can provide a wealth of spectral information from a variety of potentially useful

gas phase emitting species. In the case of particularly challenging applications such as low-open area self-aligned contact (SAC) etches, utilization of the full optical emission spectrum has been shown to accurately detect endpoint when all other endpoint systems studied failed. Production facility results regarding these and other demanding applications will be presented. The talk will largely focus on oxide etching in AMAT MXP and TEL DRM platforms. Evolving Window Factor Analysis (EWFA) is the principal multivariate techniques used in the analysis. They allow one to dynamically track the principal components of the oxide etch process. EWFA is also shown to be useful for automatic fault detection. Additionally, the detector can be modified to rapidly perform full spectrum UV-Vis absorption spectroscopy for quantitative measurement of ground state radical species involved with the etch. This additional feature is meant to augment the diagnostic capabilities of conventional OES.

14:30

NR1 6 Oxide Etch Behavior in an Inductively Coupled C4F8 Discharge Characterized by Diode Laser Spectroscopy.* HAROLD ANDERSON, *Affiliation MARCUS BARELA, Affiliation GEOFF COURTIN, Affiliation KARLA WATERS,† Dept. of Chemical and Nuclear Engineering, Univ. of New Mexico* This study reports on oxide and photoresist etch characteristics in an inductively coupled GEC Reference Cell as a function of reactor source power, bias power and pressure using C4F8. Diode laser absorption spectroscopy (DLAS) has shown that C4F8 is largely dissociated to form C2F4, CF2 and CF in the discharge. Over an oxide surface, CF2 and CF are consumed in the oxide etch process, but only when the bias power is sufficient to keep the oxide surface clean through energetic ion bombardment. For C4F8, this transition occurs at 60 eV (75 W bias power) in the GEC Cell. At higher bias powers (125 W) where oxide etching is fast (600 nm/min.), CF2 appears to be the key radical for the etch process since 50 percent (2.7-3.0 mTorr in a 15 mTorr C4F8 discharge) is consumed. These values were obtained by comparing the CF2 concentrations over non-reactive wafer surfaces versus blanket oxide wafer surfaces undergoing etching. CF is shown to display a similar trend, but its concentration is an order of magnitude less than CF2, and consequently cannot account on a mass basis for the amount of reactants necessary to balance the amount of etch products. Over a PR surface, neither CF2 nor CF concentrations vary as a function of PR etch rate. Consequently, they do not appear to be involved in the PR etch mechanism. However, PR etching is also critically dependent on bias power. PR films etch presumably due to energetic ion bombardment that degrades the PR film, making it liable to attack by fluorine.

*This project was funded by SEMATECH and NSF

†now at Intel

14:45

NR1 7 Diagnostics of $c\text{-C}_4\text{F}_8$ Plasma in an Inductively Coupled GEC Reference Plasma Reactor BING JI, *Air Products and Chemicals, Inc.* STEPHEN MOTIKA, EUGENE KARWACKI, *Air Products and Chemicals, Inc.* Electrical and spectroscopic measurements were utilized to investigate $c\text{-C}_4\text{F}_8$ based plasmas within an inductively coupled GEC reference plasma reactor. UV Absorption Spectroscopy was used to measure the concentrations of CF and CF2 radicals. These measurements were correlated with simultaneous optical emission spectroscopy (OES). We obtained plasma ion density and electron temperature from Langmuir probe, and estimated inductive power coupling efficiency by RF electrical measurements. We report here on the impact of reactor

pressure, feed gas residence time, oxygen addition, and lower electrode bias on plasma gas chemistry. Our results show that the concentrations of CF and CF₂ radicals follow similar trends with regards to changes in pressure, residence time and oxygen addition.

15:00

NR1 8 Complementary optical diagnostics of noble gas plasmas* D.J. SMITH, R.S. STEWART, *Department of Physics and Applied Physics, University of Strathclyde* In this talk we will discuss our theoretical modeling and application of an array of four complementary optical diagnostic techniques for low-temperature plasmas. These are cw laser collisionally induced fluorescence (LCIF), cw optogalvanic effect (OGE), optical emission spectroscopy (OES) and optical absorption spectroscopy

(OAS). We will briefly present an overview of our investigation of neon positive column plasmas for reduced axial electrical fields ranging from 3×10^{-17} Vcm² to 2×10^{-16} Vcm² (3-20 Td), detailing our determination of five sets of important collisional rate coefficients involving the fifteen lowest levels, the ¹S₀ ground state and the 1s and 2p excited states (in Paschen notation), hence information on several energy regions of the electron distribution function (EDF). The discussion will be extended to show the new results obtained from analysis of the argon positive column over similar reduced fields. Future work includes application of our multi-diagnostic technique to move complex systems, including the addition of molecules for EDF determination.

*We are grateful to EPSRC for their financial support to this investigation.

SESSION NR2: ATMOSPHERIC PRESSURE & DIELECTRIC BARRIER DISCHARGES

Thursday afternoon, 11 October 2001; Ballroom AB Nittany Lion Inn at 13:15; Uwe Kortshagan, University of Minnesota, presiding

Invited Papers

13:15

NR2 1 Physics and chemistry in glow dielectric barrier discharges.
FRANÇOISE MASSINES, *CNRS - LGET*

Atmospheric pressure glow discharge (APGD) are of great interest for application in gas chemistry, sterilization, surface activation or thin film deposition. But the development of a new process based on this discharge needs a clear understanding of the discharge physics and chemistry. The aim of this work is to contribute to that goal. One difficulty is the large variety of discharges called APGD. Then the first point of this talk will consist on a quick description of the different APGD families. This overview will be limited to dielectric barrier glow discharges. Then, we will focussed on those due to a Townsend breakdown. The analysis of their working domain in helium and in nitrogen shows that a lot of seed electrons are necessary to turn on the discharge through a Townsend breakdown. The main mechanism leading to these seed electrons depends (i) on the life time of the gas metastables compared to the delay between two consecutive discharges (ii) on the maximum ionisation level which can be reached without transition to FD. In helium, the origin of the seed electrons is mainly the electrons created by direct ionisation and Penning ionisation during a discharge or at the end of it, trapped in the positive column and still present in the gas when the following discharge is turned on. In nitrogen, the seed electrons are created by Penning ionisation just before the breakdown. Then in helium, the time between two discharges has to be short enough and a positive column is necessary as well as the presence of helium metastables. In N₂, metastable density just before the breakdown is a dominant parameter. Moreover, the density of N₂ molecules and then the gas temperature, is also important in order to maintain a large contribution of Penning ionisation compared to direct electronic ionisation. In all the gases, the metastables control the discharge development and then play an important role in the gas chemistry.

Contributed Papers

13:45

NR2 2 HIGH SPEED CAMERA IMAGING AND OTHER DIAGNOSTICS OF DIELECTRIC BARRIER DISCHARGES AT ATMOSPHERIC PRESSURE ION RADU, 1 FARHAD MIRALAI, 1 GREGORY CZEREMUSZKIN, 1 RAYMOND BARTNIKAS, 2 MICHAEL R. WERTHEIMER, 1 (1)DEPARTMENT OF ENGINEERING PHYSICS, ECOLE POLYTECHNIQUE, MONTREAL, QC H3C 3A7, CANADA COLLABORATION, (2)HYDRO-QUEBEC RESEARCH INSTITUTE, VARENNES, QC J3X 1S1, CANADA COLLABORATION, Synchronous, High Speed Photography (HSP, using a Princeton Instruments PI-MAX 512RB Digital ICCD Camera System) and real-time dual detection (optical-electrical) diagnostics have been carried out for the study of dielectric barrier discharges

(DBD) in flowing gases such as He, Ne, Ar, Kr, air and N₂. A phase-resolved synchronizing circuit was used to trigger the ICCD camera's shutter for durations varying from 2 ns up to 100 ms. The high voltage electrode was either bare or coated with a dielectric, while ITO coated glass was used as the ground electrode for HPS studies of discharges. Experiments have been performed for different inter-electrode distances (d), frequencies (f), and amplitudes of the electric field, in order to investigate their influence on the DBD characteristics in each gas. The DBD in He, generally characterized by a single short and intense light pulse per half-period, but under some conditions accompanied by additional pulses of equal spacing, comprises multiple luminous spots (columns, 2-9 mm in diameter), which reoccur in the same position over many thousands of cycles of the applied field. At high overvoltage, these multiple columns give way to a uniform glow over the entire electrode surface, that is, a single "column," the so-called atmo-

spheric pressure glow discharge (APGD). Similar observations are made in other noble gases, but here the spots (columns) are smaller, extremely uniform in diameter and more luminous than in He. In all noble gases they can form stable "hexagonal lattices" in the HSP image, indicative of strong electrostatic (repulsive) interactions between columns, as also reported by Miller et al. [1] for the case of lower pressure (100 Torr) He discharges. The numbers of columns vary with changes in f and d , within certain ranges. In the case of DBD in N_2 , the HSP study clearly shows the transition from a filamentary regime, like that in air, to a true glow (APGD), provided that the gas is very pure ($<$ a few hundred ppm of O_2 , for example). The observations described above are explained in terms of long-lived metastable species in the noble gases and in N_2 . A video will be shown, which illustrates the phenomena described above. [1] I. Miller, C. Punset, E. Ammelt, H.G. Purwins and J.P. Boeuf, IEEE Trans. on Plasma Sci. 27 (1999) 20.

14:00

NR2 3 Study of different discharge regimes in a dielectric barrier discharge: electrical and optical characterization*

LORENZO MANGOLINI, KONSTANTIN ORLOV, UWE KORTSHAGEN, JOACHIM HEBERLEIN, ULRICH KOGELSCHATZ, *University of Minnesota - Mechanical Engineering* We have studied dielectric barrier discharges in atmospheric pressure helium. Discharges are generated between two planar electrodes each covered with dielectric glass plates. For some measurements a mesh is used as the lower electrode which permits the optical characterization of the transverse discharge uniformity using a CCD camera. Simultaneously, discharge current and voltage are measured. By changing the discharge gap width, the amplitude, and the frequency of the applied voltage we can obtain and reproduce different discharge regimes such as filamentary microdischarges, multiple diffuse spots, and transversely uniform discharges. We demonstrate that the observation of a single current pulse per voltage half cycle is not necessarily indicative of a uniform glow discharge, as is often assumed in the literature. We have also studied the repeatable and almost periodic appearance of multiple current pulses per half cycle in the uniform discharge mode. Through the use of a radially segmented electrode, we could show that these pulses are related to alternately outward and inward traveling ionization fronts.

*This work is supported by DOE under grant ER54583 and by Du Pont.

14:15

NR2 4 Firing time jitter in a single pixel ac Plasma Display Panel

MIKE BROWN, *The University of Toledo* WOO-GEUN LEE, *The University of Toledo* ALVIN D. COMPAAN, *The University of Toledo* JERRY SCHERMERHORN, *Electro Plasma, Inc.* In order to study the timing jitter in PDP structures, we tested a single pixel electrode structure to eliminate the effects from neighboring pixels. We used a time-to-amplitude converter (TAC) and a multi-channel analyzer (MCA) to create a histogram of the discharge events in which the time delay between the leading edge of the applied voltage pulse and the discharge is measured on the x-axis. The half period of the waveform was increased from 16.67 μ s to 1.6ms to allow us to observe the effect of increasing the off time during each discharge cycle. For driving frequencies from 30kHz to 3kHz, only a small increase was observed in the length of time needed for 95% increases dramatically. A gas mixture of 4% with the balance Ne was used to study the effects on the jitter. The results show a decrease in jitter with an increase in the Xe concentration. Work supported in part by Electro Plasma, Inc.

14:30

NR2 5 Effects of cell geometry and sustain voltage waveform shape on the efficiency of plasma display panels

GEORGIOS VERONIS, UMRAN INAN, *Stanford University* Plasma display panels (PDPs) are one of the leading candidates in the competition for large-size, high-brightness flat panel displays. One of the major challenges in the process of commercializing of PDPs is the improvement of the luminous efficiency of the panel. Computer modeling is currently essential for understanding PDP physics and optimizing its operation, since diagnostic measurements in PDPs are extremely difficult due to the very small cell dimensions and complicated panel structure. In this work, a two-dimensional simulation model is used to investigate the dependence of the luminous efficiency on the sustaining voltage waveform shape and PDP cell structure. Fluid equations are solved for electrons, ions and excited species together with Poisson's equation. Electron transport coefficients and rate coefficients of electron impact reactions are calculated by using the electron energy equation. We investigate alternative cell designs (insertion of floating electrodes in the dielectric layer, variation of the shape of the sustain electrodes and variation of the parameters of the dielectric layer), and alternative voltage waveforms (non-rectangular pulses).

14:45

NR2 6 Dispersion of low Mach number shock waves in a dielectric barrier discharge.

P. BLETZINGER, *ISSI* B.N. GAN-GULY, *Air Force Research Laboratory* A. GARSADDEN, *Air Force Research Laboratory* A dielectric barrier discharge in N_2 at pressures up to 30 Torr was excited in a 3 cm diameter Pyrex tube by two external, 15 cm long electrodes. At 30 Torr and a flow rate of 100 sccm the discharge was well confined in the space between the electrodes and appeared to be diffuse. The electrical excitation was by 6 ns wide current pulses, amplitude of 20-25A and a charging voltage of 6 kV, corresponding to a peak E/N of about 190 Td at 30 Torr and an average power input of 18 W. Since the boundaries of the discharge were so well defined, laser photo-deflection measurements of shock-generated density gradients could be performed very close to where the shock enters the plasma as well as at downstream positions. At 30 Torr, 30 kHz repetition rate and at Mach 1.45, shock width increased by almost 200

15:00

NR2 7 Time-Resolved Emission Spectroscopy of High-Pressure Discharge Plasmas in Ne and Ne/H₂ Gas Mixtures

PETER KURUNCZI, *Stevens Institute of Technology; now with Plasmion Corp.* KURT BECKER, *Stevens Institute of Technology* Microhollow cathode discharge (MHCD) plasmas in pure rare gases at or near atmospheric pressure are known to be efficient sources of excimer radiation. We also demonstrated that a high-pressure MHCD plasma in Ne with a trace admixture of H_2 gives rise to very intense, monochromatic H Lyman- α emission at 121.6 nm. This is the result of a very efficient near-resonant energy transfer process between the Ne excimer and the H_2 molecule. Time-resolved emission spectroscopic studies of the Ne excimer radiation at 84 nm and of the H Lyman- α radiation at 121.6 nm were carried out in an effort to elucidate the microscopic details of the excimer formation process and the near-resonant energy transfer reaction. We report results of the determination of the rate constant of the near-resonant energy transfer process and its dependence on the gas temperature in the MHCD plasma. Work supported by NSF and DARPA.

15:15

NR2 8 Electric Impedance Measurement and Pulsed OPO Laser Induced Fluorescence Study of Capacitively Coupled VHF Plasma (He/CF₄/O₂) at Atmospheric Pressure for Chemical Vaporization Machining (CVM) Process YASUSHI OSHIKANE, SHOICHI KAWASHIMA, KENICHI TAKEMOTO, KAZUYA YAMAMURA, KATSUYOSHI ENDO, YUZO MORI, *Graduate School of Engineering, Osaka University* An capacitively coupled atmospheric VHF (150 MHz) plasma (He/CF₄/O₂) has been applied to develop a novel machining process for up-to-date optics such as X-ray mirrors for SR facilities and high reflectors for gravitational wave detectors. To optimize the process characteristics, we have been studied the plasma parameters such as radical distribution, sheath characteristics, electrical impedance,

and electric field by changing the gas concentration, VHF electric power, gap distance. In this presentation, a series of experimental results based on optical spectroscopy and VHF circuit analysis are reported and discussed. CF and CF₂ radical distribution in the plasma is observed by optical emission spectroscopy (OES) and laser induced fluorescence (LIF) spectroscopy with a frequency-doubled pulsed OPO laser. A space-dependent UV band emission of the radicals are observed by OES. The number density of the radicals are monitored by LIF technique. They are excited with UV pulses (3ns FWHM, 3mJ/pulse), respectively. Spatial distribution and streaked spectra of the LIF signals are recorded. An affection of O₂ for the plasma is also studied. And the plasma impedance is also estimated by the electric signals, distributed circuit theory, and finite element method.

SESSION OR1: LABORATORY TOURS: PENN STATE'S NSF NATIONAL NANOFABRICATION USERS NETWORK (NNUN) AND OTHER SELECTED MATERIALS RESEARCH INSTITUTE FACILITIES
Thursday afternoon, 11 October 2001; Nanfab Facility, Materials Research Institute

Buses will begin departing from the main entrance of Nittany Lion Inn beginning at 15:00.

SESSION PR1: RECEPTION AND BANQUET
Thursday evening, 11 October 2001; Atrium and Ballrooms, Nittany Lion Inn at 18:30

SESSION QF1: PLASMA BOUNDARIES: SHEATHS AND PRESHEATHS

Friday morning, 12 October 2001

Ballroom C Nittany Lion Inn at 8:15

Merle Riley, Sandia National Laboratories, presiding

8:15

QF1 1 Evidence for sheath acting as charge separator by mass

E. STAMATE, *Nagoya University, Department of Electrical Eng.*
 K. OHE, *Nagoya Institute of Technology, Department of Systems Eng.*
 H. SUGAI, *Nagoya University, Department of Electrical Eng.* We demonstrate that the sheath surrounding an one-side conductor biased target acts as an electrostatic lens that focuses the charged particles of different mass to distinct regions of the surface. Moreover, due to the particular dynamics of the charged particles within the sheath, their flux on the surface is discrete resulting in a surface separation by the charge impact into a passive edge (no impact) and an active central surface. The flux profile of charged particles on the surface was developed by sputtering a conductor film of cooper previously deposited by a magnetron discharge on one side of some gold targets of circular and square geometry. The charged species that impacted the target surface were detected by Auger electron spectrometry (AES). Due to the large difference in mass, the sheath made a very clear distinction between electron and negative ion. This property was used to detect even very low contents of negative ions in O₂ and Ar/SF₆ plasmas, a situation in which other methods such as Langmuir probes or photodetachment were not practicable. The experimental results are found in good correlation with our particle simulation. This work was partially supported by the Japan Society for the Promotion of Science.

8:30

QF1 2 Electric field and metastable density measurements in a low PD and high E/n helium discharge PETER FENDEL, *Ohio State University, Columbus, OH 43210* BISWA GANGULY, *Air Force Research Laboratory, WPAFB, OH 45433* The electric field, singlet and triplet metastable density profiles have been measured in a 1.8 Torr, 6.5 mm gap, parallel plate helium dc discharge with current density < 0.5 mA/cm² by laser induced fluorescence (LIF). The discharge was operated under the conditions where the electron impact ionization mean free path was comparable to the interelectrode gap. The axial and radial electric field profiles were measured from the LIF Stark splitting of n=11 singlet Rydberg manifold, and the electric field vectors were estimated from the laser polarization dependent intensity distributions. The on-axis electric fields remain nearly constant, from cathode to anode, indicating a near absence of space-charge at the center of the interelectrode volume. The discharge exhibits radial variation of electric fields at all the measured locations from the cathode to the anode surface. The electric field vectors were found to be nonorthogonal to the cathode surface for off-axis locations. The combined axial and radial electric field variations suggest an annular current profile which is also supported by the singlet and the triplet He metastable density measurements. Also, the electric field remains high ($E_{min} > 1000$ V/cm) indicating the absence of a plasma region in the entire interelectrode volume. A comparison of the measured singlet to the triplet metastable density ratio shows the presence of low field plasma region behind the anode.

8:45

QF1 3 Ion energy distributions in rf-biased, high-density discharges in CF₄ MARK SOBOLEWSKI, YICHENG WANG, AMANDA GOYETTE, *NIST, Gaithersburg, MD 20899* Models of ion dynamics in radio-frequency (rf) biased, high-density plasma sheaths are needed to predict ion bombardment energies in plasma simulations. To test these models, we have measured ion energy distributions (IEDs) in pure CF₄ and CF₄/argon discharges in a high-density, inductively coupled plasma reactor, using a mass spectrometer equipped with an ion energy analyzer. IEDs of CF₃⁺, CF₂⁺, CF⁺, F⁺, and Ar⁺ ions were measured as a function of rf bias amplitude and frequency, pressure, mixture, and inductive source power. Simultaneous measurements by a capacitive probe and a Faraday cup provide enough information to determine the input parameters of sheath models and allow direct comparison of calculated and measured IEDs. When the rf bias period approaches the time it takes ions to cross the sheath, IEDs predicted by analytical sheath models do not agree with measured IEDs. A model which includes a complete treatment of the time-dependent ion dynamics in the sheath, however, does accurately predict the behavior of measured IEDs over the entire range of rf bias frequency.

9:00

QF1 4 Does it make sense to talk about presheaths?* NOAH HERSHKOWITZ, *University of Wisconsin, Madison* LUTFI OKSUZ, *The Open University, Oxford, UK* GREG SEVERN, *University of San Diego* XU WANG, *University of Wisconsin* It is usually assumed that when the plasma potential is positive with respect to a boundary, ions exit the plasma at the Bohm velocity. In weakly collisional plasma, it can be shown that ions are accelerated to the Bohm velocity by a "presheath" electric field. For λ proportional to or independent of v , the plasma potential varies as $\phi = (-x/\lambda)^{1/2}$ for small x , where λ is the ion collision mean free path. This means that most of the potential drop occurs within one λ so the presheath can be thought of as a well defined region. Experimental data from emissive probes in weakly collisional dc and rf plasmas, with device size $L \gg \lambda \gg \lambda_D$, verify this dependence for argon and helium plasmas. Data are also presented for N₂ and O₂ plasmas.

*Work supported by DOE grant no. DE-FG02-97ER54437 and NSF grant no. PHY9722658

9:15

QF1 5 The unipolar ion sheath K.-U. RIEMANN, *Ruhr-University Bochum, Theoretische Physik I, (D-44780 Bochum, Germany)* L. D. TSENDIN, *St. Petersburg State Technical University, (St. Petersburg, Russia)* In technical applications, the ion sheath in front of a highly negative wall is frequently described by the well known Child-Langmuir law. Due to inaccurate boundary conditions, however, this yields only a rather poor approximation. The collisionless Child-Langmuir law can be substantially improved by accounting for universal initial conditions following from the Bohm criterion. By a semi-empirical ansatz the analysis can be generalized to account for (charge exchange) ion collisions in the sheath. As a result, we obtain a convenient analytical sheath law describing the unipolar ion sheath for arbitrary collisionality.

SESSION QF2: PLASMA INTERACTIONS WITH SURFACES

Friday morning, 12 October 2001; Ballroom AB Nittany Lion Inn at 8:15; Jean Paul Booth, Ecole Polytechnique, presiding

*Invited Papers***8:15****QF2 1 Energetic particle/surface interactions at metal and organic thin films.**NICHOLAS WINOGRAD, *Penn State University*

The interaction of kev particles with metal and polymer thin films plays a central role in the processing of many types of electronic devices. Our goal is to develop experimental and theoretical protocols to elucidate these interactions on a molecular level. The approach is to utilize laser spectroscopy to interrogate the vibrational and excited electronic states of neutral species desorbed from the sample after irradiation. The predicted behavior of desorbed atoms and molecules is determined using molecular dynamics computer simulations. These simulations are quite reliable for metallic systems, and are now being developed for molecular thin films. For example, we employ a Brenner hydrocarbon potential to describe the motion of aromatic molecules, benzene being the model system. These calculations can produce quantum specific information that can be directly compared with experiment. This strategy is illustrated for benzene adsorbed onto a Ag111 surface at various coverages, ranging from a fraction of a monolayer to several monolayers. The spectroscopy is carried out using multiphoton resonance ionization of benzene molecules from either ground vibrational or excited vibrational levels. Moreover, the Ag atoms that desorb from the surface may also be monitored by resonance ionization from ground and excited states. The experimental observables such as yield, kinetic energy distribution and angle distribution are then compared to predictions of the molecular dynamics computer simulations. The results show general agreement between theory and experiment, providing a confirmation of the molecular picture provided by the theory. The significance of this agreement will be discussed in terms of a general picture of radiation damage in organic thin films.

8:45**QF2 2 Plasma treatments of polymers for various applications: A route for controlling processes and performances.**RICCARDO D'AGOSTINO, *University Bari*

This abstract not available.

*Contributed Papers***9:15**

QF2 3 Charge Conversion in Low Energy Scattering of H₂⁺ and H₃⁺ from a Polycrystalline Tungsten Surface J.N. DEFAZIO, T.M. STEPHEN, B.L. PEKO, *Department of Physics and Astronomy, University of Denver* Measurements of charge conversion in collisions of H₂⁺ and H₃⁺ with a polycrystalline tungsten surface are presented. Experiments are performed under high vacuum conditions (< 10⁻⁸ Torr). Measurements have been accomplished for H₂⁺ and H₃⁺ energies of 100-1000 eV, at an incident angle of 18 deg. Specularly scattered positive and negative products are energy analyzed and detected. Two distinct energy distributions for negative ions are observed, while positive ions show one. Results indicate pre-collision neutralization and dissociation, and post-collision ionization processes. Energy distributions are in qualitative agreement with TRIM (Transport of Ions in Matter) Monte Carlo calculations.

SESSION RF1: PLASMA DIAGNOSTIC V

Friday morning, 12 October 2001

Ballroom C Nittany Lion Inn at 10:00

Greg Hebner, Sandia National Laboratories, presiding

10:00

RF1 1 A new method of electron temperature measurement in Si process plasmas TAKESHI K.GOTOH*, *Keio university at Yokohama, Japan* TOSHIAKI MAKABE, *Keio university at Yokohama, Japan* When plasmas are jointed to a wall surface with trench patterns made of dielectric materials, a positive charge-build-up occurs at the bottom of the trench. It is called "local charge build-up" or "electron shading effect"¹. When the aspect ratio of the trench is high, the bottom potential would almost equal to the plasma potentials. Because the ion flux toward the bottom must decrease substantially to balance the slight electron flux toward the bottom. Therefore, the bottom completely would charge up and the potential difference between the trench bottom and wall surfaces would be almost sheath voltage, which is related linearly to electron temperature; T_e in plasmas. In the present study, T_e in an inductively coupled plasma in Ar were measured by using a

glass plate with an array of capillaries. Two small pieces of Si wafer with an thin Au film were set on the dielectric chamber wall. One piece was uncovered and the other was completely covered with the glass plate with an array of 0.4mm long and 20 μ m diameter capillaries. The potential difference between both of the pieces were observed by voltage probes. (Tektro P6009). The measurement was performed by changing Te from 2.2 eV to 4.0 eV in Ar plasma. The values of potential difference almost varied linearly from 8.0 V to 16.5 V with respect to Te and were nearly close to theoretical values. *Permanent address : Fujitsu Lab. LTD. at Atsugi, Japan

¹T.Kamata and H.Arimoto, J.Appl.Phys. 80 p2637,(1996)

10:15

RF1 2 A seven harmonic actively compensated Langmuir probe for the GEC Cell* A. GOODYEAR, L. NOLLE, A.A. HOPGOOD, P.D. PICTON, N. BRAITHWAITE, *The Open University, Oxford Research Unit, Boars Hill, Oxford, OX1 5HR, UK* The uncertainty of Langmuir probe measurements in capacitively coupled discharges depends to a great extent on how well harmonic components in the plasma potential are accounted for. The extent to which individual harmonics distort a probe characteristic has been determined across power and pressure parameter-space in the GEC cell. Langmuir probe current-voltage measurements are distorted by RF components across the probe sheath. A seven harmonic waveform was applied to the probe tip to actively match that generated by the plasma. In some circumstances harmonics above the 3rd contributed RF components of the order of the electron temperature in magnitude. Measurement of the EEDF was found to be particularly sensitive to these components. Optimization of the applied waveform (seven amplitudes and seven phases) was achieved using artificially intelligent control. This is advantageous given the large number of (possibly interacting) parameters and permits tracking of changes in plasma conditions. An algorithm utilizing simulated annealing determines the optimum waveform in a far shorter time than a skilled human operator can.

*Work supported by the EPSRC (UK), Grant No. GR/M71039

10:30

RF1 3 Microwave Interferometer for Steady-State Plasmas EARL SCIME, ROBERT BOIVIN, JOHN KLINE, *Department of Physics, West Virginia University* MATTHEW BALKEY, *Naval Research Laboratory* Standard single frequency, "fringe-counting," microwave interferometers are of limited use for steady-state plasma experiments. We have constructed a swept frequency microwave interferometer, similar to a classic zebra-stripe interferometer, optimized for electron density measurements in steady-state plasma experiments. The key element in the system is a frequency doubled YIG oscillator capable of sweeping from 20 to 40 GHz. As the source frequency is swept, the sum of the reference and plasma leg signals exhibits a series of beats. Both the frequency shift and phase shift of the beat pattern due to the addition of plasma in one leg of the interferometer is used to determine the line-integrated electron density.

10:45

RF1 4 Ion Flux Measurements in Electron Beam Produced Plasmas in Atomic and Molecular Gases* S.G. WALTON,[†]D. LEONHARDT, D.D. BLACKWELL,[‡]D.P. MURPHY, R.F. FERNSLER, R.A. MEGER, *Plasma Physics Division, Naval Research Laboratory, Washington, DC 20375* In this presentation, mass- and time-resolved measurements of ion fluxes sampled from pulsed, electron beam-generated plasmas will be discussed. Previ-

ous works have shown that energetic electron beams are efficient at producing high-density plasmas (10^{10} - 10^{12} cm⁻³) with low electron temperatures ($T_e < 1.0$ eV) over the volume of the beam. Outside the beam, the plasma density and electron temperature vary due, in part, to ion-neutral and electron-ion interactions. In molecular gases, electron-ion recombination plays a significant role while in atomic gases, ion-neutral interactions are important. These interactions also determine the temporal variations in the electron temperature and plasma density when the electron beam is pulsed. Temporally resolved ion flux and energy distributions at a grounded electrode surface located adjacent to pulsed plasmas in pure Ar, N₂, O₂, and their mixtures are discussed. Measurements are presented as a function of operating pressure, mixture ratio, and electron beam-electrode separation. The differences in the results for atomic and molecular gases will also be discussed and related to their respective gas-phase kinetics.

*Work supported by the Office of Naval Research

[†]SFA Inc., Largo, MD

[‡]NRC Postdoctoral Research Associate

11:00

RF1 5 Electron Beam Diagnostics in Plasmas Based on Electron Beam Ionization* DARRIN LEONHARDT, EDBERTHO LEAL-QUIROS,[†]DAVID BLACKWELL,[‡]SCOTT WALTON,[§]DONALD MURPHY, RICHARD FERNSLER, ROBERT MEGER, *US Naval Research Laboratory, Plasma Physics Division* Over the last few years, electron beam ionization has been shown to be a viable generator of high density plasmas with numerous applications in materials modification. To better understand these plasmas, we have fielded electron beam diagnostics to more clearly understand the propagation of the beam as it travels through the background gas and creates the plasma. These diagnostics vary greatly in sophistication, ranging from differentially pumped systems with energy selective elements to metal 'hockey pucks' covered with thin layers of insulation to electrically isolate the detector from the plasma but pass high energy beam electrons. Most importantly, absolute measurements of spatially resolved beam current densities are measured in a variety of pulsed and continuous beam sources. The energy distribution of the beam current(s) will be further discussed, through experiments incorporating various energy resolving elements such as simple grids and more sophisticated cylindrical lens geometries. The results are compared with other experiments of high energy electron beams through gases and appropriate disparities and caveats will be discussed. Finally, plasma parameters are correlated to the measured beam parameters for a more global picture of electron beam produced plasmas.

*Work supported by the Office of Naval Research

[†]US Navy - ASEE Summer Faculty. Permanent Address: Polytechnique University of Puerto Rico, Hato Rey, P.R. 09918

[‡]NRL/NRC Postdoctoral Research Associate

[§]SFA Inc., Largo, MD

11:15

RF1 6 Ions Near Bumps - Experimental measurements of ion trajectories near surface features on rf-biased wafers J. R. WOODWORTH, *Sandia National Laboratories* I. C. ABRAHAM, P. A. MILLER, R. J. SHUL, B. P. ARAGON, T. W. HAMILTON, C. G. WILLISON, *Sandia National Laboratories* We are studying ion trajectories near small wafer surface features in an inductively-driven Gaseous Electronics Conference Reference Cell. In this talk we will report ion trajectory measurements

near 300-micron tall "walls" and at the bottom of 300-micron tall "corners" on rf-biased silicon wafers. We make these measurements by coupling ions through 6-micron diameter pinholes located near the features of interest and then analyzing them with a gridded ion energy and angle analyzer developed previously. Our intent in taking this data is to facilitate the development of theoretical models that will describe ion trajectories in and around surface features, pushing our understanding of the plasma-surface interface down to a finer level of detail. In our experiments, we find that the ion beam moves off axis and is non uniform near walls and corners, the ion energy distributions are different at different angles to the wafer surface, and the ion fluxes are not strongly dependent on the rf bias voltage. Sandia is a multiprogram laboratory operated by Sandia Corporation, a Lockheed Martin Company, for the United States Department of Energy under Contract DE-AC04-94AL85000.

11:30

RF1 7 Electron Collision Excitation Rate and Electron Density in a Rare Gas Discharge* M. A. BRATESCU, Y. SAKAI, M. YANAGIDA, *Hokkaido University, Sapporo 060-8628, Japan* In the present work we introduced an optical diagnostics method

based on laser collisionally induced fluorescence (LCIF) to determine electron collision excitation rate. LCIF means a change of the emitted light of plasma due to the resonant light absorption corresponding to an atomic species present in the plasma. The experiment was done in 1 Torr pressure Xe discharge at 1 mA current. The laser pumping wavelength was corresponding to the transition from $1s_5$ to $2p_6$ at 823.389 nm. Measuring the intensities in the emitted spectra from the discharge we calculated the electron collision excitation rates from $2p_6$ to other upper levels i.e. $3p_8$, $3p_5$, $2p_4$, $5d'_4$, $2p_2$, $2p_1$, $3p_7$. In the same discharge we measured the absorption line from resonant level $1s_4$ to $2p_5$ at 828.239 nm in order to determine the number density of $1s_4$ level, $N(1s_4)$. The excitation to $1s$ levels in rare gas discharges is mainly due to electron impact excitation. Radiative deexcitation occurs in case of resonant levels $1s_4$ and $1s_2$. Using a simple balance equation we evaluate electron density. For the case that $N(1s_4) \sim 10^8 \text{ cm}^{-3}$, an electron excitation rate of $1s_4$ level $\sim 1.6 \times 10^{-13} \text{ cm}^3 \text{ s}^{-1}$ at $T_e \sim 0.6 \text{ eV}$, we obtained $n_e \sim 10^{13} \text{ cm}^{-3}$.

*Work supported by Grant-in-Aid for Scientific Research (C) of JSPS.

SESSION RF2: LOW AND ULTRALOW ENERGY ELECTRON-MOLECULE INTERACTIONS

Friday morning, 12 October 2001; Ballroom A, B Nittany Lion Inn at 10:00; A. Chutjian, Jet Propulsion Laboratory/California Institute of Technology, presiding

Invited Papers

10:00

RF2 1 Attachment of slow electrons to molecules and clusters at high energy resolution.

ASCHWIN GOPALAN, *Universität Kaiserslautern, Fachbereich Physik, D-67663 Kaiserslautern, Germany*

Collisions between electrons and atoms, molecules or clusters at low energies are of great fundamental and applied interest. Especially, the attachment of electrons to molecules XY with formation of either dissociated products $X + Y^-$ (dissociative attachment) or long-lived anions XY^- (associative attachment, e.g. SF_6^-) is an important process in connection with the dielectric breakdown strength of gases. Processes involving vibrational excitation and negative ion formation are strongly mediated through resonances in the collision complex. Apart from the well known shape resonances, vibrational Feshbach resonances have recently been observed to play an important role. In these studies, it became clear that very high energy resolution (energy width around 1 meV) is necessary to reveal the details of the resonance structure and – in electron attachment experiments – the steep rise in the cross-section towards zero energy (s-wave attachment). Over the last ten years, our group has developed laser photoelectron sources with (sub) meV energy widths. They rely on resonant two step laser photoionization of metastable Ar^* or ground state K atoms with tunable narrow-band lasers in conjunction with a careful characterization and minimization of the residual electric field in the reaction region. So far, most of the experiments have addressed electron attachment processes with selected molecules and molecular clusters. In these studies, the photoelectrons react with a collimated target nozzle beam in the region of their production. At very low photoelectron currents, energies down to $E = 0.02 \text{ meV}$ and energy width down to 0.015 meV were achieved, but more typically, effective energy widths between 0.2 and 2 meV were used at currents between 1 and 50 pA. For the first time, the $E^{-1/2}$ behaviour ($E \rightarrow 0$) for s-wave attachment processes was clearly verified and step-like structure was found in the attachment yield at onsets for vibrational excitation. Prominent, narrow vibrational Feshbach resonances were recently observed in electron attachment reactions with CH_3I and CH_2Br_2 molecules as well as with clusters of N_2O and CO_2 . Experiments are under way to exploit the potential of these laser photoelectron sources for scattering experiments involving atoms in a well collimated supersonic beam. Our work has been supported by the Deutsche Forschungsgemeinschaft, the Graduiertenkolleg *Laser- und Teilchenspektroskopie* and the *Zentrum für Lasermeß technik und Diagnostik*.

10:30

RF2 2 Dissociative Electron Attachment in the condensed phase: sample morphology and bio-molecules.A.D. BASS, *Groupe des Institues de Recherche en Santé du Canada en Sciences des Radiations, Dépt. de Médecine Nucléaire et de Radiobiologie, Faculté de Médecine, Université de Sherbrooke, Sherbrooke, Quebec, CANADA*.*

Recent electron impact experiments on condensed plasmid DNA have shown low energy electrons to be remarkably effective in causing damage and reveal that electron-scattering phenomena, such as transient anion formation and their decay via dissociative electron attachment, play a central role in this process. Such experiments may prompt a revision of our understanding of the mutagenic effects of radiation and have significant implications for both radiotherapy and radio-protection. These results can be better understood by investigating electron scattering with the various functional constituents of DNA in condensed environments. Recent work, to be presented here, has focused on electron attachment processes in condensed DNA bases and sugar-like analogues of the DNA backbone, as evidenced by the desorption of fragment anions. Despite this progress, a complete understanding of these processes requires parallel study of simpler 'model' systems, which allow the characteristic condensed-phase phenomena modulating electron-scattering to be identified. Factors affecting anion formation and DEA can be classed as either intrinsic (affecting the properties of the resonance) or extrinsic (modifying the energy of electrons before attachment and/or the reactions of fragments, post-dissociation). In this talk we will present new results in which the extrinsic factors of porosity and phase of a sample are probed via the desorption of anionic fragments from either the pure film or from probe molecules condensed upon its surface. We show that anion desorption and hence our ability to observe DEA process, is highly sensitive to sample morphology and phase, a property which can be exploited to study the morphology of the film itself.

*In collaboration with L. Sanche.

Contributed Papers

11:00

RF2 3 Electron Transport Properties and Collision Cross Sections in C2F4

K. YOSHIDA, S. GOTO, *Kitami Institute of Technology* H. TAGASHIRA, *Muroran Institute of Technology* C. WINSTEAD, B.V. MCKOY, *California Institute of Technology* W.L. MORGAN, *Kinema Research & Software** We have measured the electron drift velocity, longitudinal diffusion coefficient, and ionization coefficient in C2F4 (tetrafluoroethylene). Using these data, ab initio calculations of the elastic and momentum transfer cross sections and of the neutral excitation cross sections, and measurements of the partial ionization cross sections, we have performed a swarm analysis in order to construct a self-consistent set of electron impact cross sections for C2F4. The swarm analysis is based on solutions to Boltzmann's equation for electrons in C2F4 for values of $E/N < 500$ Td and direct Monte Carlo simulation of electron transport in C2F4 for $500 \text{ Td} < E/N < 2000$ Td. We present an analysis and discussion of the sensitivity of cross sections derived from swarm data to uncertainties in the electron transport measurements. We also discuss the failure of the two-term spherical harmonic solution to Boltzmann's equation for $E/N > 500$ Td, which necessitated the use of Monte Carlo simulations for high values of E/N .

*The authors would like to thank Dr. Peter Ventzek for his encouragement and support of this work.

11:15

RF2 4 Electron Interactions with BCl₃

LOUCAS CHRISTOPHOROU, *NIST* JAMES OLTHOFF, *NIST* In this paper we review and assess the cross sections for collisions of low-energy electrons with boron trichloride (BCl₃), a plasma processing gas used for the etching of metals and semiconductors. There are no experimental data on the total electron scattering, total elastic, differential elastic, momentum transfer, or inelastic electron scattering cross sections. There are only calculated values for the total elastic, differential elastic, momentum transfer, and some electronic excitation cross sections, and derived cross sections for vibrational excitation and dissociation. The only available experi-

mental cross section data are for partial and total ionization and electron attachment. The electron attachment data are uncertain. To characterize the electron attachment processes, measurements are needed for both the absolute magnitude of the electron attachment cross section and temperature dependence of the production of Cl⁻ and BCl₃⁻. Similarly, besides some rather uncertain data on electron attachment rate constants, there are no measurements of the electron attachment, ionization, or transport coefficients for this gas. The experimental data on the electron affinity, electron attachment, and electron scattering, allowed identification of negative ion states of BCl₃ at -0.3 eV, 1.0 eV, 2.8 eV, 5.2 eV, 7.6 eV, and 9.0 eV. The existing electron collision data will be discussed and relevant data on photon impact will be elaborated upon.

11:30

RF2 5 Observation of the Even Rotational States of the Helium Molecular Ion

C. CARABALLO, M. FAXAS, A. PACHECO, J. ROJAS, L. SIMONS, K. HARDY, *Florida International University** The Dissociative Recombination (DR) reaction of the helium molecular ion results in the production of two final state product atoms, one being in an excited state, and the other normally being in the ground state. We observed DR reactions of He⁺ from rotational states of the $v=3, 4, \text{ and } 5$ vibrational levels of the molecule. Energies of DR transitions are measured by time-of-flight (TOF) spectroscopy. Even though parity conservation prohibits the existence of even angular momentum states, we have obtained observations of these states. We observed the $J=0, 2, 4, 6, 8, 10, 14$ and 16 from $v=3, 4, \text{ and } 5$ vibrational levels. Using the expression for the energies of rotational states, $F_v(J) = B_v J(J+1) + D_v J^2(J+1)^2$, rotational constants B_v and D_v can be determined. In obtaining these constants the states were examined in the following way: first the even and odd states were combined, then only the odd ones were examined, and finally only the even ones. The rotational constants for the combined odd and even rotational states and for the odd rotational states alone are $B_v(c) = 6.49 \pm 0.05$ and $B_v(o) = 6.53 \pm 0.09$ for the $v=3$ level respectively. For the $v=4$ level they are $B_v(c) = 6.12 \pm 0.05$ and $B_v(o) = 6.17 \pm 0.05$. Finally, for the $v=5$ level they are $B_v(c) = 5.78 \pm 0.15$ and $B_v(o) = 5.64 \pm 0.14$. The rotational constants for only

even angular momentum states are slightly higher but within experimental error.

*Support by LLNL Research Collaborations for HBCU/MI, NSF REU and NASA

11:45

RF2 6 Ion-Ion Plasmas Produced by Electron Beams* R. F. FERNSLER, D. LEONHARDT, S. G. WALTON,[†]R. A. MEGER, *Plasma Physics Division, Naval Research Laboratory* The ability of plasmas to etch deep, small-scale features in materials is limited by localized charging of the features. The features charge because of the difference in electron and ion anisotropy, and thus one solution now being explored is to use ion-ion plasmas in place of electron-ion plasmas. Ion-ion plasmas are effectively electron-free and consist mainly of positive and negative ions. Since the two ion species behave similarly, localized charging is largely eliminated. However, the only way to produce ion-ion plasmas at low gas

pressure is to convert electrons into negative ions through two-body attachment to neutrals. While the electron attachment rate is large at low electron temperatures ($T_e < 1$ eV) in many of the halogen gases used for processing, these temperatures occur in most reactors only during the afterglow when the heating fields are turned off and the plasma is decaying. By contrast, T_e is low nearly all the time in plasmas produced by electron beams, and therefore electron beams can potentially produce ion-ion plasmas continuously. The theory of ion-ion plasmas formed by pulsed electron beams is examined in this talk and compared with experimental results presented elsewhere [1]. Some general limitations of ion-ion plasmas, including relatively low flux levels, are discussed as well. [1] See the presentation by D. Leonhardt et al. at this conference.

*Work supported by the Office of Naval Research

[†]SFA Inc., Largo, MD

A

- Abou-Ghazala, Amr LR2 3
 Abraham, I.C. MR1 1, RF1 6
 Abramzon, Nina DTP 58
 Adamovich, Igor V.
 JWP 79, JWP 81, JWP 82
 Adibzadeh, Mehrdad
 DTP 51
 Aithal, Shashi M. JWP 80
 Akatsuka, Hiroshi DTP 67,
 JWP 49
 Akira, Tonegawa DTP 66
 Akiyama, Hidenori LR2 3
 Alaoui, M. JWP 2
 Amanatides, Eleftherios
 LR1 6
 Anderson, Harold NR1 5,
 NR1 6
 Anderson, L.W. AT1 3,
 DTP 55
 Anderson, Scott JWP 34
 Angel, Gordon DTP 26
 Aragon, B.P. RF1 6
 Aranda Gonzalvo, Y.
 JWP 30
 Arndt, Stefan ET2 2
 Arnell, R.D. DTP 13
 Arslanbekov, Robert
 DTP 8, GW2 5
 Ayres, Virginia KW1 6

B

- Baldwin, K.G. AT1 4
 Balkey, Matthew RF1 3
 Balkey, M.M. MR1 7
 Baravian, G. JWP 3, LR2 1
 Barela, Marcus NR1 6
 Barrett, Richard GW2 3
 Barroy, P.R.J. DTP 22
 Barthelémy, O. GW2 6
 Bartnikas, Raymond NR2 2
 Bartschat, K. DTP 53,
 KW2 5, KW2 6
 Basner, Ralf DTP 61
 Bass, A.D. RF2 2
 Bass, Andrew D DTP 50
 Basurto, Eduardo DTP 65
 Bäcker, H. DTP 13
 Becker, K. DTP 58,
 DTP 60, ET2 1
 Becker, Kurt DTP 61,
 GW1 2, NR2 7
 Behnke, J. DTP 7
 Behnke, J.F. DTP 7,
 DTP 12, DTP 14, DTP 15
 Belkind, A. ET2 1
 Benck, Eric NR1 1
 Benhacene, K.M. DTP 2
 Bernal, Sara KW1 6

Bhandarkar, Upendra

KW1 3

- Biloiu, C. JWP 37
 Biloiu, I.A. JWP 37
 Blackwell, David DTP 46,
 JWP 48, RF1 5
 Blackwell, D.D. RF1 4
 Bletzinger, P. NR2 6
 Boeuf, J.-P. JWP 61
 Boffard, John B. AT1 3,
 DTP 55
 Bogaerts, Annemie **KW2 3**
 Boivin, R.F. MR1 7
 Boivin, Robert AT2 5,
 DTP 18, DTP 40, RF1 3
 Booth, Jean-Paul **MR2 2**
 Bose, Deepak **BT2 3**,
MR1 3
 Boulos, Maher LR2 5
 Bowden, Mark JWP 53
 Bradley, J.W. DTP 13,
 GW2 4, JWP 30
 Braithwaite, N.St.J.
 DTP 22, DTP 28, RF1 2
 Brake, Mary JWP 34,
 KW1 6
 Bratescu, M.A. RF1 7
 Bray, Igor DTP 54
 Brown, Michael DTP 35
 Brown, Mike JWP 56,
 NR2 4
 Browning, P.K. GW2 4
 Buckman, S.J. AT1 4,
 GW1 3
 Buff, James DTP 26
 Buss, R.J. BT1 4
- C**
- Cao, Jin **BT1 6**
 Caraballo, C. **RF2 5**
 Carter, Dan LR1 5
 Chaker, M. BT1 7, GW2 6,
 LR1 4
 Chang, Hong-young
 JWP 20
 Chang, H.Y. JWP 28
 Cho, Moo-Hyun DTP 47
 Cho, Sang-Hoon JWP 24
 Choi, Yong-Sup DTP 24
 Christophorou, Loucas
RF2 4
 Chung, ChinWook JWP 28
 Chung, Kyu-Sun DTP 24
 Colla, M. AT1 4
 Collaboration,
 (1)Department of
 Engineering Physics Ecole
 Polytechnique Montreal
 QC H3C 3A7 Canada
 NR2 2

Collaboration,

- (2)Hydro-Qubec Research
 Institute Varennes QC
 J3X 1S1 Canada NR2 2
 Collaboration, CRTP LR2 5
 Collaboration, Electro
 Plasma Inc. Millburg OH
 JWP 56
 Collaboration, ETP LR2 5
 Collaboration, *Grad.
 School of Eng. Tohoku
 Univ. MR1 6
 Collaboration, National
 Institute for Fusion
 Science DTP 66
 Collaboration, Sharp Corp.
 MR1 6
 Collard, Corey JWP 34,
KW1 6
 Collins, G.J. JWP 65
 Compaan, Alvin D.
 JWP 56, NR2 4
 Coppins, M. GW2 4
 Corr, Cormac JWP 27
 Corr, C.S. JWP 26
 Costa i Bricha, E. JWP 26
 Costa i Bricha, Elm
 JWP 14
 Courtin, Geoff NR1 6
 Cowan, Robert D. DTP 52
 Craig, Gary NR1 3
 Crimp, Marty KW1 6
 Cruden, Brett A. JWP 76,
 JWP 77, KW1 4, **MR2 4**
 Csambal, C. DTP 12
 Csanak, George DTP 52
 Cummings, James DTP 26
 Czarnetzki, U. JWP 52
 Czeremuszkin, Gregory
 NR2 2
- D**
- d'Agostino, Riccardo
QF2 2
 Dahiya, R.P. **BT1 8**
 Dasgupta, A. **DTP 53**
 Dateo, Christopher DTP 69
 Dave, Bakul JWP 5,
 JWP 31
 Davies, P.B. DTP 39
 De Urquijo, Jaime DTP 65
 DeFazio, J.N. **QF2 3**
 Defrance, P. DTP 60
 DeJoseph, Charles DTP 62
 DeJoseph Jr., C.A. **JWP 44**
 DeJoseph Jr., Charles A.
 DTP 34
 Delaney, Michael JWP 34
 Delprat, S. LR1 4
 Delzeit, Lance **KW1 4**

- Den Hartog, E.A. JWP 57
 Deutsch, H. **DTP 60**
 Deutsch, Hans DTP 61
 Dhali, Shirshak **JWP 5**,
JWP 31
 Diamant, Stela JWP 2
 Dietz, Doug **JWP 80**
 Diong, C.H. JWP 6
 Diver, Declan GW2 3
 Döbele, H.F. DTP 41
 Döbele, H.F. JWP 52
 Doebele, Hans Friedrich
 DTP 45
 Doll, Gary JWP 63
 Donko, Zoltan JWP 11
 Dorai, Rajesh **LR2 2**
 Doughty, D.A. ET1 6
 Dubin, D.H.E. BT1 2
 Duten, Xavier DTP 38

E

- Economou, Demetre **BT2 5**,
DTP 48, **JWP 47**
 Endo, Katsuyoshi DTP 4,
 NR2 8
 Ernst, Uwe JWP 58
 Escoffier, C.N. JWP 26

F

- Fang, Y. KW2 5, **KW2 6**
 Faxas, M. RF2 5
 Fedchak, J.A. JWP 57
 Fendel, Peter **QF1 2**
 Fernsler, R. F. DTP 20
 Fernsler, R.F. RF1 4,
RF2 6
 Fernsler, Richard DTP 46,
 JWP 48, RF1 5
 Foest, Rüdiger **JWP 68**
 Font, G.I. BT2 2, **JWP 8**
 Fontes, Christopher J.
DTP 52
 Francis, Terry JWP 2
 Frank, Klaus JWP 58
 Franklin, Raoul **QF1 6**
 Fraser, Gerald NR1 1
 Fraser, Hamish L. JWP 82
 Frederickson, Kraig JWP 82
 Fresnet, F. **JWP 3**, LR2 1
 Frommhold, Lothar ET2 4
 Fruchtman, Amnon **DTP 17**
 Fry, Bob NR1 5
 Fujita, Hiroharu JWP 9
 Funahashi, H. JWP 51,
 NR1 2
 Fursa, Dmitry DTP 54,
KW2 2

G

Ganachev, Ivan **ET2 7**
 Ganguli, Gurudas **BT1 5**
 Ganguly, Biswa **DTP 35**,
QF1 2
 Ganguly, B.N. **NR2 6**
 Garscadden, A. **NR2 6**
 Garscadden, Alan **DTP 35**,
DTP 62
 Gaskill, D.K. **LR1 1**
 Gavrishchaka, Valeriy
BT1 5
 Gilbert, S.J. **GW1 3**
 Gilgenbach, Ronald **JWP 63**
 Girshick, Steven **KW1 3**
 Glembocki, O.J. **DTP 20**,
LR1 1
 Golkowski, C. **ET1 3**
 Golubovskii, Yu.B. **DTP 7**,
DTP 14, **DTP 15**
 Golubyatnikov, Guerman
NR1 1
 Gomez, S. **DTP 42**, **JWP 26**
 Gomez, Sergi **JWP 38**
 Goodyear, A. **DTP 22**,
DTP 28, **RF1 2**
 Gopalan, Aschwin **RF2 1**
 Goree, J. **BT1 1**, **BT1 2**
 Gorshkov, Oleg **LR2 4**
 Goto, S. **RF2 3**
 Gotoh, Takeshi K. **RF1 1**
 Gottschalk, Jeff **JWP 56**
 Govindan, T.R. **BT2 3**,
MR1 3
 Goyette, Amanda **JWP 23**,
QF1 3
 Gozadinos, George
DTP 25, **ET2 5**
 Graham, Bill **NR1 3**
 Graham, W.G. **DTP 42**,
JWP 26
 Graham, William G.
JWP 14, **JWP 27**, **JWP 38**
 Gravelle, Denis **LR2 5**
 Greenberg, K.E. **DTP 30**
 Greenwood, C.L. **JWP 46**
 Gregori, Gianluca **NR1 4**
 Grum-Grzhimailo, A.N.
DTP 53
 Guay, D. **BT1 7**
 Gulley, R.J. **AT1 4**
 Gunther, Steve **NR1 5**
 Guo, Wei **JWP 44**

H

Haas, F.A. **DTP 28**
 Hajime, Suzuki **DTP 66**
 Hamilton, T.W. **RF1 6**

Hammer, David **ET1 3**
 Hammer, Dominik **ET2 4**
 Hanne, G. Friedrich **KW2 1**
 Hardy, K. **RF2 5**
 Harikai, Atsushi **DTP 32**
 Hartmann, Ralf **DTP 10**
 Hash, David **BT2 3**,
KW1 5
 Hatton, P.J. **JWP 45**
 Heberlein, Joachim **DTP 10**,
NR1 4, **NR2 3**
 Hebner, G.A. **BT1 4**,
DTP 30, **JWP 54**, **MR1 1**
 Hempel, F. **DTP 39**
 Henry, R. **LR1 1**
 Hernandez, Jose Luis
DTP 65
 Hershkowitz, Noah **DTP 23**,
QF1 4
 Hinshelwood, D. **DTP 20**
 Ho, P. **BT1 4**
 Holm, R.T. **DTP 20**
 Hondou, T. **JWP 60**
 Hong, Bo-Han **DTP 24**
 Hoogerland, M. **AT1 4**
 Hopgood, A.A. **RF1 2**
 Hopwood, Jeffrey **JWP 74**
 Hori, Masaru **KW1 1**
 Horie, Ikuya **JWP 33**
 Hseuh, Hsin-Pai **JWP 66**
 Hubert, J. **DTP 2**
 Huo, Winifred **DTP 59**
 Hur, M.S. **JWP 64**
 Hwang, Helen **LR1 3**
 Hwang, H.H. **BT2 4**

I

i Cabarrocas, P. Roca
KW1 2
 Iizuka, Satoru
MR1 6
 Ikeda, Masami **JWP 72**,
MR2 5
 Ikuta, Nobuaki **JWP 16**
 Iliin, A.A. **LR2 4**
 Inan, Umran **NR2 5**
 Irissou, E. **BT1 7**
 Isaacs, W.A. **DTP 56**
 Isao, Shirota **DTP 66**
 Ishijima, Tatsuo **JWP 72**,
MR2 5

J

Jayaraman, RaviPrakash
JWP 66
 Ji, Bing **NR1 7**
 Jiang, Chunqi **JWP 4**

Jiang, N. **JWP 6**, **JWP 39**,
LR1 2
 Jiang, Ning **DTP 31**,
JWP 21
 Jiao, Charles **DTP 62**
 Johnson, D. **BT1 4**
 Johnston, T.W. **GW2 6**
 Jonston, Mark **JWP 63**
 Joung, Me **DTP 47**
 Joyce, Glenn **BT1 5**
 Jung, Min-joong **DTP 19**,
DTP 24

K

Kadota, K. **DTP 16**,
DTP 64, **JWP 71**
 Kano, Katsuhiko **DTP 67**
 Karahashi, Kazuhiro
JWP 36
 Karwacki, Eugene **NR1 7**
 Kashiwazaki, Ryouji
JWP 49
 Katsch, Hans-Michael
DTP 45
 Katsuki, Sunao **LR2 3**
 Kawashima, Shoichi
DTP 4, **NR2 8**
 Kazuo, Takayama **DTP 66**
 Kazutaka, Kawamura
DTP 66
 Kelly, P.J. **DTP 13**
 Ken'ichi, Yoshida **DTP 66**
 Khare, Bishun **JWP 75**
 Khazratov, Toir **DTP 68**
 Kim, Chang-Koo **JWP 47**
 Kim, Dae-Chul **DTP 47**
 Kim, Doosik **BT2 5**
 Kim, Gon-ho **DTP 19**,
DTP 24, **DTP 47**
 Kim, Jong-Sik **DTP 47**
 Kim, S.J. **JWP 64**
 Kim, S.S. **JWP 28**
 Kim, Yong-Ki **KW2 4**
 Kimura, T. **DTP 9**, **JWP 22**
 Kimura, Yasuo **JWP 67**
 Kitamori, Kazutaka
JWP 33, **JWP 69**
 Kitamura, S. **JWP 50**
 Kline, J.L. **MR1 7**
 Kline, John **AT2 5**,
DTP 18, **DTP 40**, **RF1 3**
 Koga, Kazunori **DTP 32**
 Kogelschatz, Ulrich **NR2 3**
 Koleske, D. **LR1 1**
 Kolobov, Vladimir **BT2 7**,
DTP 8, **GW2 5**, **MR1 2**
 Kono, A. **JWP 51**, **NR1 2**

Kortshagen, Uwe **ET1 7**,
KW1 3, **MR1 4**, **NR1 4**,
NR2 3
 Kovaleski, Scott **AT2 2**,
AT2 3
 Kroesen, Gerrit **JWP 53**
 Kroesen, G.M.W. **BT1 8**
 Kudriavtsev, Vladimir
BT2 7, **MR1 2**
 Kudrna, P. **DTP 12**,
DTP 15
 Kudryavtsev, Anatoly
DTP 8
 Kumar, Sunil **DTP 31**
 Kurihara, Kazuaki **JWP 36**
 Kurunczi, Peter **NR2 7**
 Kushner, Mark J. **BT1 3**,
ET1 1, **ET1 2**, **LR2 2**
 Kuwano, Takayuki **JWP 67**

L

Lampe, Martin **BT1 5**
 Lang, N. **DTP 37**
 Larsen, M. **DTP 55**
 Lau, Y.Y. **JWP 63**
 Laverty, S.J. **DTP 42**
 Laville, S. **GW2 6**
 Lavrov, B.P. **DTP 36**,
DTP 37
 Lawler, J.E. **ET1 6**,
JWP 57
 Lazarides, A. **JWP 63**
 Le Drogoff, B. **BT1 7**,
GW2 6
 Leal-Quiros, Edbertho
RF1 5
 Lee, Bong-Joo **DTP 47**
 Lee, Dong Seok **JWP 20**
 Lee, H.J. **JWP 64**
 Lee, H.S. **JWP 64**
 Lee, J.K. **JWP 64**
 Lee, Kangil **DTP 19**
 Lee, Woo-Geun **JWP 56**,
NR2 4
 Lee, Yongkwan **JWP 20**
 Lee, Young D. **GW2 1**
 Leipold, Frank **DTP 43**
 Lempert, Walter R. **JWP 82**
 Leonhardt, D. **RF1 4**,
RF2 6
 Leonhardt, Darrin **DTP 46**,
JWP 48, **RF1 5**
 Lho, Taihyoep **DTP 19**
 Lian, Jie **JWP 63**
 Lin, Chun C. **AT1 3**,
DTP 55
 Lister, G.G. **ET1 6**

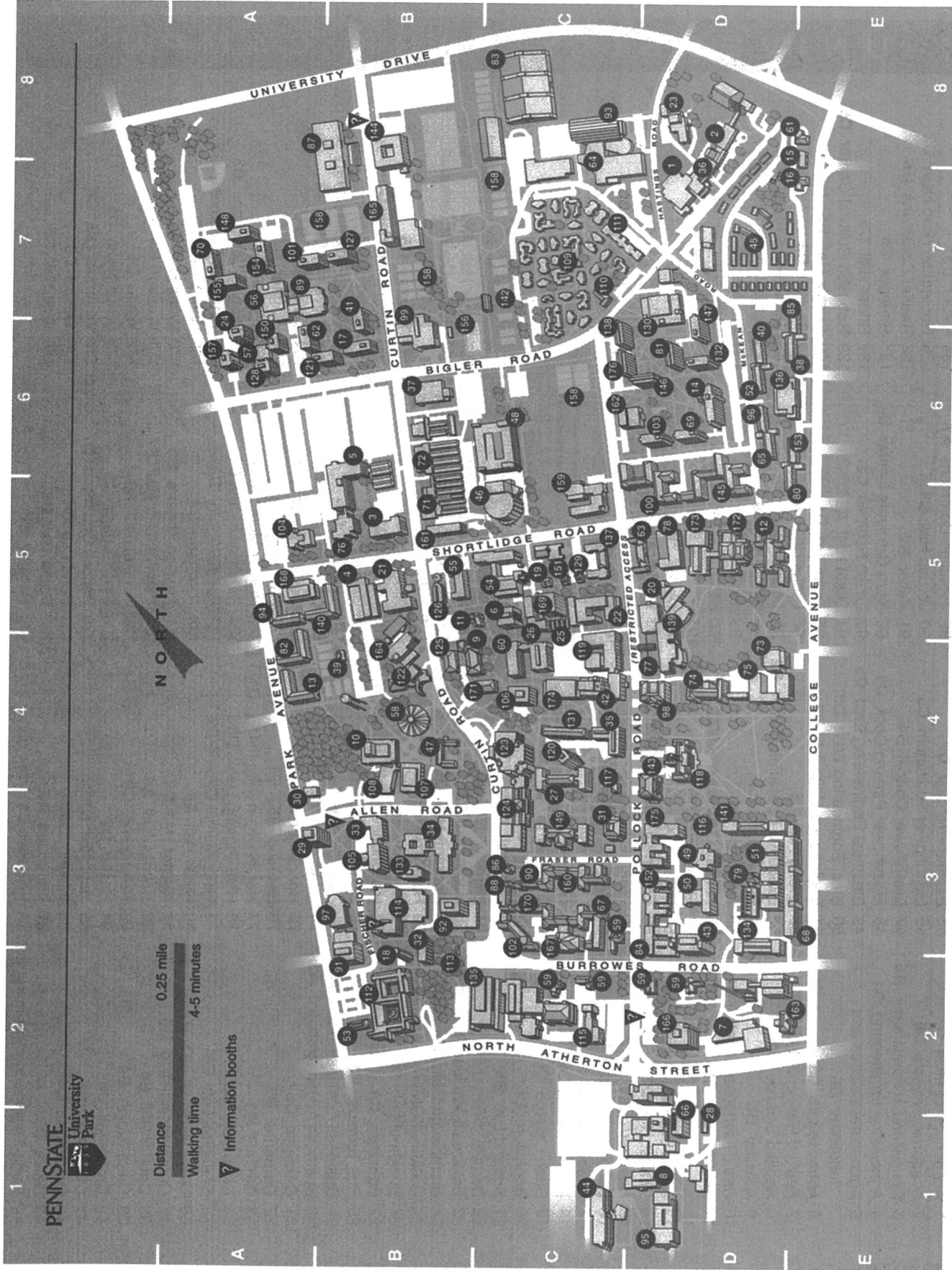
- Lister, Graeme G. **DTP 54**,
ET1 2
- Loffhagen, Detlef **JWP 11**,
JWP 17
- Long, J.D. **JWP 6**, LR1 2
- Lovtsov, A.S. LR2 4
- Luggenhölscher, D.
JWP 52
- Luo, W. **JWP 39**
- M**
- Ma, Z.W. BT1 2
- Madison, D.H. **DTP 53**
- Madison, Don **AT1 2**
- Maeshige, K. BT2 1
- Maeshige, K. **GW2 2**
- Maeshige, K. **JWP 25**
- Magne, L. **JWP 3**, LR2 1
- Maguire, P.D. **DTP 42**,
JWP 26
- Mahony, Charles M.O.
JWP 14
- Mahony, C.M.O. **DTP 42**,
JWP 26
- Maiorov, V.A. **DTP 7**
- Makabe, T. **BT2 1**
- Makabe, Toshiaki **GW2 2**,
JWP 25, RF1 1
- Makrinich, Gennady
DTP 17
- Mangolini, Lorenzo **NR2 3**
- Manheimer, W. **DTP 20**
- Manthey, Claudius **DTP 45**
- Maresca, Antonio **MR1 4**
- Margot, J. **DTP 2**,
GW2 6, LR1 4
- Mark, T. **DTP 60**
- Marler, J.P. **GW1 3**
- Martus, K. **DTP 58**
- Maruyama, Kouichi
JWP 33
- Masataka, Ono **DTP 66**
- Massines, Franoise **NR2 1**
- Mataras, Dimitrios **LR1 6**
- Mathieu, Thomas **JWP 32**
- Matsoukas, Themis BT1 6
- Matt, S. **DTP 60**
- McAninch, Ian **KW1 4**
- McCarthy, T. **DTP 3**
- McConkey, Bill **HW1 1**
- McCurdy, C.W. **DTP 56**
- McGrath, Robert T. **JWP 66**
- McKoy, B.V. **RF2 3**
- McKoy, Vincent **DTP 57**
- McNeill, Donald H. **DTP 6**
- Mechold, L. **DTP 39**
- Mechold, Lars **DTP 38**
- Meger, R.A. **RF1 4**, **RF2 6**
- Meger, Robert **DTP 46**,
JWP 48, **RF1 5**
- Mehanna, E.A. **AT2 4**
- Messier, Russell **JWP 66**
- Meyyappan, Meyya **BT2 3**,
JWP 75, **JWP 76**,
JWP 77, **KW1 4**, **KW1 5**,
MR1 3, **MR2 4**
- Midha, Vikas **DTP 48**
- Miller, P.A. **RF1 6**
- Mills, D. **JWP 46**
- Mills, Randell **ET1 8**
- Minayeva, Olga **JWP 74**
- Miralai, Farhad **NR2 2**
- Mohamed, Abdel-Aleam
Hufney **DTP 43**
- Moore, John **LR1 5**
- Morgan, W.L. **BT2 2**,
JWP 8, **RF2 3**
- Mori, Yuzo **DTP 4**, **NR2 8**
- Morrow, Tom **NR1 3**
- Moselhy, Mohamed **ET1 5**
- Moskowitz, Phil **JWP 59**
- Moss, Richard **ET1 1**
- Motika, Stephen **NR1 7**
- Muminov, T.M. **DTP 68**
- Muraoka, K. **JWP 50**,
JWP 60
- Muratore, Chris **LR1 5**
- Murnick, Daniel E. **ET1 4**
- Murnick, D.E. **DTP 3**
- Murphy, Donald **DTP 46**,
JWP 48, **RF1 5**
- Murphy, D.P. **RF1 4**
- Muthuswamy, Navin
JWP 31
- N**
- Nakagawa, D **JWP 25**
- Nakai, Yusuke **ET2 7**
- Nakajima, M. **JWP 37**
- Nakamoto, M. **DTP 16**
- Nakamura, Moritaka
JWP 36
- Nanbu, K. **MR1 5**
- Narishige, S. **JWP 50**
- Neale, I.D. **JWP 45**,
JWP 46
- Niemi, K. **DTP 41**
- Nishida, S. **DTP 9**
- Niwanō, Michio **JWP 67**
- Nobuyoshi, Ohyabu
DTP 66
- Noguchi, Y. **JWP 60**
- Nolle, L. **RF1 2**
- Nonkawa, Kiyohide
JWP 69
- Nosenko, V. **BT1 1**, **BT1 2**
- Nunomura, S. **BT1 1**
- O**
- Oh, J.J. **GW2 1**
- Ohe, K. **DTP 9**, **JWP 22**,
QF1 1
- Ohno, J. **NR1 2**
- Ohtsu, Yasunori **JWP 9**
- Okpalugo, Osmond A.
DTP 42
- Oksuz, Lutfi **QF1 4**
- Olthoff, James **RF2 4**
- Onthong, U. **DTP 60**
- Orel, A.E. **DTP 56**
- Orlov, Konstantin **MR1 4**,
NR2 3
- Oshikane, Yasushi **DTP 4**,
NR2 8
- Osiac, M. **DTP 36**
- Ostrikov, K.N. **JWP 6**,
JWP 39, **LR1 2**
- Ostrikov, Kostya **DTP 31**,
JWP 21
- P**
- Pacheco, A. **RF2 5**
- Paeva, G. **BT1 8**
- Palm, Peter **JWP 79**,
JWP 81, **JWP 82**
- Parenteau, Luc **DTP 50**
- Pasquiers, S. **JWP 3**, **LR2 1**
- Peko, B.L. **QF2 3**
- Petzenhauser, Isfried
JWP 58
- Pfender, Emil **NR1 4**
- Phelps, A.V. **DTP 63**
- Picton, P.D. **RF1 2**
- Pilione, Lawrence J.
JWP 66
- Pitchford, L.C. **JWP 61**
- Ploenjes, Elke **JWP 79**,
JWP 81, **JWP 82**
- Popp, Hanns-Peter **JWP 32**
- Porokhova, I.A. **DTP 14**,
DTP 15
- Porshnev, P.I. **JWP 2**
- Postel, C. **JWP 3**, **LR2 1**
- Probst, M. **DTP 60**
- Puech, V. **JWP 3**, **LR2 1**
- Punset, C. **JWP 61**
- Q**
- Qi, Bo **JWP 63**
- Queney, D. **LR1 4**
- R**
- Radovanov, Svetlana
DTP 26
- Radu, Ion **NR2 2**
- Rajaraman, Kapil **ET1 2**
- Ramamurthi, Badri **DTP 48**
- Rao, M V V S **MR2 4**
- Rao, M.V.V.S. **JWP 76**,
JWP 77
- Raoux, Sebastien **JWP 2**
- Rapakoulias, Dimitrios
LR1 6
- Rauf, S. **BT2 4**, **MR1 1**
- Rauf, Shahid **BT2 6**
- Ray, Paresht **ET1 8**
- Raynor, T. **DTP 58**
- Rees, J. Alan **LR1 5**
- Rees, J.A. **JWP 45**,
JWP 46
- Rescigno, T.N. **DTP 56**
- Rich, J. William **JWP 79**,
JWP 81, **JWP 82**
- Riemann, K.-U. **DTP 27**,
QF1 5
- Riley, M.E. **BT1 4**, **DTP 30**
- Riley, Merle E. **GW1 4**
- Ritchie, A. Burke **GW1 4**
- Rizakhanov, R.N. **LR2 4**
- Roche, Greg **LR1 5**
- Rojas, J. **RF2 5**
- Röpcke, J. **DTP 36**,
DTP 37, **DTP 39**
- Röpcke, Jürgen **DTP 38**
- Rousseau, A. **JWP 3**, **LR2 1**
- Rousseau, Antoine **DTP 38**
- Russell, T.H. **JWP 45**
- Rusz, J. **DTP 12**
- S**
- Sabsabi, M. **GW2 6**
- Sakai, Y. **JWP 18**, **JWP 37**,
RF1 7
- Sakai, Yosuke **ET2 6**
- Sakoda, T. **JWP 50**
- Salikhbaev, U.S. **DTP 68**
- Salvermoser, M. **DTP 3**
- Salvermoser, Manfred
ET1 4
- Sanche, Leon **DTP 50**
- Sarwar, Ivan **JWP 40**,
JWP 41, **JWP 42**
- Sasaki, K. **DTP 16**,
DTP 64, **JWP 71**
- Sato, Noriyoshi
MR1 6
- Satoh, K. **JWP 18**
- Sawada, Takayuki **JWP 69**
- Schermerhon, Jerry **JWP 56**
- Schermerhorn, Jerry **NR2 4**
- Schmidt, Martin **DTP 61**,
JWP 68

- Schoenbach, Karl H.
DTP 43, ET1 5, JWP 4,
LR2 3
- Schram, DC LR2 5
- Schulz-von der Gathen, V.
DTP 41
- Scime, Earl AT2 5,
DTP 18, DTP 40, RF1 3
- Scime, E.E. MR1 7
- Seetamsetty, Sreeram
JWP 5
- Sekine, Makoto JWP 36
- Selezneva, Svetlana LR2 5
- Severn, Greg DTP 23,
QF1 4
- Shamamian, V. DTP 20,
LR1 1
- Shao, May JWP 56
- Sharma, Surendra P.
JWP 76, JWP 77, MR2 4
- Shaw, D.M. JWP 65
- Shcherbakov, Yuri V.
DTP 5
- Shi, Wenhui ET1 5
- Shin, Jai K. GW2 1
- Shinohara, Masanori
JWP 67
- Shiozawa, M. MR1 5
- Shiratani, Masaharu
DTP 32
- Shon, Jong LR1 3
- Shul, R.J. RF1 6
- Sigeneger, F. ET2 3,
JWP 12
- Sigeneger, Florian JWP 68
- Simons, L. RF2 5
- Smith, D.J. JWP 73,
NR1 8
- So, Soon-Youl ET2 6
- Sobbia, R. GW2 4
- Sobolewski, Mark JWP 23,
QF1 3
- Song, Byungmoo ET1 3
- Song, Susan KW1 6
- Sosov, Yuriy JWP 13
- Spangler, Robert AT2 5
- Spanjers, Greg AT2 1
- Stafford, L. LR1 4
- Stamate, E. QF1 1
- Stark, Robert H. JWP 4
- Steen, Philip G. JWP 14,
JWP 27, NR1 3
- Steffens, Kristen MR2 1
- Stephen, T.M. QF2 3
- Stewart, R.S. JWP 73,
NR1 8
- Stoffels, E. BT1 8
- Stoffels, W.W. BT1 8
- Stone, Tom AT1 3
- Stout, Phillip BT2 6
- Stout, P.J. BT2 4
- Strak, Robert H. ET1 5
- Subramaniam, Vish V.
JWP 79, JWP 80, JWP 82
- Suda, Y. JWP 37
- Sugai, H. QF1 1
- Sugai, Hideo DTP 31,
ET2 7, JWP 72, MR2 5
- Sugawara, H. JWP 18,
JWP 37
- Sugawara, Hirotake ET2 6
- Sugiyama, Akira
MR1 6
- Sullivan, J.P. GW1 3
- Sun, Xuan AT2 5
- Surko, C.M. GW1 1,
GW1 3
- Suzuki, Takuma JWP 33,
JWP 69
- Syssoev, Vladimir S. DTP 5
- T**
- Tadera, Takamitsu MR1 6
- Tagashira, H. RF2 3
- Takeda, Akihide JWP 16
- Takemoto, Kenichi DTP 4,
NR2 8
- Takizawa, K. JWP 71
- Tatsumi, Tetsuya MR2 3
- Team, 2Department of
Nuclear Energy School of
Engineering Tokai
University DTP 66
- Team, Department of
Physics School of Science
Tokai University DTP 66
- Team, Department of
Physics University of
Toledo Toledo OH
JWP 56
- Team, Institut für Laser-
und Plasmaphysik DTP 41
- Team, Plasma Application
Lab DTP 19
- Team, Plasma Application
Modeling Group JWP 64
- Team, Research Institute of
Science and Technology
Tokai University DTP 66
- Team, Sheath DTP 23
- Teii, K. JWP 50
- Theodosiou, Constantine
DTP 51, JWP 13
- Thompson, Catherine
NR1 3
- Tichý, M. DTP 12, DTP 14
- Tichy, M. DTP 15
- Tran, Phuoc DTP 6
- Trudeau, M. BT1 7
- Tsakadze, E.L. LR1 2
- Tsakadze, Erekle JWP 21
- Tsakadze, Z.L. LR1 2
- Tsakadze, Zviadi JWP 21
- Tsendin, L.D. QF1 5
- Tsendin, Lev DTP 8
- Tsuboi, Hideo JWP 36
- Tuguhro, Watanabe
DTP 66
- Turner, Miles M. DTP 25,
ET2 5
- U**
- Uchino, K. JWP 50,
JWP 60
- Uhlmann, L.J. AT1 4
- Uhrlandt, Dirk ET2 2
- Ulrich, Andreas ET1 4
- V**
- Vaid, D. DTP 53
- van de Sanden, Richard
LR2 5
- Vender, David DTP 25,
ET2 5
- Ventzek, Peter L.G. BT2 6
- Ventzek, P.L.G. MR1 1
- Veronis, Georgios NR2 5
- Vidal, F. GW2 6
- Visser, Bram JWP 53
- Viswanathan, G. Babu
JWP 82
- Vyas, Vivek BT1 3
- W**
- Walter, Lempert JWP 78
- Walton, Scott DTP 46,
JWP 48, RF1 5
- Walton, S.G. RF1 4, RF2 6
- Wang, Luming JWP 63
- Wang, Xu DTP 23, QF1 4
- Wang, Yicheng JWP 23,
QF1 3
- Watanabe, M. JWP 65
- Watanabe, Yukio DTP 32
- Waters, Karla NR1 6
- Weik, Fritz DTP 50
- Wertheimer, Michael R.
NR2 2
- Wickliffe, M.E. JWP 57
- Wieser, Jochen ET1 4
- Williams, Jim AT1 1
- Williamson, James M.
DTP 34
- Willison, C.G. RF1 6
- Winkler, R. ET2 3, JWP 12
- Winkler, Rolf ET2 2,
JWP 11, JWP 17
- Winograd, Nicholas QF2 1
- Winstead, C. RF2 3
- Winstead, Carl DTP 57
- Woehrman, Michael AT2 5
- Woehrman, Micheal
DTP 40
- Wonchul, Lee JWP 78
- Woodworth, J.R. MR1 1,
RF1 6
- Woolston, Mike JWP 2
- X**
- Xu, S. JWP 6, JWP 39,
LR1 2
- Xu, Shuyan DTP 31,
JWP 21
- Y**
- Yagisawa, T. GW2 2
- Yamaguchi, H. DTP 64
- Yamamoto, Tatsushi MR1 6
- Yamamura, Kazuya DTP 4,
NR2 8
- Yamaoka, Yoshikazu
JWP 36
- Yanagida, M. RF1 7
- Yang, H.Q. GW2 5
- Yoo, Suk-Jae DTP 47
- Yoshida, K. RF2 3
- You, S.J. JWP 28
- Z**
- Zdravkovic, D. GW2 4
- Zhang, Da BT2 6
- Zhao, Z. ET2 1
- Zholonko, Nick JWP 41,
JWP 42
- Zhou, Ning BT2 7, MR1 2
- Zimmerman, Todd A.
DTP 55

NOTES

Distance 0.25 mile
Walking time 4-5 minutes

Information booths

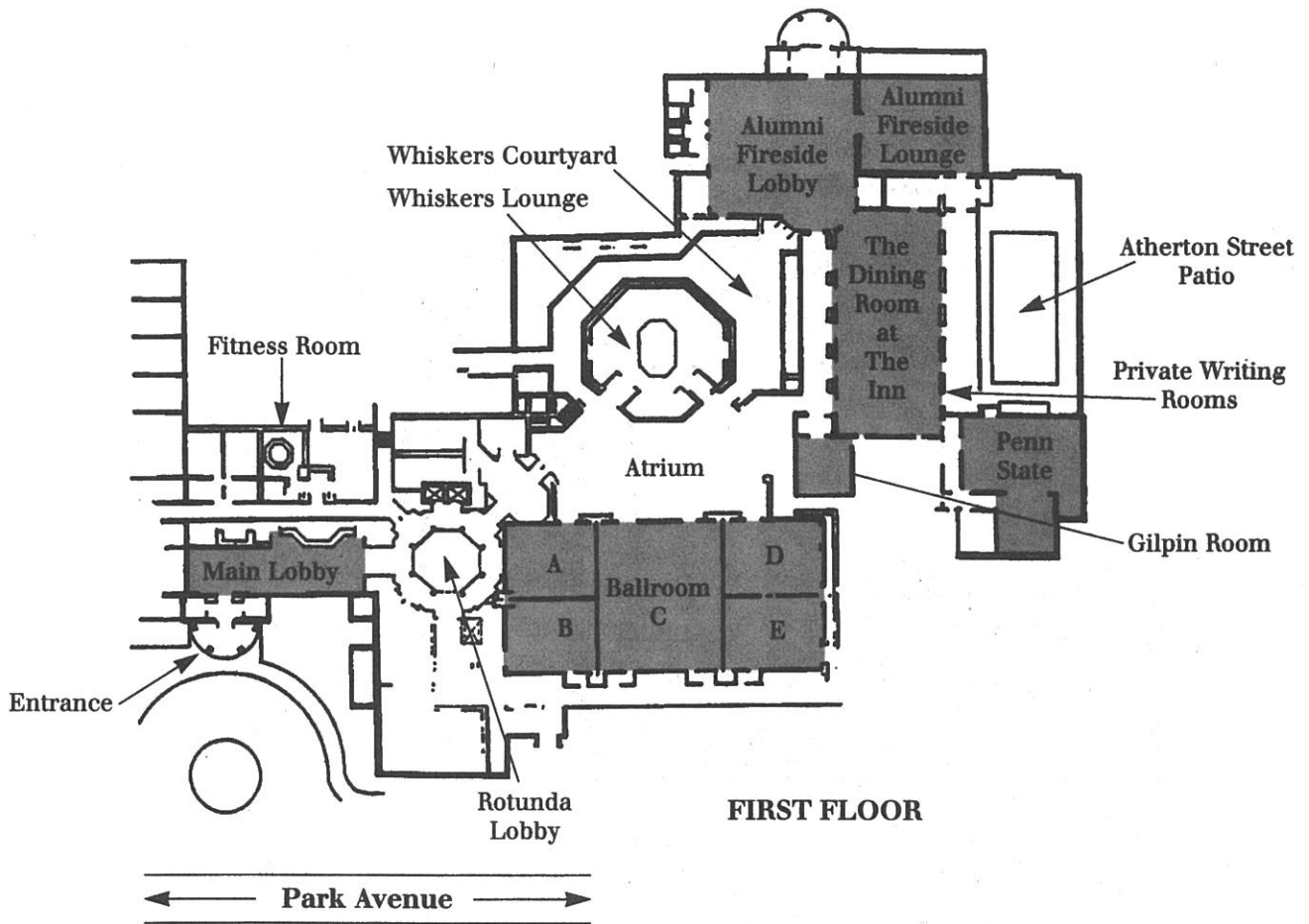


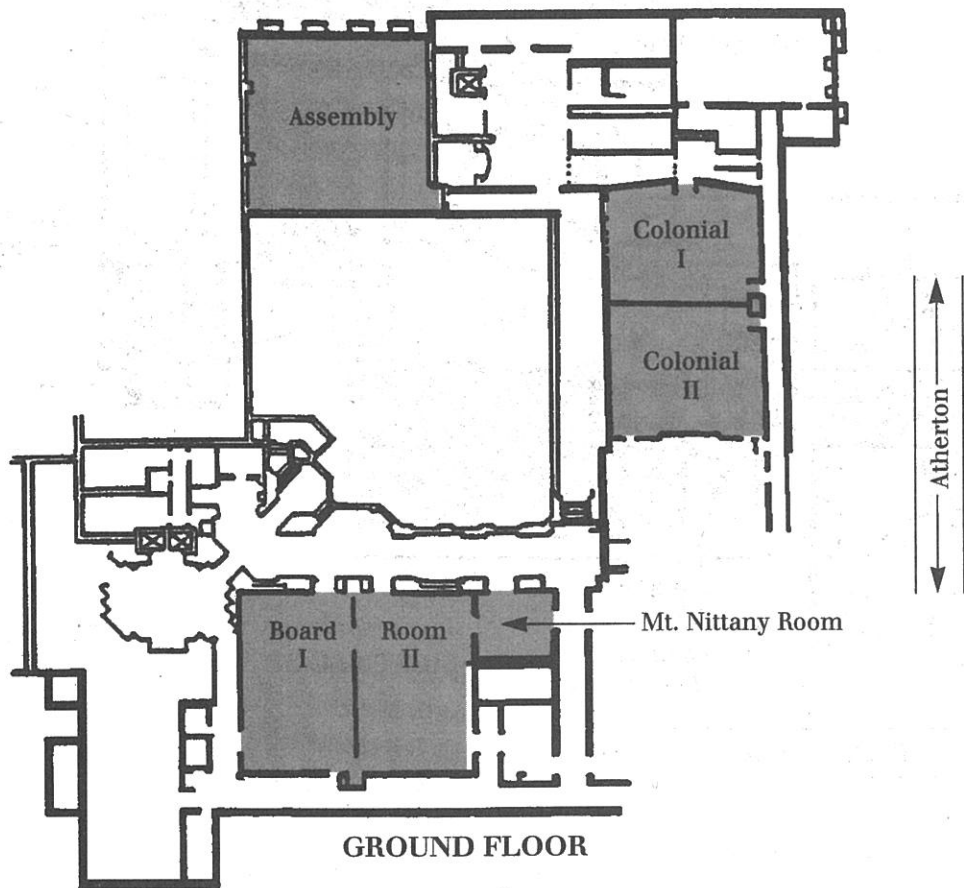
UNIVERSITY PARK CAMPUS

- | | | |
|--|--------------------------------|--------------------------------------|
| 1 Academic Activities D7 | 89 Johnston Commons A7 | 134 Reber D3 |
| 2 Academic Projects D8 | 90 Jordan Hall C3 | 135 Recreation (Rec Hall) C2 |
| 3 Agricultural Administration B5 | 91 Keller B2 | 136 Redifer Commons D6 |
| 4 Agricultural Engineering B4 | 92 Kern Graduate Center B3 | 137 Rittenour C5 |
| 5 Agricultural Science and Industries B6 | 93 Lasch Football C8 | 138 Ritner Hall C6 |
| 6 Althouse Lab C5 | 94 Leete Hall A5 | 139 Robeson Cultural Center C5 |
| 7 Applied Research Lab D2 | 95 Leonhard D1 | 140 Runkle Hall B5 |
| 8 Applied Science D1 | 96 Lyons Hall D6 | 141 Sackett D3 |
| 9 Armsby B4 | 97 Mateer B3 | 142 Sarni Tennis Facility C7 |
| 10 Arts (Playhouse Theatre) B4 | 98 McAllister D4 | 143 Schwab Auditorium D4 |
| 11 Arts Cottage B5 | 99 McCoy Natatorium B6 | 144 Shields B8 |
| 12 Atherton Hall D5 | 100 McElwain Hall D5 | 145 Simmons Hall D5 |
| 13 Beam Business Admin. A4 | 101 McKean Hall A7 | 146 Shulze Hall D6 |
| 14 Beaver Hall D6 | 102 McKee Hall C3 | 147 Shunk Hall D7 |
| 15 Beecher/Dock House E8 | 103 Miffilin Hall D6 | 148 Snyder Hall A7 |
| 16 Benedict House E7 | 104 Mitchell Inst. Services A5 | 149 Sparks C3 |
| 17 Bigler Hall B6 | 105 Moore B3 | 150 Sprout Hall A6 |
| 18 Biomechanics Lab B2 | 106 Mueller Lab C4 | 151 Spruce Cottage C5 |
| 19 Birch Cottage C5 | 107 Music I B4 | 152 Steidle D3 |
| 20 Bookstore D5 | 108 Music II B4 | 153 Stephens Hall E6 |
| 21 Borland Lab B5 | 109 Nittany Apartments C7 | 154 Stone Hall A7 |
| 22 Boucke C5 | 110 Nittany Community Cntr. C7 | 155 Stuart Hall A7 |
| 23 Breazeale Nuclear Reactor D8 | 111 Nittany Hall C7 | 156 Swimming Pool (outdoor) B6 |
| 24 Brumbaugh Hall A6 | 112 Nittany Lion Inn B2 | 157 Tener Hall A6 |
| 25 Buckhout Greenhouses C5 | 113 Nittany Lion Shrine B2 | 158 Tennis Courts (outdoor) A/B7, C6 |
| 26 Buckhout Lab C5 | 114 Nittany Parking Deck B3 | 159 Thomas C5 |
| 27 Burrows C4 | 115 Noll Lab C2 | 160 Thompson Hall C3 |
| 28 Bus Terminal D1 | 116 Obelisk D3 | 161 Tyson B5 |
| 29 Business Administration I A3 | 117 Old Botany C4 | 162 Undergraduate Library C6 |
| 30 Business Administration II A3 | 118 Old Main D4 | 163 University Club E2 |
| 31 Carnegie C3 | 119 Osmond Lab C4 | 164 Visual Arts B4 |
| 32 Carpenter B2 | 120 Oswald Tower C4 | 165 Wagner B7 |
| 33 CEDAR B3 | 121 Packer Hall A6 | 166 Walker D2 |
| 34 Chambers B3 | 122 Palmer Museum of Art B4 | 167 Waring Commons C3 |
| 35 Chandlee Lab C4 | 123 Paterno Library C4 | 168 Warnock Commons A5 |
| 36 Coal Utilization Lab D7 | 124 Pattee Library C3 | 169 Wartik Lab C5 |
| 37 Computer Building B6 | 125 Patterson B4 | 170 Watts Hall C3 |
| 38 Cooper Hall E6 | 126 Pavilion Theatre B5 | 171 Weaver B4 |
| 39 Credit Union B4 | 127 Pennypacker Hall B7 | 172 White D5 |
| 40 Cross Hall D6 | 128 Pinchot Hall A6 | 173 White North D5 |
| 41 Curtin Hall B7 | 129 Pine Cottage C5 | 174 Whitmore Lab C4 |
| 42 Davey Lab C4 | 130 Pollock Commons D7 | 175 Willard D3 |
| 43 Deike D3 | 131 Pond Lab C4 | 176 Wolf Hall C6 |
| 44 Earth-Engineering Sciences C1 | 132 Porter Hall D6 | |
| | 133 Rackley B3 | |

PENNSTATE







Epitome of the Gaseous Electronics Conference 2001 of the American Physical Society

8:00 TUESDAY MORNING
9 OCTOBER 2001

- AT1 **Electron Collisions with Rare Gases**
Williams, Madison
Ballroom C, Nittany Lion Inn
- AT2 **Plasma Propulsion**
Spanjers
Ballroom AB, Nittany Lion Inn

10:00 TUESDAY MORNING
9 OCTOBER 2001

- BT1 **Dusty Plasmas and Plasmas for Nanostructured Materials**
Ballroom AB, Nittany Lion Inn
- BT2 **Plasma Modeling: Needs and Opportunities**
Ballroom C, Nittany Lion Inn

11:45 TUESDAY MORNING
9 OCTOBER 2001

- CT1 **Plasma Modeling Discussion**
Ballroom C, Nittany Lion Inn

13:15 TUESDAY AFTERNOON
9 OCTOBER 2001

- DTP **Poster Session I**
Board Room, Nittany Lion Inn

15:30 TUESDAY AFTERNOON
9 OCTOBER 2001

- ET1 **Lighting**
Ballroom C, Nittany Lion Inn
- ET2 **Glows: DC Pulsed RF, Microwave, Inductive, Other**
Ballroom AB, Nittany Lion Inn

19:15 TUESDAY EVENING
9 OCTOBER 2001

- FT1 **Positive Column Workshop**
Assembly Room, Nittany Lion Inn

8:00 WEDNESDAY MORNING
10 OCTOBER 2001

- GW1 **Collisions with Molecules**
Surko, Becker
Ballroom C, Nittany Lion Inn
- GW2 **Computational Methods for Plasmas**
Ballroom AB, Nittany Lion Inn

10:00 WEDNESDAY MORNING
10 OCTOBER 2001

- HW1 **Foundations of Gaseous Electronics**
McConkey
Ballroom C, Nittany Lion Inn

11:15 WEDNESDAY MORNING
10 OCTOBER 2001

- IW1 **GEC Business Meeting**
Ballroom C, Nittany Lion Inn

13:15 WEDNESDAY AFTERNOON
10 OCTOBER 2001

- JWP **Poster Session II**
Board Room, Nittany Lion Inn

15:30 WEDNESDAY AFTERNOON
10 OCTOBER 2001

- KW1 **Plasmas for Nanostructured Materials**
Hori, i Cabarrocas
Ballroom C, Nittany Lion Inn
- KW2 **Electron Collisions with Metal Vapors**
Hanne, Fursa, Bogaerts
Ballroom AB, Nittany Lion Inn

8:00 THURSDAY MORNING
11 OCTOBER 2001

- LR1 **Materials Processing**
Ballroom C, Nittany Lion Inn
- LR2 **Environmental Applications and Thermal Plasmas**
Ballroom AB, Nittany Lion Inn

10:00 THURSDAY MORNING
11 OCTOBER 2001

- MR1 **Inductively-Coupled Plasmas and Magnetically-Enhanced Plasmas**
Ballroom C, Nittany Lion Inn
- MR2 **Fluorocarbon Plasmas**
Steffens, Booth, Tatsumi
Ballroom AB, Nittany Lion Inn

13:15 THURSDAY AFTERNOON
11 OCTOBER 2001

- NR1 **Plasma Diagnostics III**
Ballroom C, Nittany Lion Inn
- NR2 **Atmospheric Pressure & Dielectric Barrier Discharges**

Massines
Ballroom AB, Nittany Lion Inn

15:30 THURSDAY AFTERNOON
11 OCTOBER 2001

- OR1 **Laboratory Tours: Penn State's NSF National Nanofabrication Users Network (NNUN) and Other Selected Materials Research Institute Facilities**
Nanfab Facility, Materials Research Institute

19:00 THURSDAY EVENING
11 OCTOBER 2001

- PR1 **GEC Reception and Banquet**
Ballroom C, Nittany Lion Inn

8:15 FRIDAY MORNING
12 OCTOBER 2001

- QF1 **Plasma Boundaries: Sheaths and Pseudosheaths**
Ballroom C, Nittany Lion Inn
- QF2 **Plasma Interactions with Surfaces**
Winograd, d'Agostino
Ballroom AB, Nittany Lion Inn

10:00 FRIDAY MORNING
12 OCTOBER 2001

- RF1 **Plasma Diagnostic V**
Ballroom C, Nittany Lion Inn
- RF2 **Low and Ultralow Energy Electron-Molecule Interactions**
Gopalan, Bass
Ballroom A, B, Nittany Lion Inn

13:30 FRIDAY AFTERNOON
12 OCTOBER 2001

- SF1 **Workshop: Innovations in Gaseous Electronics Education**
Ballroom C, Nittany Lion Inn



0003-0503(200110)46:6;1-3